Structural Analysis of the Hohonu Thrust Fault and Relationships with the Neogene Tectonic Evolution of the Grey Valley Region.

A thesis submitted in partial fulfillment of the requirements for the degree of Master of Science in Geology in the University of Canterbury by

Jan Sintenie

June 2014

FOR SHARON

FRONTISPIECE

Looking south along the trace of the Hohonu Fault with Bell Hill, Lake Brunner and the Hohonu Range to the left.

ABSTRACT

The main aims of this study are to; (1) constrain the kinematics and tectonic evolution of the Hohonu Fault; (2) understand the Neogene tectonic history of the Greymouth area and its context in terms of regional plate motions; and (3) determine if Late Cretaceous extensional structures in the study area are influencing deformation and Neogene tectonic development.

Two major extensional tectonic episodes have significantly affected the crustal architecture of the study area prior to Neogene compression. The first being NNE-SSW directed extension as new Zealand broke away from Gondwana between c. 115 and c. 82 Ma. This was accompanied by granitoid intrusion, core complex formation, and was culminated with rifting and opening of the Tasman Sea. The second being WNW-ESE directed extension that was related to the propagation of the Challenger Rift System through New Zealand between c. 45 and c. 23 Ma. This phase was characterised by the development of NNE-SSW trending normal faulted basins. Both of these tectonic episodes have left strong structural discontinuities in the crust.

During the phase of Neogene compression since c. 23 Ma, the change from WNW-ESE extension to compression in the same direction resulted in inversion of many of the basins that had formed in the Paleogene to early Neogene stage of extension. The compressional reactivation of the inherited NNE-SSW normal faults has been illustrated by many authors, and therefore their presence as a seismic hazard is relatively clear. The possible reactivation of the easterly trending Late Cretaceous structures in the current stress field is less well understood, and therefore represent an unquantified seismic hazard.

This study uses a diverse range of data including a large amount from petroleum exploration (open source) as well as recently released (2013) aeromagnetic data, and kinematic data from fieldwork done during this study. A principal tool used to synthesise the data is the 3D structural geology software Move. This software was used to map structures across the study area as well as create two balanced geological cross sections which were restored to significant Neogene horizons.

Findings from this study include a new hypothesis that suggests the existence of a c. 25 km wide, WNW-ESE trending Late Cretaceous extensional structure between the Hohonu Range and the Takutai Half Graben offshore Greymouth. The presence of this Cretaceous extensional structure appears to have significantly effected Neogene tectonic development across the Grey Valley Trough and Hohonu Range. In the Grey Valley Trough, the Cretaceous extension zone is coincident with an area where Neogene subsidence is c. 2km greater than the largest amounts of subsidence occurring to the north or south. On the southwest margin, and to the north of the

Hohonu Range, the inferred presence of conjugate strike slip faults indicates the reactivation of the Cretaceous extensional structures in the current stress field and may present a seismic hazard risk. The concept of the Greymouth area developing as craton-ward migrating foreland system during the Late Miocene is also suggested.

CONTENTS

TABLE OF FIGURES

ACKNOWLEDGMENTS

Firstly I would like to thank my supervisors: Francesca Ghisetti, who taught me how to use the Move software and provided lightning-quick, in-depth edits to the final draughts of my thesis; Catherine Reid who was my reliable in-house supervisor, and Uwe Ring who travelled all the way from Stockholm to do some fieldwork with me.

Thanks to all of those who helped me in the field during this study. It was great to have someone to yell kinematic, bedding and cleavage measurements to when half submerged in those cold creeks.

Thanks to the Canterbury University Mason Trust for funding the fieldwork section of this study. This involved many nights in a tent at the Moana Campground and the fuel costs for driving between the field area and Christchurch.

Thanks to all the support I have received from the staff and fellow students from the Department of Geological Sciences, University of Canterbury. This included the use of a laptop on which to run the Move software, and staff who answered many questions about various forms of geophysical data and fieldwork.

Finally, thanks to my parents, Catherine and Ad, my sister, Anna and my partner Sharon who helped me get to the end of this thesis when a number of other life issues made it a lot harder at times.

CHAPTER 1. INTRODUCTION

1.1 Overview of tectonic context

1.1.1 Present tectonic setting and location of the study area

The deformational response of the Australian Plate continental crust to the development of the plate boundary in the West Coast region of South Island, New Zealand is the subject of present debate (e.g. Ghisetti et al., 2014). This investigation looks into the deformational effects of both reactivated inherited structures and lithospheric flexure due to thrust loading on the Australian crust during Neogene plate boundary development. This study focusses on the Greymouth region (see Figure 1-1), which is situated in the transition zone between foreland basin and inverted basin-and-range. The main aim of this study is to define the style of deformation that has developed in the study area during the Neogene, and to understand whether and to what extent pre-existing structures have influenced this style of deformation.

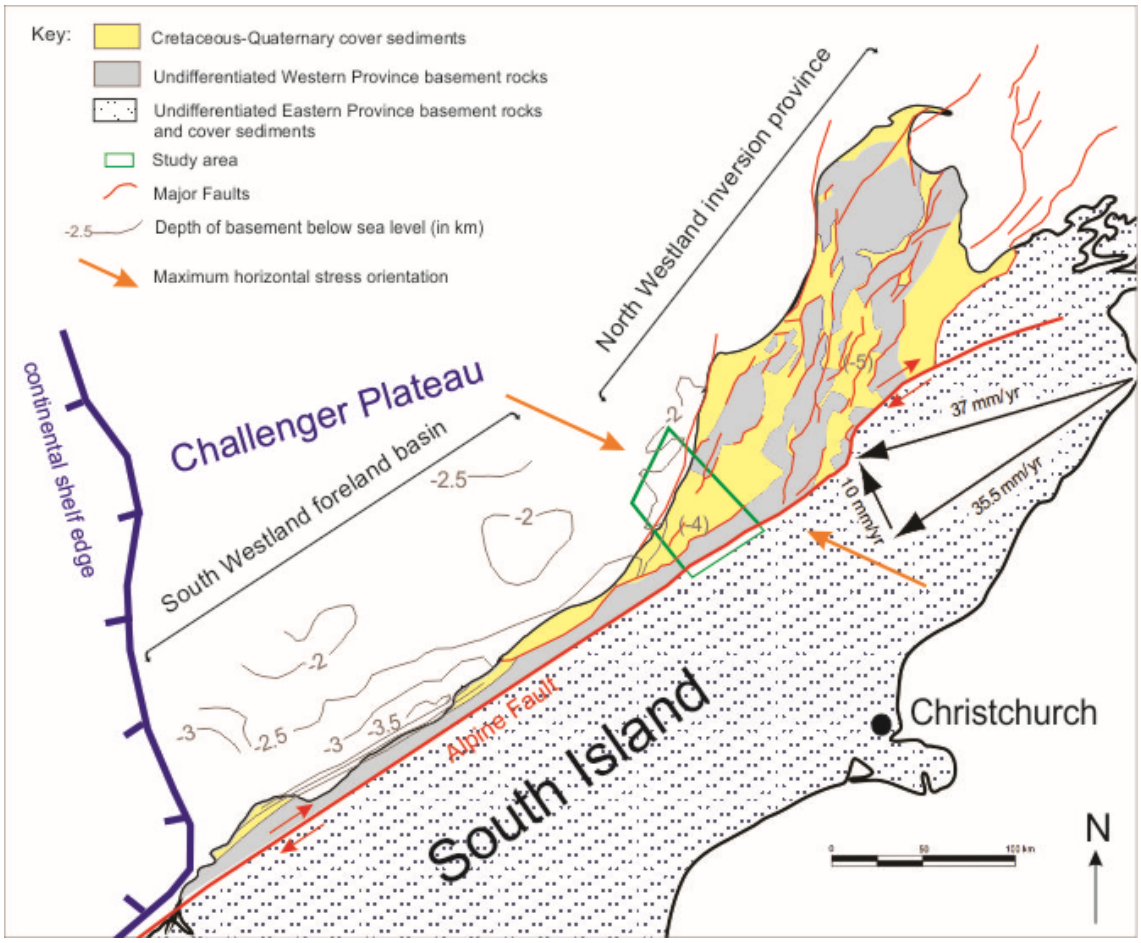

Figure 1-1: Regional tectonic sketch map showing the position of the study area between the North Westland inversion province to the north and the South Westland foreland basin to the south. Redrawn from Sircombe and Kamp (1998) and Ghisetti and Sibson, (2006). Partitioning of the interpolate velocity vector after Norris and Cooper (2000). Maximum horizontal stress orientation after Townend et al (2012).

At present, in the region of the study area, the Pacific Plate is obliquely colliding with the Australian Plate with a relative plate motion vector of 37mm/year with a 35.5 mm/year component parallel to the plate boundary and a 10 mm/year component perpendicular to it (Norris & Cooper 2000) (see Figure 1-1). Studies of principal stress directions based on extensive studies of earthquake focal mechanisms, show a very consistent principal stress direction of 115 ± 5° throughout the northern South Island (Townend et al. 2012).

1.1.2 South Westland Sedimentary Basin as a foreland basin

A number of previous workers have identified the South Westland Basin as a foreland basin system (Sircombe and Kamp, 1998; Sircombe, 1993; Harrison, 1999) (see Figure 1-2). Foreland basin systems are associated with convergent plate margins where orogenic fold and thrust belts form in colliding continental crust. They form by flexural subsidence of the lithosphere in response to loading either within or beneath the adjacent orogen (DeCelles and Giles, 1996; Catuneanu, 2004). Foreland systems contain four depozones as recognised by DeCelles and Giles (1996). These are (starting from the margin of the fold-thrust belt of the orogeny): the wedge top; foredeep; forebulge; and back bulge depozones (see Figure 1-3)

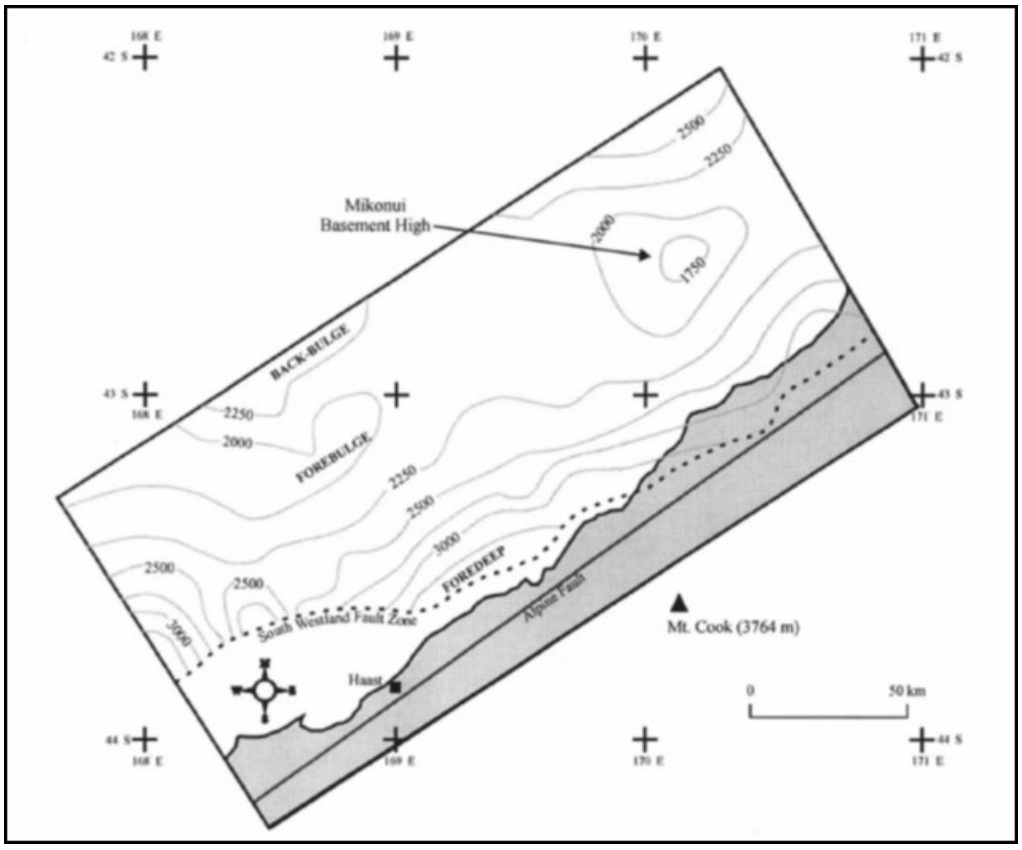

Figure 1-2: South Westland Foreland Basin structure (from Harrison, 1999). Depth to basement contours, with values shown in metres

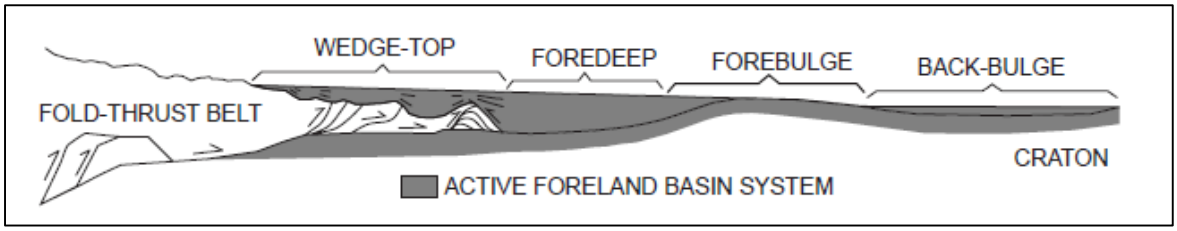

Figure 1-3: Depozones of a foreland basin system (taken from DeCelles and Giles, 1996).

Foreland basins are divided into two types; pro- and retro- foreland basins (see Figure 1-4) (Catuneanu, 2004; Naylor and Sinclair, 2008). Pro-foreland basins form on the subducting lithospheric slab side of the orogen, and the creation of a foredeep is primarily controlled by the supra-lithospheric orogenic load (Catuneanu, 2004). These form on the side of the orogen where more accretion occurs and as a result, they migrate outwards as the orogeny builds and the thrust front advances (Naylor and Sinclair, 2008). Retro foreland basins form on the over-riding lithosphere, and additional to the adjacent orogenic load, their subsidence is also controlled by sublithospheric loading by the down-going slab and broad wavelength dynamic loading of the lithosphere caused by viscous mantle flow (Catuneanu, 2004). These form on the side of the orogeny where less accretion occurs, and the thrust-front remains relatively stable as the orogen grows. This means that retro foreland systems tend to remain stationary as they develop. The outward migration of a foreland basin system during the building of an orogen can be observed by noting the changes in depositional environment characteristic of each depozone (cf. Horton and DeCelles, 1997)

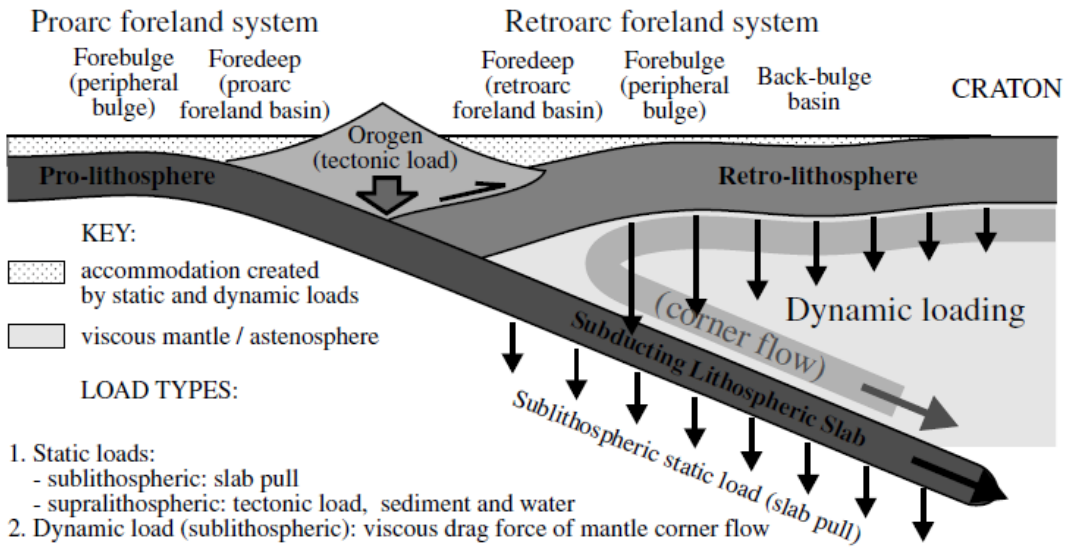

Figure 1-4: Pro arc and retroarc foreland systems – tectonic setting and controls on accommodation (from Catuneanu, 2004). Foreland systems form by the flexural deflection of the lithosphere under a combination of supra- and sublithospheric loads.

The Taranaki Basin (c. 300 km northeast of the study area) has been identified as a classic retro foreland basin that formed primarily during the Miocene (Holt and Stern, 1994; Decelles and Giles, 1996, Baur et al 2013). This occurred in response to the Pacific Plate subducting beneath the Australian Plate which caused regional subsidence due to sublithospheric dynamic loading as well as more localised flexural subsidence adjacent to the orogenic load (Holt and Stern, 1994). The South Westland Basin has also been identified as a retro-foreland basin by Naylor and Sinclair (2008). This classification relies on the assumption that the lower part of the Pacific Plate lithosphere is being subducted beneath the Australian Plate lithosphere. The westward subduction of the lower Pacific Plate lithosphere beneath the Australian Plate lithosphere is the model suggested for the central and northern parts of the Southern Alps Orogen by Beaumont et al. (1996). The fact that the Alpine Fault has evolved from a pure transform feature (Sutherland et al., 2000), and that subduction must change polarity at some point along the fault, may mean that classification of the foreland basin type is not applicable. The hypothesis that the South Westland Basin has developed as a foreland basin since the Late Miocene has been challenged by Sutherland (1996) and Walcott (1998), who suggested that the subsidence along the southeastern boundary of the Westland Basin can be entirely attributed to sediment loading, with no orogenic loading and flexure occurring in the Australian Crust. This argument is countered by Sircombe and Kamp (1998) and Harrison (1999) who show the Australian crust to have a profile characteristic of loading-induced flexure.

1.1.3 Inherited Cretaceous structures

Prior to the development of the early Cenozoic extensional basins, the Westland area also underwent an intense phase of NNE-SSW-directed extension as it rifted away from Australia and Antarctica during the Cretaceous (Bradshaw, 1989, Laird and Bradshaw, 2004). Evidence for structures that developed during this extensional phase are present across the North Westland region (Tulloch and Kimbrough, 1989, Laird, 1993, Bishop, 1992b, Waight et al., 1998a,b). However, it is poorly understood what tectonic influence the structures inherited from the Cretaceous extensional phase have had during the Neogene compressional regime.

1.1.4 Inversion of Paleogene extensional faults

In North Westland, the Neogene inversion of Early Cenozoic NNE-SSW trending extensional basins has been well documented (Wellman, 1949, Laird, 1968, Bishop and Buchanan, 1995, Ghisetti and Sibson, 2006, Ghisetti et al, 2014,). Specifically in the study area, the Paparoa Inversion Zone is an area where the locus of subsidence during the Eocene became a locus of uplift during the Neogene through the process of inversion of its bounding faults.

1.2 Gaps in present understanding of tectonic development of region

Specific gaps in this understanding that will be addressed during this study are as follows:

- Very little work has been done to understand fault kinematics in the area of basement exposure between the Hohonu and Alpine Faults
- Recently released (from www.nzpam.govt.nz) aeromagnetic data has not been interpreted in detail for the study area.
- Although the Neogene re-activation of Eocene extensional faults in the form of inversion has been well documented (Wellman, 1949; Laird, 1968; Bishop and Buchanan, 1995; Ghisetti and Sibson, 2006), the influence of WNW-ESE trending Late Cretaceous extensional structures on Neogene structural development is under-recognized.
- As a whole, the tectonic evolution of the Australian crust in the Greymouth region in the context of being situated at a collisional margin is poorly understood. This involves understanding why, and what time did: 1) inherited fault sets re-activate; and 2) new orogenic wedge thrusting occur during the Neogene convergent phase.

1.3 Investigation outline

The main focus of this study is to constrain the tectonic evolution of one of the main fault zones in the immediate footwall of the Alpine Fault: the Hohonu Fault. Field studies were undertaken to constrain the kinematics and timing of activity on the Hohonu Fault. Data were collected in both the hangingwall and footwall sections of the fault, with some exposures of the principal fault plane itself being described. A synthesis of the tectonic setting for the study area has also been attempted by putting together field data, subsurface data (from wells and seismic reflection surveys) and regional geophysical surveys. A principal output of this regional synthesis is the construction and restoration of two geological cross sections across the study area using Move software, and a map of the main faults inferred across the study area. The main points to be discussed in this study are: 1) The Neogene tectonic history of the study area; and 2) whether structures that developed during Late Cretaceous NNE-SSW directed extension have influenced the deformation of the study area during the Neogene.

1.4 Thesis structure

Chapter 2 of this thesis outlines the geological setting of the study area. This consists of firstly, briefly describing the stratigraphy of the study area, secondly, describing the main structures and faults of the study area, and thirdly, summarizing the geological history of the study area.

Chapter 3 describes the fieldwork that was undertaken during this study. This consists of describing the basement between the Hohonu and Alpine Faults, summarizing the fieldwork that looked at important parts of the Neogene basin sediments, and describing observations that help constraining the activity of the Hohonu Fault itself.

Chapter 4 outlines the work done to synthesise subsurface, mapped and geophysical data. Firstly, the different data are described, this is followed by a description of the methods and results of interpretation of aeromagnetic and seismic data. The methods for how cross sections were created, validated and restored using Move software is then described, followed by a presentation of the results of this part of the study.

Chapter 5 discusses what implications there are from this study on understanding the influences of pre-existing Late Cretaceous extensional structures on Neogene tectonic development. Relationships to seismic activity and possible earthquake hazards are also discussed

Chapter 6 outlines the main conclusions of this study. It also outlines recommendations for future work.

CHAPTER 2. GEOLOGICAL SETTING AND TECTONIC HISTORY OF THE STUDY AREA

2.1 Introduction

This chapter synthesises the large amount of geological data and interpretations on the study area produced by previous workers. Work including many decades of petroleum and coal exploration, surface mapping, stratigraphic studies, core complex analysis, interpretation of the basement terranes, and studies of the intrusive rocks in the Greymouth region has allowed the geology of the study area to be well constrained. This chapter will summarize the stratigraphic units of the study area as seen in Figure 2-2. Most of these units outcrop to some degree across the study area and can be seen on the accompanying geological map (Figure 2-3). Also on this map is an outline of the structural geology of the study area. This is described by dividing the study area into a series of domains which are bounded by major structural features. The chapter finishes with an outline of the geological history, relating it to large scale changes in plate motions.

2.2 Physiography of study area

The area of focus for this study is located in the Greymouth region of the West coast, New Zealand (Figure 2-1). The area is bounded by the Southern Alps in the southeast and the Tasman Sea in the northwest. The Taramakau and the Grey are two major rivers with mouths along the coast of the study area. Adjacent to where it enters the Tasman Sea, the Grey River orthogonally cuts between two north-south trending ridges - the Rapahoe Range and the Peter Ridge. At its southern end, the Peter Ridge curls round to the east, to connect with the southern end of the northeast-southwest trending Kaiata Range. The Grey River cuts across the northern end of the Kaiata Range as it exits the Grey Valley. The Grey Valley consists of a 15-30 km wide, NNE-SSW trending strip of land with low, undulating topography and flat terraces rising no higher than 400m above sea level. This strip of low topography continues to the south of the Kaiata Range and Peter Ridge, adjacent to the coast for a distance of around 50 km. Before it exits the Grey Valley, the Grey River runs southward along the eastern side of the Paparoa Range. This is a range with crestal elevations of between 1000 – 1500 m and continues in a NNE direction for around 60 km to the Buller River. To the east of the lowland strip, there is a parallel ca. 10 km wide lineament of discrete, glacier-cut hills and mountains, the largest of which are >1300 m high. From south to north within the study area, these are; Mt Turiwhate, Hohonu Range, Mt Te Kinga, Granite Hill and Bell Hill. Some of the glacially eroded gaps along the line of hills are exploited by rivers such as the Taramakau and Crooked Rivers, some others are at least partially filled by lakes such as Kaneire, Brunner and Haupiri. To the south east of the line of discrete hills and mountains, there is a narrow 1-3 km wide strip of low, and often flat topography of which the Taramakau River flows down part of. This

strip of low topography is bounded to the south east by a straight NW-SE trending edge of steep topography that leads up to the main range of the Southern Alps.

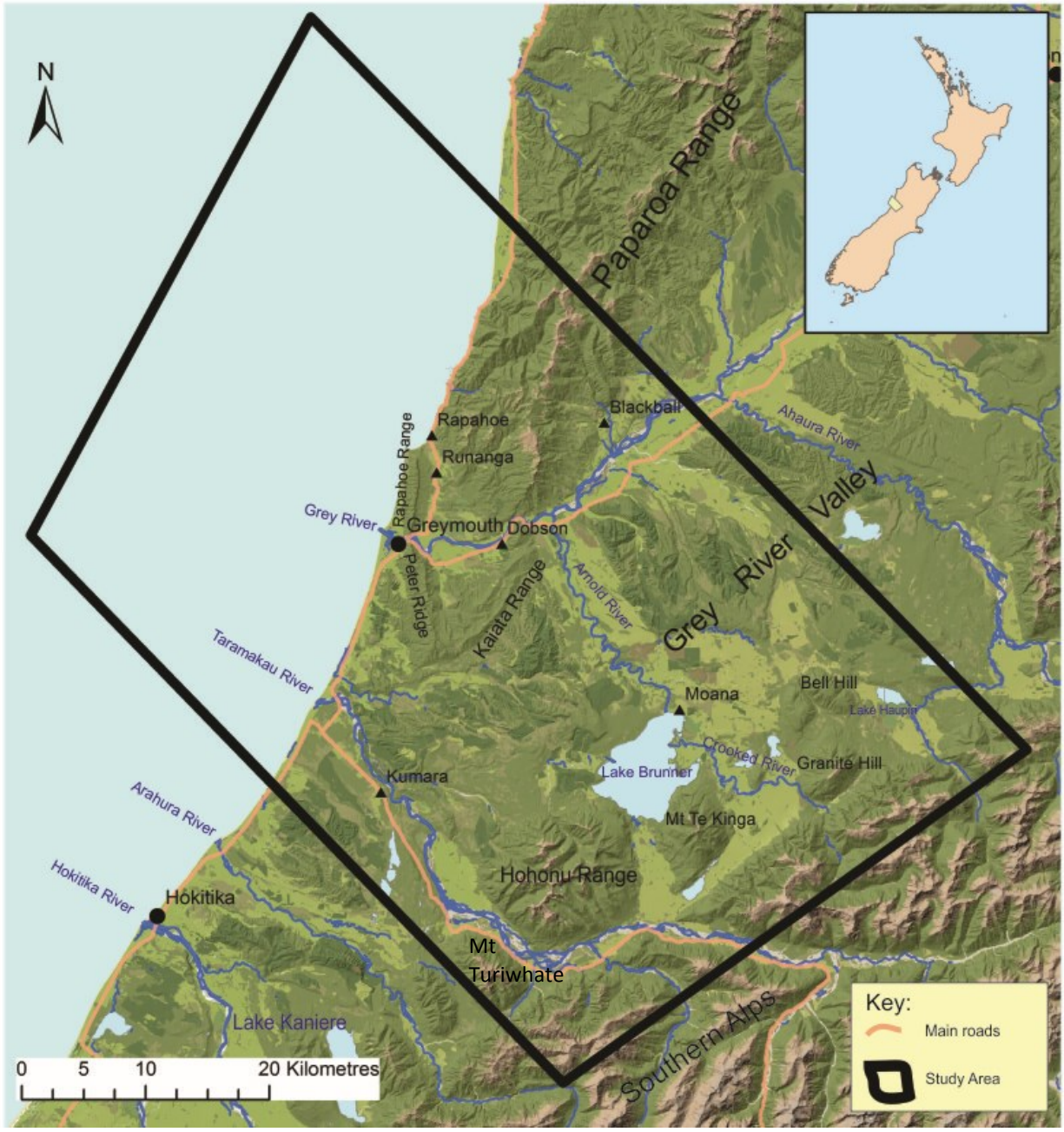

Figure 2-1: Physiography and extent of study area.

2.3 Generalised stratigraphy of the study area

The stratigraphy of the study area can be simplified into a transgressive sequence lasting from the Cretaceous through to the Oligocene followed by a regressive sequence in the Neogene. Although no one location in the basin contains the full sequence of stratigraphic units, collectively, the study area as a whole has a close to complete sedimentation record stretching back to the Late

Cretaceous. Figure 2-2 summarizes the stratigraphy of the study area and Figure 2-3 shows the surface geology. Following is a summary of the main stratigraphic units in the study area. The Neogene sediments will be described in most detail as these provide information of the tectonic development during that time; a principal focus in this study. Most information, unless otherwise specified is taken from Suggate and Waight (1999):

2.3.1 Basement rocks

In the study area, the basement rock west of the Alpine Fault, into which Palaeozoic and Mesozoic igneous rocks have intruded, and Cretaceous to Recent sediments have overlain, are variably metamorphosed siliciclastic sandstones and mudstones of the Greenland Group. Greenland Group makes up most of the Buller Terrane; one of the terranes of the Western Province of New Zealand, and before Cretaceous continental break up, the closest to the interior of Gondwana (Mortimer, 2004). The Greenland Group is composed of a thick succession of interbedded argillite and greywacke that are interpreted to have been deposited as turbidites on a proximal submarine fan off the continental margin of Gondwana during the Ordovician (Laird and Shelley, 1974). Few estimates have been made as to the overall thickness of the Greenland Group, with Laird (1988)

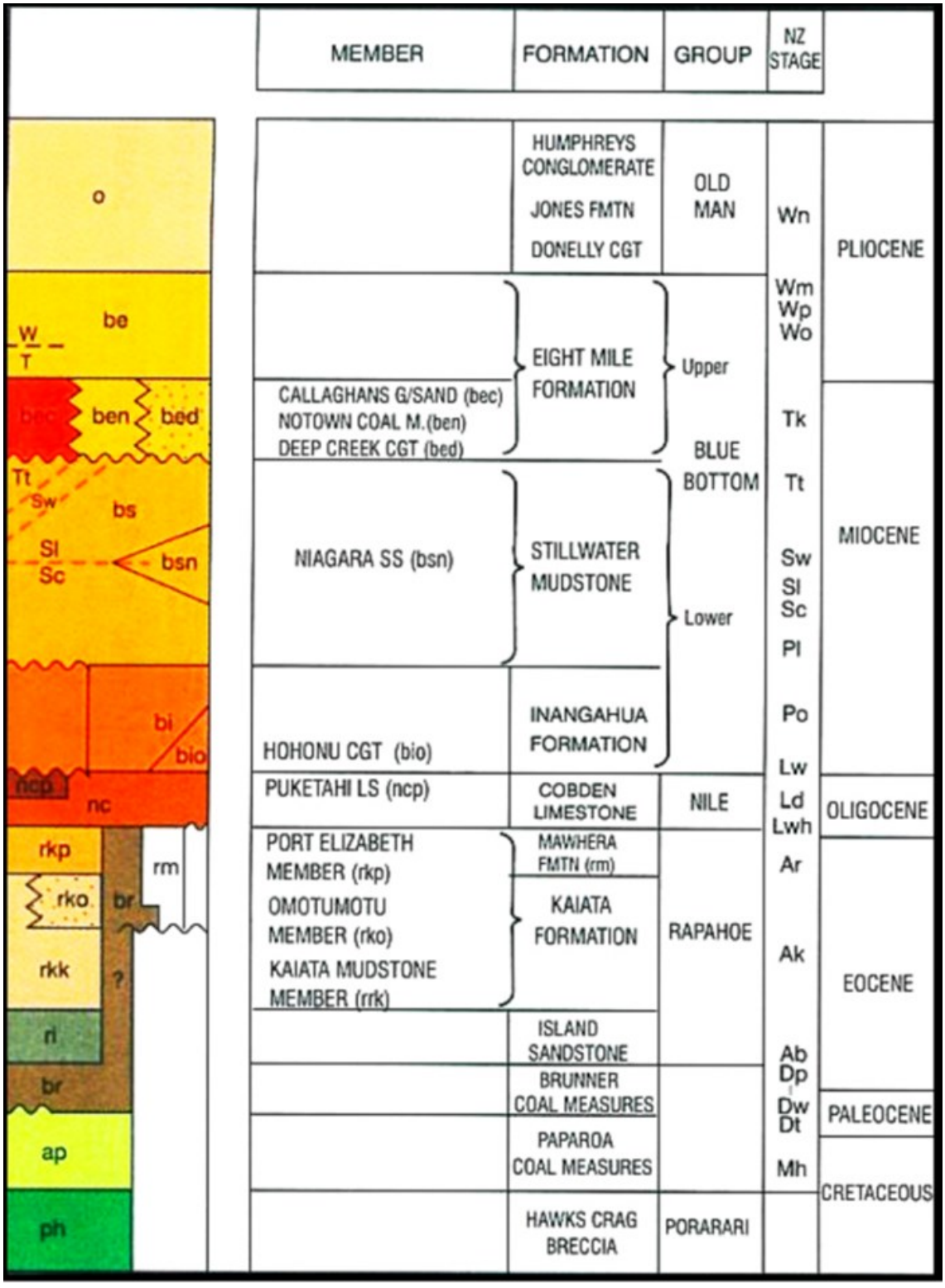

Figure 2-2: Generalised stratigraphy for the study area (From Suggate and Waight, 1999).

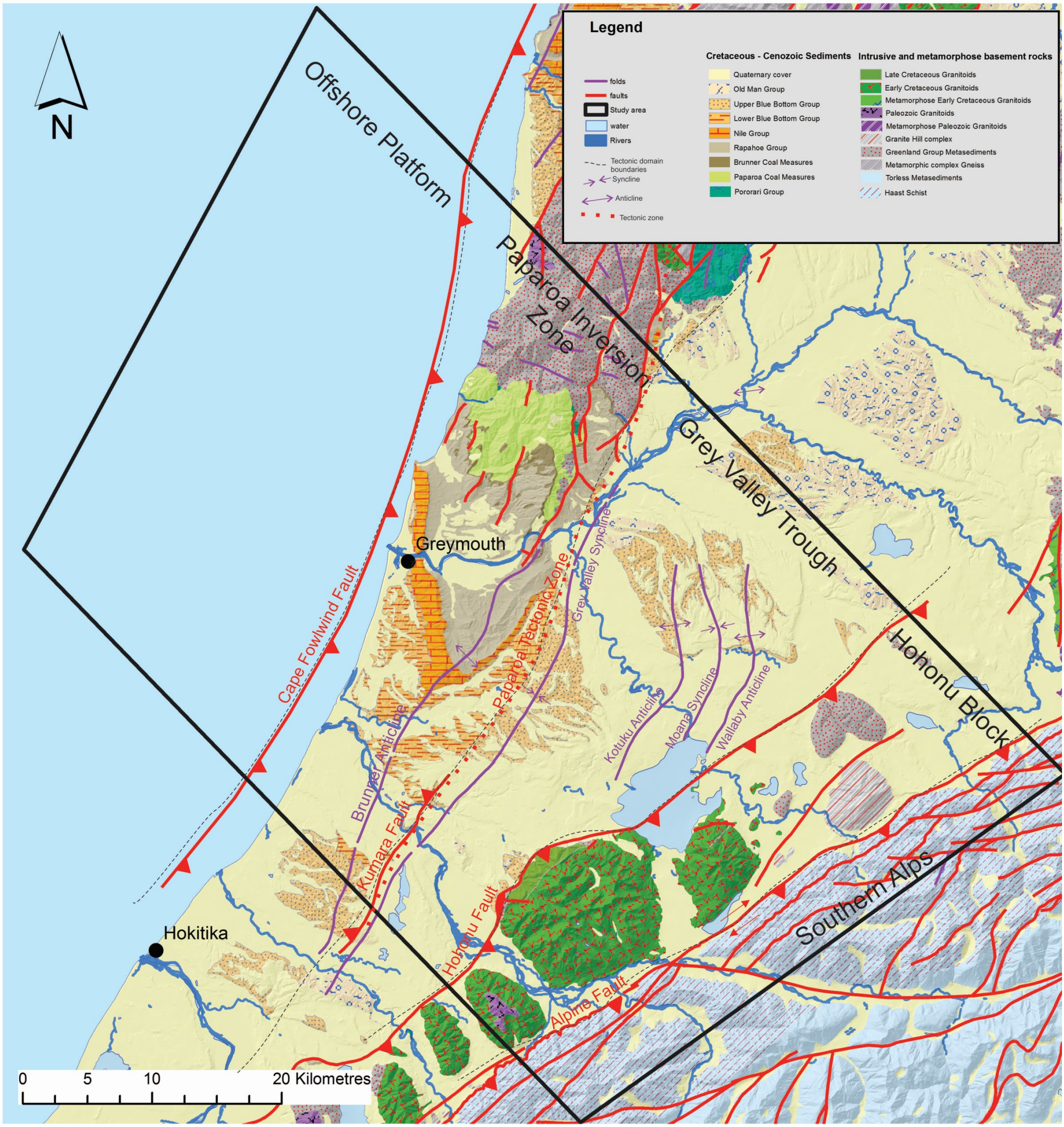

Figure 2-1: Geological map of study area. Showing surface geology from the Greymouth Qmap (Nathan et al, 2002), tectonic domains and major structural elements. Fold axes are those shown on the Kumara-Moana Geological Map (Suggate and Waight, 1999)

indicating a thickness “considerably greater than the 1600 m minimum”. Most Greenland Group outcrops show low grade, chlorite-zone metamorphism that has been dated as Late Ordivician to Early Silurian (Adams 2004). This metamorphism and deformation is the cause of the penetrative cleavage which exists in most outcrops, and the folding of bedding which ranges from open to isoclinal.

In all wells drilled deep enough in the study area, the rock directly underlying the basement unconformity is Greenland Group. However, Palaeozoic and Mesozoic granitoids comprise the basement of some wells drilled to the north of the study area (cf. Ghisetti et al., 2014), outcrop extensively across the Hohonu Block (see Figure 2-3), and large areas of the northwest South Island in general. The granitoid plutons that comprise the bulk of the Hohonu Range, Mt Te Kinga and Mt Turiwhate were emplaced between 114 and 109 Ma. Granitoids that intruded during this episode have been mapped by Waight (1995) and include (from oldest to youngest) Uncle Bay Tonalite; Deutgam Granodiorite; Pah Point Granite; Jays Creek Granodiorite; and Te Kinga Monzogranite. The A-type French Creek Granite intruded in a separate episode of magmatism at c.82 Ma and outcrops in an isolated band across the northwest margin of the Hohonu Range. Mafic dykes of the Hohonu Dyke Swarm which cut across the older granitoids of the Hohonu Range and Mt Te Kinga are also associated with the same c.82 Ma magmatic episode (Waight et al., 1998b).

Other basement rocks that outcrop in relatively small areas west of the Alpine Fault (see Figure 2-3) include: the Granite Hill Complex which is interpreted as belt of mid crustal, amphibolite facies rocks that have been uplifted adjacent to the Alpine Fault (see Kamp et al., 1992) and have Buller Terrane affinity (Heiss et al., 2010); and small areas of Devonian granitoids.

To the east of the Alpine Fault, the basement is biotite to garnet zone Haast Schist. This is a relatively highly metamorphic part of the Torlesse Composite Terrane which is Triassic in age (Nathan et al, 2002).

2.3.2 Hawks Crag Breccia, Pororari Group

These are terrestrial deposits that are typically late Early Cretaceous in age and were deposited in half-graben basins adjacent to rapidly uplifting ranges (Laird, 1988). The Hawks Crag Breccia is typically massive, angular, poorly sorted Greenland Group or Granite derived conglomerate and breccia, and is usually distinguished by being orange-red in colour (Suggate and Waight, 1999). Small outcrops occur across the southern end of the Paparoa Range. Some boreholes (e.g. Taramakau -1) in the Paparoa Inversion Zone have intersected thin successions (< 100 m thick) of breccias attributed to the Pororari Group. The general thickness which reaches >1000 m elsewhere

in the North Westland region, is not known across most of the study area (Suggate and Waight, 1999).

2.3.3 Paparoa Coal Measures

The Paparoa Coal Measures consist of fluvial and lacustrine deposits that range from uppermost Cretaceous to Paleocene in age. This unit typically consists of relatively minor lacustrine mudstones with large amounts of sandstone with coal interbeds. In the Greymouth Coalfield, the Paparoa Coal Measures have been divided into 7 members, 4 being predominantly terrestrially deposited, with 3 intervening members deposited in lacustrine environments. In stratigraphic order from base to top these are; Jay Coal Measures Member; Ford Mudstone Member; Morgan Coal Measures Member; Waiomo Mudstone Member; Rewanui Coal Measures Member; Goldlight Mudstone Member; and Dunollie Coal Measures Member. In the Greymouth Coalfield, the Jay Coal Measures Member appears to lie conformably upon the Hawks Crag Breccia. Conglomerates are common in the lower coal measures members. In the Greymouth Coalfield, there is a >500 m thick volcaniclastic pile within the Morgan Member. This has been linked with Basaltic volcanism observed at Mt Camelback, in the Arahura-1 well and in the Greymouth and Pike Coalfields which has been collectively dated at c. 68 Ma (Laird, 1993; Suggate and Waight, 1999). The formation was deposited across a broad floodplain with lake-filled basins. This setting has been related to deposition coeval with extensional faulting (Bowman, 1984). This formation outcrops in a broad area across the southern end of the Paparoa Range. The formation is thought to have been deposited throughout the study area. In some places it has been removed by erosion as is evidenced by coal pebbles within the younger Rapahoe Group sediments that are able to be assigned through palynology to the Paparoa Coal Measures. The formation still exists in large areas across the Paparoa Inversion Zone and the middle northern part of the Grey Valley Trough. In both of these areas, the thickness of the formation reaches 800 m thick (Suggate and Waight, 1999).

2.3.4 Brunner Coal Measures

The Brunner Coal Measures were deposited in coastal flood plain and fluvial environment. They consist of predominantly quartzose grit and sandstones that are sourced from deeply weathered material with a low erosion rate (Gage, 1952). Occasional carbonaceous shale and coal seams up to 4 m thick are also present. This unit is diachronous, with ages of Early Eocene in the Paparoa Inversion Zone, and Late Eocene up to earliest Oligocene in the Grey Valley Trough. This formation outcrops across the southern end of the Paparoa Range where it is typically <100 m thick. Boreholes (e.g. Taramakau–1, Card Creek-1 and Kumara-2) show it to be present in thicknesses no greater than 200 m across almost all of the Paparoa Inversion Zone. In the Grey

Valley Trough, the presence of the Brunner Coal Measures is sparse with it only occasionally being present in boreholes and in thicknesses of 22 m or less (Suggate and Waight, 1999).

2.3.5 Rapahoe Group

The Rapahoe Group was deposited in an inner shelf to upper bathyal environment (Suggate and Waight, 1999). In the Paparoa Inversion Zone, the Rapahoe Group consists of predominantly marine mudstones (Kaiata Mudstone Member and Port Elizabeth Member) with minor sandstone and conglomerate at the base (Island Sandstone) and in the middle of the unit, (Omotumotu member) and is late Middle Eocene to earliest Oligocene in age. The Paparoa Inversion Zone was the main locus of deposition for the group with thicknesses ranging from around 500 m in the south to over 2 km at the southern end of the Paparoa Range. Here, the group extends in age from late Middle Eocene to Early Oligocene. In the Grey Valley Trough, the Rapahoe Group is represented in a small area close to the crest of the Kotuku Anticline by the < 150 m thick Mawhera Formation. This conglomerate, sandstone and siltstone unit is Late Eocene in age and was deposited in a near-shore marine environment (Suggate and Waight, 1999).

2.3.6 Nile Group

The Nile Group consists of predominantly limestone, Early to Late Oligocene in age that was deposited almost everywhere across the study area. The limestone is generally hard, crystalline and white but is in parts muddy, contains glauconitic bands, sometimes sandy, and occasionally pink coloured. In the Paparoa Inversion Zone, the limestone is typically between 100 and 400 m thick and was deposited in an outer shelf to upper bathyal environment. This contrasts with the Grey Valley Trough where the limestone is <80 m thick and was deposited in an inner shelf environment (Suggate and Waight, 1999).

2.3.7 Blue Bottom Group

The Blue Bottom Group consists of marine mudstones and sandstones with minor near-shore conglomerate that are Miocene to Late Pliocene in age. This group was deposited across most of the study area, although in many locations the upper portion of the unit has been removed by Late Pliocene and Quaternary erosion. Differing degrees of basin subsidence across the study area have resulted in the thickness of the group varying widely across the study area with it being only c. 100 m on the crest of the Kotuku Anticline to >5000 m in the Grey Valley Trough directly west of the Hohonu Range. Differing degrees of subsidence are also reflected in depositional depths with wells drilled close to the northern margin of the Hohonu Range (eg. Hohonu-1, Niagara-1 and Niagara-2) showing middle to lower bathyal environments during the deposition of the lower Blue Bottom (Inangahua Formation and Stillwater Mudstone) during Early and Middle Miocene, other

areas ranged up to outer shelf environments for the same period (Spanninga, 1993). The lower Blue Bottom is predominantly mudstone that is typically brown to brown-grey with some sandstone and limestone layers near the base (Inangahua Formation), and a uniform, massive blue-grey in the upper portion (Stillwater Mudstone). A significant unconformity is present within the Blue Bottom Group that occurred during the Late Miocene. In the Paparoa Inversion Zone, this unconformity is overlain by a layer of greensands 10-15 m thick (Callaghans Greensand). This contrasts with the Grey Valley Trough, where the unconformity is overlain by a unit of interbedded pebble conglomerate and sandstone which in some places contains thin coal seams (the Deep Creek Conglomerate and Notown Coal Measures). Above these basal members that overlie the Late Miocene unconformity, the muddy sandstones of the greater part of the Eight Mile Formation were deposited. Towards the top of the Blue Bottom Group, bands of conglomerate become increasingly common, marking the change in depositional environment to coastal and towards terrestrial (Suggate and Waight, 1999).

2.3.8 Old Man Group

The Old Man Group is a unit of terrestrial gravels that were deposited prior to and during the early Pleistocene glaciations. It consists predominantly of gravels with rounded clasts that are composed mostly of greywacke, with some granites and rare schist. The unit also contains some layers of sand, silt, clay and lignite up to 4 m thick. This unit is nowhere more than 500 m thick and has been either eroded or covered with Quaternary sediment over most of the study area. Outcrops of the Old Man Group are present in the northern and southern parts of the axis of the Grey Valley Syncline (Suggate and Waight, 1999).

2.3.9 Quaternary fluvial and glacial deposits

An unconformity representing at least 1.5 million years separates the youngest Old Man Group gravels from the oldest of the Quaternary deposits (less than 500 ka). The Quaternary sediments consist of fluvial, glacial, lacustrine and coastal marine deposits primarily derived from greywacke eroded from the uplifting Southern Alps, with relatively minor amounts of granite, schist, and basic volcanic rocks (Suggate and Waight, 1999).

2.4 Local tectonic setting

In a broad sense the study area can be divided into five north to northwest trending tectonic domains (See figure 2.2), with each separated from the next by a fault controlled boundary. These domains are named here, starting from the eastern side of the study area as: the Southern Alps; the Hohonu Block; the Grey Valley Trough; the Paparoa Inversion Zone; and the Offshore Platform. Nathan (1978b) provides a similar scheme for the structural layout of the study area. Below is a description of each of the tectonic domains and their bounding structures, progressing from east to

west across the study area. The fault controlled boundaries between each of the tectonic domains will be described between the ones they separate.

2.4.1 Southern Alps

Starting at the Eastern side of the study area, this domain is predominantly comprised of Haast Schist, which outcrops along the western edge of the Southern Alps. Fission track analysis shows that over 15km of uplift has occurred in this section of the study area since the early Neogene with greatest amount of exhumation has occurred adjacent to the Alpine Fault (Tippet and Kamp, 1993).

2.4.2 Alpine Fault

The Alpine Fault is a crustal scale, east dipping dextral-reverse fault marks the eastern boundary to the Hohonu block, the second tectonic domain to the west and is generally considered to be the principal feature that defines the plate boundary in the South Island. It is a c. 800 km long continuous dextral transform which links subduction zones of opposite polarity (Pacific Plate subducting to the north and Australian Plate subducting to the south). The offset of basement rocks suggests that about 460 km of dextral displacement has occurred across the fault over the past 45 Ma (Sutherland et al., 2000) of during the Neogene (Nathan et al., 2002). Satellite photographs (from Google Earth) and geological maps (e.g. Nathan et al., 2002) show that between latitudes 42.5°S and 44.5ºS, the Alpine Fault is remarkably straight, striking at 055°. This fault is commonly referred to as the boundary between the Pacific and Australia plates, taking up 60-80% of the lateral motion with an average slip rate of 25-30 mm per year in the last 5 Ma (Norris and Cooper, 2001). Seismic refection imaging of the fault at depth shows the Alpine Fault to dip southeast at c. 50° to depths of around 25 km (Davey et al., 1995).

2.4.3 Hohonu Block

In the Hohonu Block, basement gneisses, Cretaceous granitoids and Greenland Group metasediments have been uplifted as part of what has been considered simply as a frontal thrust block infront of the Alpine Fault (Kamp et al. 1992, Batt et al, 2004). The Granite Hill Fault is a poorly exposed fault that is thought to be another range-front thrust within the Hohonu block. Like the Fraser Fault further south (cf. Kimbrough et al, 1994), the Granite Hill Fault brings gneissic rocks from deeper levels in the crust to the surface (Nathan et al., 2002). Further west in the Hohonu Block, other faults have been mapped by Waight (1995) but the timing and tectonic context of these is poorly understood. The Rocky Creek Fault is one example, and strikes east-west across the Northern side of Mt Te Kinga.

2.4.4 Hohonu Fault

The east dipping Hohonu thrust fault marks the boundary between the Hohonu Block and the Grey Valley Trough. This is a fault that has been active during the Neogene, but it is not fully understood whether it was continuously active for this whole period, or if there was a particular phase during which the majority of fault movement occurred. One outcrop of the fault in the Hohonu River has been used to indicate that the fault is shallowly dipping to the east at 30° (Nathan 1978b, Wellman, 1950). The basin-bounding Hohonu Fault appears to vary considerably in the amount of offset that has occurred across it during the Neogene. In the southern part, adjacent to the Hohonu Range, the high topography (>1000m) in the hanging wall and seismic interpretation (c.f Haskell, 2009) of the footwall suggests that greater than 7km of vertical offset has occurred. In the northern part around Bell Hill, the fault's exact position and offset is less well known due to the large amount of Quaternary sediment covering the fault zone. Relatively subdued topography in the hanging wall and limited seismic interpretation in the footwall by Matthews (1990), suggests that vertical offset may be as little as 1km. Taken as a straight line between the points where it is mapped west of Lake Kaniere to where it is mapped west of Bell Hill, the Hohonu Fault strikes close to parallel with the Alpine Fault, but more locally, the strike of the Hohonu Fault is highly variable, especially adjacent to the Hohonu Range. Here, it can vary from striking east-west on the northern side of the Hohonu Range to NNW-SSE on the western side of the range (almost orthogonal to the Alpine Fault). Coupled with the highly variable strike adjacent to the Hohonu Range, it is also the part of the fault where the surface trace is most clearly defined topographically. Deep seated glacial erosion and lower rates of movement elsewhere on the fault are possible reasons for it being harder to define.

2.4.5 Grey Valley Trough

The Grey Valley Trough is the third tectonic domain to the west and comprises a sedimentary basin that is infilled by mostly Neogene sediments. The thickness of Neogene sediment is inconsistent across the basin and can range from c. 200 m to over 5 km thick. Subsurface geometry (Nathan et al., 1986; Matthews, 1990; Buchan, 1997; Suggate and Waight, 1999) suggests that fault bounded basement blocks were initially in a half-graben configuration, inherited from Late Cretaceous to Paleogene extensional faulting. After Neogene infilling and inversion of the adjacent Paparoa and Hohonu blocks, shortening has modified the geometry of the trough by creating a series of anticlines and synclines. The most important of these is the Grey Valley Syncline, Kotuku Anticline and Moana Syncline which all tend to trend between N-S and NE-SW (see Figure 2-3). All three of these folds are east-verging. This is seen in the asymmetric nature of the synclines, which both have a much steeper western limb (dipping between 50° and 90º to the east) than the eastern limb (dipping 5° to 10º to the west). The structure between the axis of the Moana Syncline

and the Hohonu Fault is less well constrained. Matthews (1990) marks two NNE-SSW striking, west dipping thrust faults with basement remaining close to c. 1km below sea level. Due to the scarcity and poor quality of seismic profiles in this area, these interpretations must be treated with caution. Suggate and Waight (1999) have inferred the presence of another anticline, the Wallaby Anticline in this area, but likewise, they have accepted that the scarcity of data in this location means that this interpretation is difficult to constrain. The southern part of the Grey Valley Trough is much narrower (only c. 10km) than the northern part and is bounded by two large thrust faults – the Kumara Fault and the Hohonu Fault. Here, seismic interpretation suggests that basement has subsided right across the trough to c. 4.5 - 5.5 km below sea level (Haskell, 2009). It is poorly understood why the Grey Valley Trough becomes deeper and narrower to the south.

2.4.6 Kumara Fault / Paparoa Tectonic Zone

A large NNE-SSW striking, west dipping inverted normal fault within the basement marks the boundary between the Grey Valley Trough and Paparoa Inversion Zone. The separation on this fault is expressed near the surface by the re-orientation of Cenozoic sediments to dip between 50° and 90º to the east, and in the south of the study area, the propagation of the fault to the surface (where it is named the Kumara Fault). Laird (1968) described this fault zone as part of the Paparoa Tectonic Zone, a NNE-SSW trending faulted lineament along which Eocene and Oligocene normal faults have been inverted to become reverse faults in the Neogene.

2.4.7 Paparoa Inversion Zone

The Paparoa Inversion Zone is the fourth tectonic domain heading west. The Paparoa Inversion Zone is named as such due to its history as a NNE-SSW trending trough that developed under extensional tectonic episodes in the Late Cretaceous and Paleogene, which was subsequently inverted to form a basement high during the compressional tectonic episode of the Neogene (Wellman, 1949). The southward younging of the outcropping Cretaceous-Neogene sequence (Nathan et al., 2002) shows that as a whole, the Paparoa Inversion Zone plunges to the south.

2.4.8 Cape Foulwind Fault

The Cape Foulwind Fault runs sub parallel to the coast of the study area, around 5km offshore. It is a NNE striking reverse fault that dips to the east at c. 50-60° and has a vertical separation of the top basement unconformity of that varies from c. 250 m to up to 3400 m along strike from north to south (Ghisetti et al., 2014, Bishop, 1992a). In the broader region, this fault continues adjacent to the coast south towards Ross, and north toward Westport for a length of around 180km (Ghisetti et al., 2014). It is likely that the position of the present coastline is controlled by activity on this fault (Suggate, 1987).

2.4.9 Offshore Platform

The outermost tectonic domain, on the western margin of the study area is that of the offshore platform. The good coverage of seismic profiles (Figure 4-5) show that as a whole the area is relatively stable and undeformed (Bishop, 1992a). However, as with the Grey Valley Trough and Paparoa Inversion Zone, there is a contrast between the northern and southern parts of the tectonic domain. To the north, a number of small c. NNE-SSW trending thrust faults penetrate the basement unconformity and gently fold the overlying Paleogene and Neogene sediments. To the south there is large ESE-WNW trending half graben structure (Takutai Half Graben) underlying the Paleogene and Neogene sediments interpreted as being Late Cretaceous in age (Bishop, 1992b). The Paleogene and Neogene sediments that overlie this feature are gently down-warped. It is uncertain whether this down-warping is due to re-activation of the normal faults that control the structure, simply greater compaction of the graben infill compared to the surrounding basement, or both of these.

2.5 Review of the geo-tectonic evolution of the study area

2.5.1 Pre-Cretaceous basement formation

As described in section 2.3.1, the Greenland Group was deposited on the Gondwana margin and subsequently underwent chlorite –zone metamorphism during the Ordovician. This metamorphic episode was the start of an extended period stretching through the rest of the Palaeozoic, and into the late Mesozoic where the Greenland Group rocks were part of the edge of the Gondwana supercontinent. Other than the intrusion of granitoids during the Late Devonian and Carboniferous Tuhua Orogeny, very little tectonic activity appears to have affected the Greenland group rocks during this time.

2.5.2 Cretaceous NNE-SSW directed extension

A significant change occurred to the tectonic regime of the Gondwana margin around 105±5 Ma where convergent margin tectonics ceased, giving way to extensional tectonics within the Western Province. The likely cause for this change was the collision of an oceanic spreading ridge with the subduction margin (Bradshaw, 1989). The NNE-SSW directed crustal extension that began at this point in time, continued for c. 30Ma before culminating in the opening of the Tasman Sea.

The initial effect of the change of tectonic regime in the study area was the intrusion of the Hohonu Suite Granitoids between 114 and 109 Ma. These granitoid rocks are what makes up the majority of basement outcrop across the Hohonu Range and Mt Te Kinga. These late Early

Cretaceous plutons are likely to have been generated during adiabatic melting of the lower crust and underlying mantle during isothermal uplift and thinning of the previously over-thickened continental crust (Waight et al, 1998a).

Another product of the change in tectonic regime was the development of the Paparoa Metamorphic Core Complex (PMCC) described by Tulloch and Kimbrough (1989). The core complex is a feature of extending continental crust where high-grade metamorphic and granitic mid-lower crustal rocks (lower plate) have been exhumed along low-angle detachment faults to become juxtaposed against low grade upper crustal rocks (upper plate). Secondary to the main detachment faults, steeper normal faults form in the upper plate creating domino-like blocks and forming half-graben basins at the surface. Although their overall form is poorly preserved in the PMCC, these basins appear to have a WNW-ESE trend which suggests a NNE – SSW axis of extension (Tulloch and Kimbrough, 1989).

Given the extensive presence of the low-grade Greenland Group rocks, most of the basement outcropping or drilled in the study area is part of the upper plate of the core complex. Directly to the north of the study area in the Paparoa Range, the Pike Detachment Fault juxtaposes the high-grade Charleston Gneiss of the lower plate against Greenland Group and contemporaneous half-graben fill, the Pororari Group, of the upper plate. It is likely that a continuation of the low-angle, south-dipping Pike Detachment Fault extends beneath the study area. Evidence for this can be seen with the sporadic presence of the contemporaneous Pororari Group at the northern margin of the Greymouth coalfield, within the Taramakau-1 well (see Figure 4-3 for location) and outcrops in the Gentle Annie area and Mt Camelback to the south of the field area (Nathan et al., 2002). Further evidence of a southward-extending detachment fault can be seen with the presence of the high grade metamorphic Granite Hill and Fraser complexes directly west of the Alpine Fault trace. These are interpreted to be lower plate rocks and the detachment that separates them from the upper plate has been re-oriented and over-thrust through movement along the Alpine Fault during the Neogene (Kimbrough et al 1994, Waight 1995).

The detachment faults of the PMCC are thought to have been active well into the Late Cretaceous (Tulloch and Kimbrough, 1989). This appears to have been part of a continuous thinning of the crust throughout the Westland region that culminated in lithospheric failure and the opening of the Tasman Sea at c. 82 Ma (Weissel et al., 1977). The contemporaneous French Creek Granite and Hohonu Dyke Swarm present in the Hohonu range provide evidence for extension to near-failure of the continental crust within the study area at a time almost exactly coinciding with the opening of the Tasman Sea (Waight et al., 1998b). The French Creek Granite is an A-type granite that cooled from a highly fractionated, asthenosphere-sourced magma. The Hohonu Dyke Swarm is

predominantly made up of lamprophyre and dolerite dykes that are possibly from the same source magma as the French Creek Granite, but it is not so highly evolved (Waight et al, 1998b). Both of these are indicative of a continental rift setting. The preferred orientation of the dykes in the Hohonu Dyke Swarm is WNW-ESE (Waight, 1995). This indicates that extension was still occurring in a NNE - SSW direction at the point of continental breakup. This is backed up by Al-hornblende geobarometry of the 82 Ma French Creek Granite by Waight (1995), suggests it was emplaced at c. 1 kb or about 3 km depth. This method was also used for the late Early Cretaceous granitoids and were found to be emplaced at c. 4 kb or about 12 km depth (i.e. about 9 km of exhumation appears to have occurred in the intervening time). This is consistent with the development of a core complex where upper crustal blocks are tilted and lower crustal material is brought to the surface along detachment faults.

Bishop (1992b) identified a WNW-ESE trending half-graben structure between the base-Miocene and top basement horizons in the seismic grid offshore Greymouth. This structure has been interpreted to have formed during the NNE-SSW directed extension regime between 110 and 80 Ma.

2.5.3 Late Cretaceous-Paleocene coal measures deposition

Seafloor spreading continued in the Tasman Sea until gradually stopping at c. 52 Ma (Weissel et al, 1977). Within the field area, the start of the opening of the Tasman Sea is marked by the beginning of deposition of the Paparoa Coal Measures. During their deposition that extends through to the Early Paleocene, the Paparoa Coal Measures record a number of significant changes in palaeo-environment that are likely to be tectonically controlled. In the Greymouth Coalfield area, the apparent lack of an unconformity between the Hawks Crag Breccia and lowest member of the Paparoa Coal Measures (Jay Member) indicates that there was apparently continuous sedimentation through the time of continental break up between New Zealand and Gondwana. As shown in Figure 2-4, deposition of the Jay, and the overlying Ford member show a distinctive WNW-ESE depositional trend in borehole-derived isopach maps (Gage, 1952, Bowman, 1984). The WNW-ESE striking basin-bounding faults that are likely to control these depositional trends have been suggested by Laird (1993) to be associated with the opening of the Tasman Sea and remained active during the early phase of sea-floor spreading.

At some stage during the period of seafloor spreading in the Tasman Sea, the New Caledonia Trough is also thought to have opened. Laird (1993) and Thrasher (1990) suggest that a significant NNE-SSW trending sinistral transform fault zone was active through the Westland region, linking the eastern end of the New Caledonia Trough with the main spreading centre of the Tasman Sea. During its development, it appears that extension occurred across the transform fault zone due to

slight changes in Australia-pacific plate motions. Evidence of the onset of extension of the transfer fault system at this point in time is shown in isopach maps of the Morgan and subsequent members of the Paparoa Coal Measures where the depositional trend appears to change to NNE-SSW (Figure 2-4). Basaltic volcanism dated at c. 68 Ma provides further evidence for this extension in the study area (Laird, 1993).

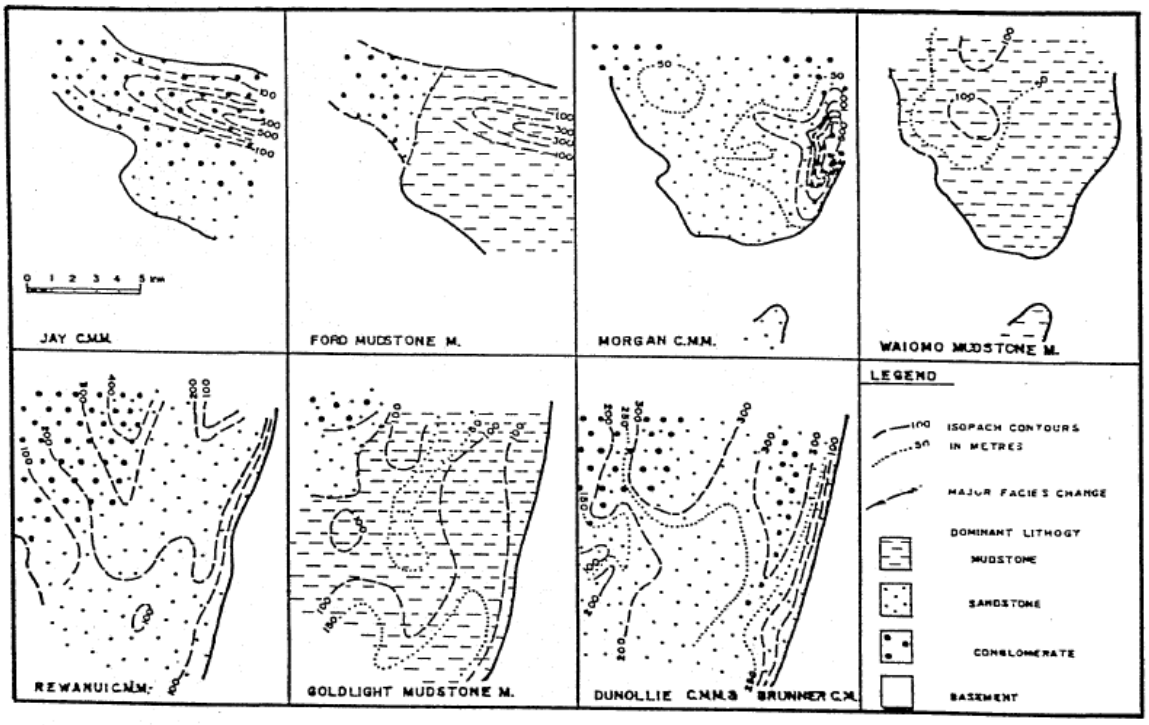

Figure 2-4: Simplified Isopachs for members of the Paparoa Coal Measures, showing broad lithological variations (from Bowman, 1984). All to same scale. Isopachs in metres.

From the Late Paleocene through to the Early Eocene the study area appears to have gone through a phase of tectonic quiescence. The remnant topography eroded down and the crust thermally subsided as a New Zealand-wide marine transgression began to occur. In the study area, this is represented by a paraconformity at the top of the Paparoa Coal Measures and the deposition of the time-transgressive Eocene Brunner Coal Measures above this paraconformity. The Brunner Coal Measures are thought to have been deposited on a coastal plain with sediment input from a maturely weathered source on a low lying landscape (Suggate and Waight, 1999).

In total, the coal measures in the Greymouth Coalfield can range up to over 800 m thick (Newman, 1985). Although the coal measures appear to be thin or not present in a large part of the Grey Valley Trough, Suggate and Waight (1999) suggest that in some places, based on seismic interpretation, they range up to a similar thickness to that in the Greymouth Coalfield and also appear to be structurally controlled by NNE-SSW trending faults.

2.5.4 Eocene – Oligocene Rifting

During the Late Eocene to Early Oligocene, the Challenger Rift System developed along of the western margin of New Zealand (Kamp, 1986). This was likely to be associated with the acceleration of seafloor spreading between Australia and Antarctica and the opening of the Emerald Basin which both began c. 42 Ma (Mutter et al, 1985, Furlong and Kamp, 2013). This occurred concurrently with continuing widespread marine transgression of the New Zealand continent.

In the study area, the formation of the Challenger Rift System is expressed with the onset of WNW-ESE directed extension and the development of the NNE-SSW trending normal faults. The most significant of these was a fault that was located along the eastern side of the present-day Paparoa Inversion Zone. Activity on this normal fault was the primary mechanism by which the Paparoa Trough formed (Nathan, 1978b).

As tectonic subsidence and deposition of marine sediments occurred in the Paparoa Trough during the Eocene and Early Oligocene, it appears that the area now occupied by the Grey Valley Trough acted as a rift-shoulder and remained close to or above sea level. This is indicated by a number of boreholes and outcrops in which thin Cobden Limestone directly overlies basement. The Kaiata Formation of the Paparoa Trough also contains the coarser Omotumotu Member which appears to be derived from eroding coal measures to the east (Suggate and Waight, 1999). A secondary, much smaller basin appears to have been actively subsiding close to the apex of the Kotuku Anticline and is associated with the deposition of the Mawhera Formation (Suggate and Waight, 1999).

2.5.5 Neogene Compression

During the Late Oligocene and Early Miocene, the weak corridor of crust of the Challenger Rift System began to be exploited by a change in plate motions. This involved the inception of a new dextral transform plate boundary across the continent, a structure that was to evolve into the present-day Alpine Fault (King, 2000, Sutherland et al., 2000).

In the study area, this transition is represented stratigraphically by a sudden change from carbonate to clastic sedimentation (Cobden Limestone to Inangahua Formation). Geohistory analysis by Spanninga (1993) and Christie (2007) on the wells drilled in the Grey Valley Trough show that the stratigraphic change was accompanied by a basin wide rapid tectonic subsidence that ranged in magnitude from c. 200 m on the crest of the Kotuku anticline to c. 1 km along the axis of the Grey Valley Syncline and up to 2 km in wells adjacent to the Hohonu Range. This happened at rate much faster than the sedimentary infilling of the basin could keep up with, and the depositional depths of the Inangahua Formation (Figure 2-2) reflect this. On the Paparoa Inversion Zone,

measured sections published by Nathan (1978b) and well completion reports (from www.nzpam.govt.nz) show an unconformity above the Cobden Limestone which typically extends for most of the length of the Early Miocene. The combination of an unconformity in the Paparoa Inversion Zone and rapid increase in depositional depth in the Grey Valley Trough indicates that an early phase of inversion had occurred (Kamp et al, 1999).

By the Middle Miocene, the Stillwater Mudstone (see Figure 2-2) had begun to be deposited at relatively consistent depositional depths across the study area (Suggate and Waight, 1999, Spanninga, 1993). This suggests that the area had become more tectonically quiescent, and a phase of infilling the accommodation space provided by the previous phase of subsidence occurred.

As mentioned in the stratigraphic description of the Blue Bottom Group, there is a significant unconformity present between the Stillwater Mudstone and the overlying Eight Mile Formation (see Figure 2-2). This represents a phase of regional uplift that occurred between 10 and 7 Ma, which was followed by renewed subsidence (Nathan, 1978b). Suggate and Waight (1999) point out that the ages of top of the Stillwater Mudstone generally get older from the east (on top of the Brunner Anticline) towards the west (around the Kotuku Anticline) meaning that more up-warping and erosion had occurred on the eastern side of the study area during the formation of the unconformity. The apparent tectonic activity that produced the Late Miocene unconformity roughly coincides with the timing of a change across the plate boundary where a greatly increased degree of convergence occurred c. 6.4 Ma (Walcott, 1988). A number of workers consider increased convergence and development of a retro-foreland type-setting to have begun on the West Coast region between 10 Ma and 5 Ma (Beaumont et al., 1996, Batt et al., 2004, Kamp et al., 1992, Sircombe and Kamp, 1998). Haast Schist clasts first appear in conglomerates at the base of the Eight Mile Group which indicates that uplift had begun in the Southern Alps around this time (Suggate and Waight, 1999).

As the Southern Alps were rising in the Late Miocene and Pliocene, the Eight Mile Formation infilled a subsiding area that had formed across the Grey Valley Trough and Paparoa Inversion Zone. Further infilling, coupled with regional uplift during the Late Pliocene resulted in a regression and the terrestrial Old Man Group was deposited across a broad alluvial plane (Suggate and Waight, 1999).

Suggate and Waight (1999) suggest that a major phase of uplift has occurred in the Paparoa Inversion Zone since the Old Man Group was deposited (c. 2 Ma - present). This was coupled with initiation of activity on the Kumara Fault. Suggate (1987) provided evidence of Quaternary tectonic activity in the Paparoa Inversion Zone by describing the warping of fluvial terraces across it.

Kamp et al. (1999) presented apatite fission track data for the Greymouth Coalfield which show that three phases of uplift occurred during the Neogene. These occurred at 20-15 Ma, 12-7 Ma and 2 Ma to the present. Each of these phases of uplift is linked to unconformities present across the Paparoa Inversion Zone, and all have been used to summarize the Neogene tectonic development of the study area described above. The 20-15 Ma phase of uplift is associated with the early inversion phase which produced an unconformity across the uplifting Paparoa Inversion Zone and the deposition of the Inangahua Formation in the subsiding Grey Valley Trough. The 12-7 Ma phase of uplift was associated with the development of the widespread Middle-Late Miocene unconformity, probably associated with the beginnings of increased convergence across the plate boundary. The 2 Ma to the present phase of uplift is associated with a renewed phase of inversion resulting from continuing convergence across the plate boundary (Kamp et al., 1999).

CHAPTER 3. FIELDWORK

3.1 Introduction

Fieldwork was undertaken during this study primarily with the aim of gaining data on fault geometry and kinematics, but also to further constrain the relative timing of fault activity and deposition of basin sediments. Figure 3-1 shows the entire field area with the locations of the specific areas visited. Figures 3-2 through to 3-7 are maps of these specific areas and show stereonets of fault data, surface traces of faults observed during fieldwork, and cleavage and bedding plane orientations. The maps are organized into groups showing: (1) deformation across the uplifted basement of the Hohonu Block (figures 3-2, 3-3, and 3-4); (2) environment of deposition and deformation of sediments across the Grey Valley Trough, and Paparoa Inversion Zone (figure 3-5); (3) the Hohonu Fault zone where information on footwall deformation and sedimentation, kinematic and orientation data of the fault plane itself, and deformation of the hanging wall basement rocks have been gathered (figures 3-6 and 3-7).

Specific kinematic data are described in terms of strike, dip and cardinal dip direction of the fault plane, with trend and plunge of striae and a predominant sense of movement if observed being either normal or reverse and/or either dextral or sinistral. If fault planes observed contained striae with a determinable sense of movement (cf. Petit, 1987), these were plotted using faultkin software (produced by R.W. Allmendinger). Faultkin also enables principal stress directions to be determined for a fault zone through linked Bingham analysis of the available kinematic data (cf. Marrett and Allmendinger, 1990, Allmendinger et al, 2012). The orientation planar fabric such as cleavage, foliation and bedding will be described in terms of strike and dip cardinal dip direction. For large groups of plane orientations (eg cleavage or bedding for a section of creek bed), or singular planes that vary in orientation in different sections (such as a fault plane) orientation may be described collectively as follows:

Strike will be given in cardinal (e.g.; N, S, E, W , intercardinal(e.g.; NW, SW etc.) and secondary intercardinal (NNE, WNW etc.) directions, i.e. the 360° of the compass is separated into 16 segments of 22.5° with the cardinal direction name marking the centre of each segment. For example if a cleavage plane was striking north, that means its strike must measure between 348.75° and 011.25°

Dip will be given as one of 5 subdivisions between vertical and horizontal, followed by a cardinal dip direction. These subdivisions are; sub-horizontal, 0-10°; shallowly dipping, 10-35°; moderately dipping, 35-55°; steeply dipping, 55-80°; and sub-vertical 80-90°.

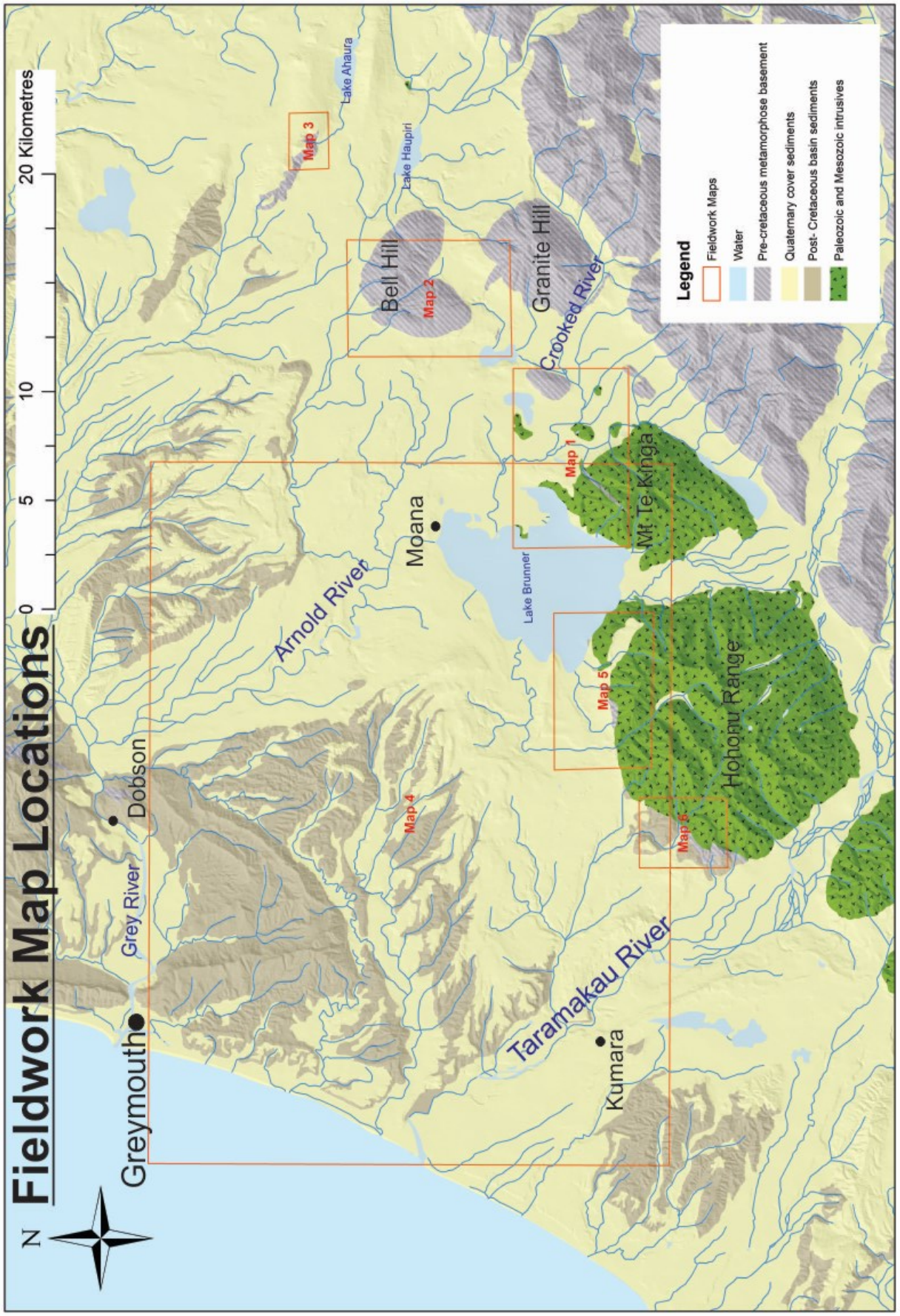

Figure 3-1: Simplified regional geology map showing positions of maps that show detailed geology of areas visited during fieldwork

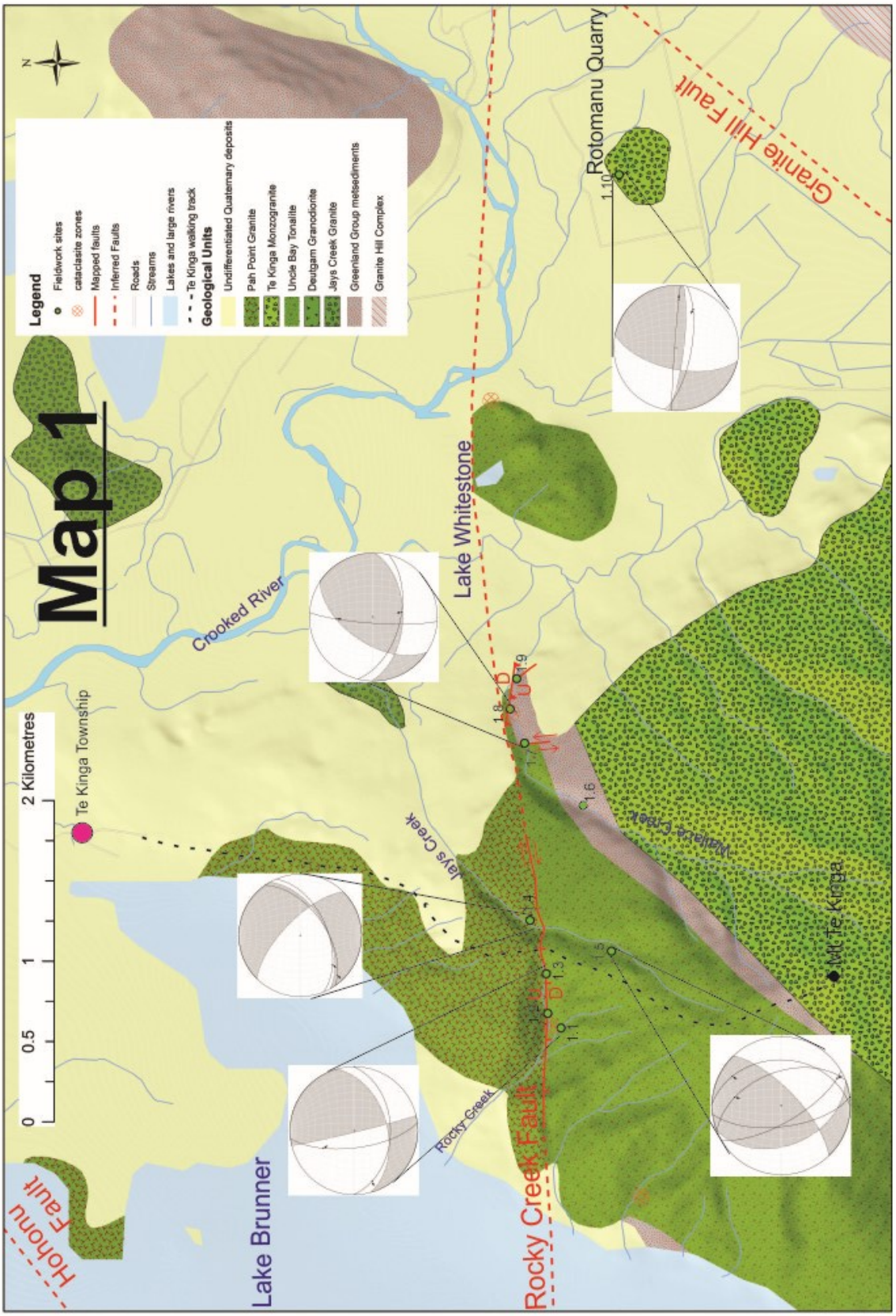

Figure 3-2: Map 1: North Te Kinga

Map 2

N

0 0.5 1 2 Kilometres

Hohonu Fault

Bell Hill Retreat

Jones Creek

Bell Hill

Deep Creek

Cleavage measurements

Gouge zone

Bedding measurements showing fold axis

Cleavage directly above gouge zone

Fault planes

Lady Lake

Sam Creek

Granite Hill Fault

Granite Hill

2m from fault

7m from fault

15m from fault

Key:

- Fault plane
- Hanging wall cleavage planes
- Foot wall cleavage planes
- Average cleavage planes from surrounding area
- Striations on hanging wall cleavage plains

Legend

- Fieldwork sites
- cataclasite zones
- Mapped faults
- Inferred Faults
- Roads
- Streams
- Lakes and large rivers

Geological Units

- Undifferentiated Quaternary deposits
- Greenland Group metsediments
- Granite Hill Complex
- cleavage
- bedding
- fold axis (plunging syncline)

Figure 3-3: Map 2, Bell Hill Area

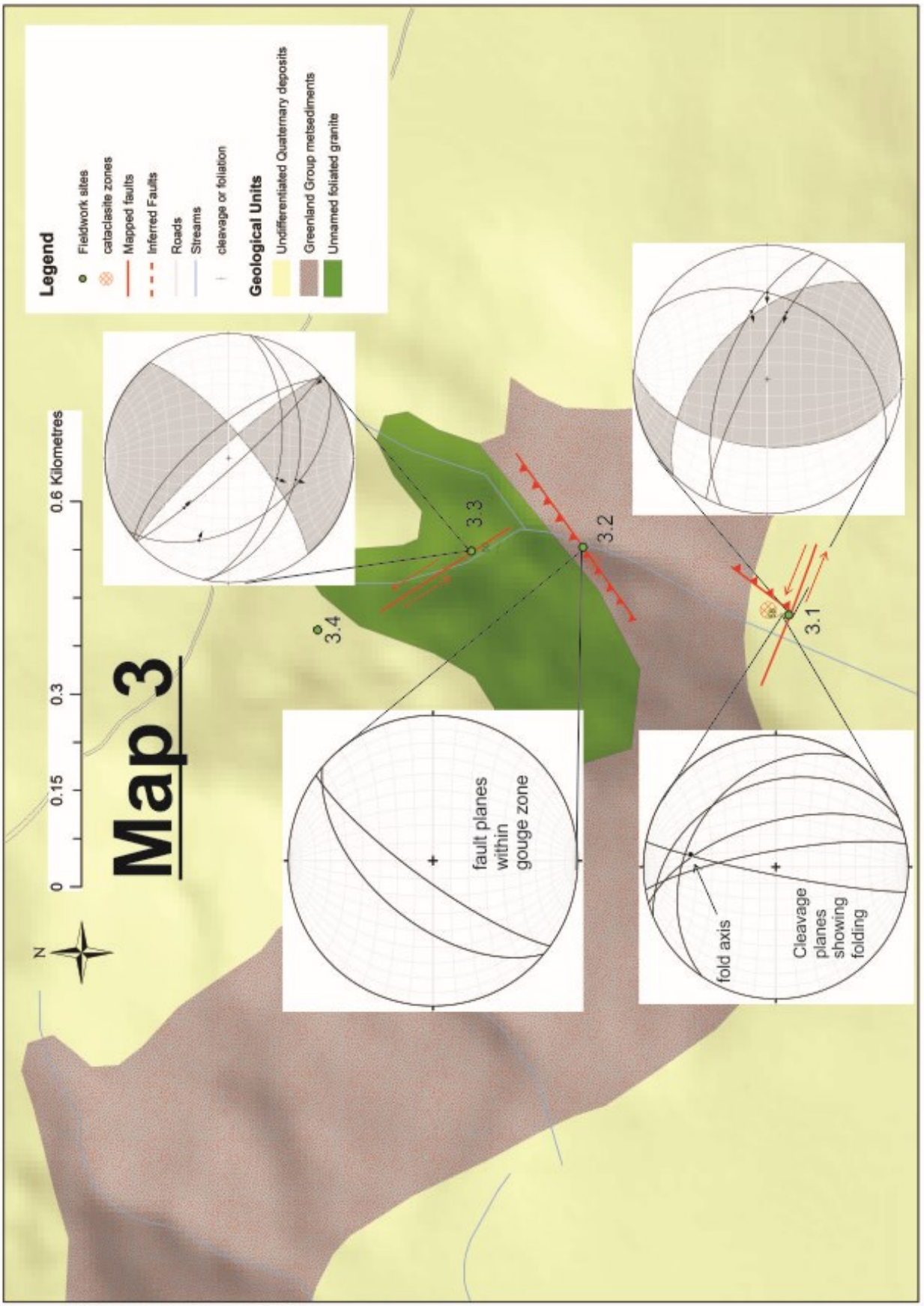

Figure 3-4: Map 3, unnamed hill to the northwest of Lake Ahaura

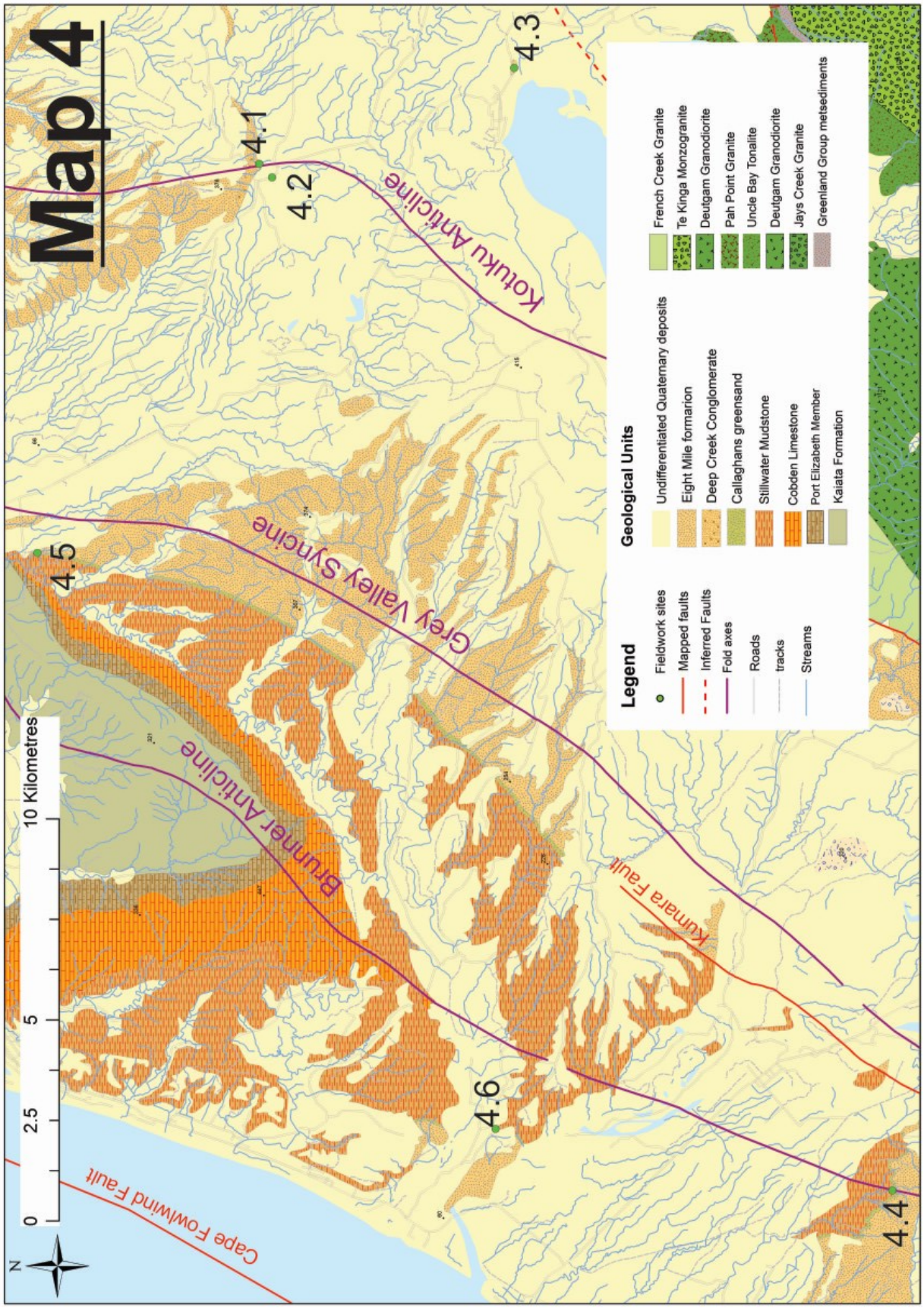

Figure 3-5: Map 4, Stratigraphically significant outcrops across the Paparoa Inversion Zone and Grey Valley Trough visited during this study

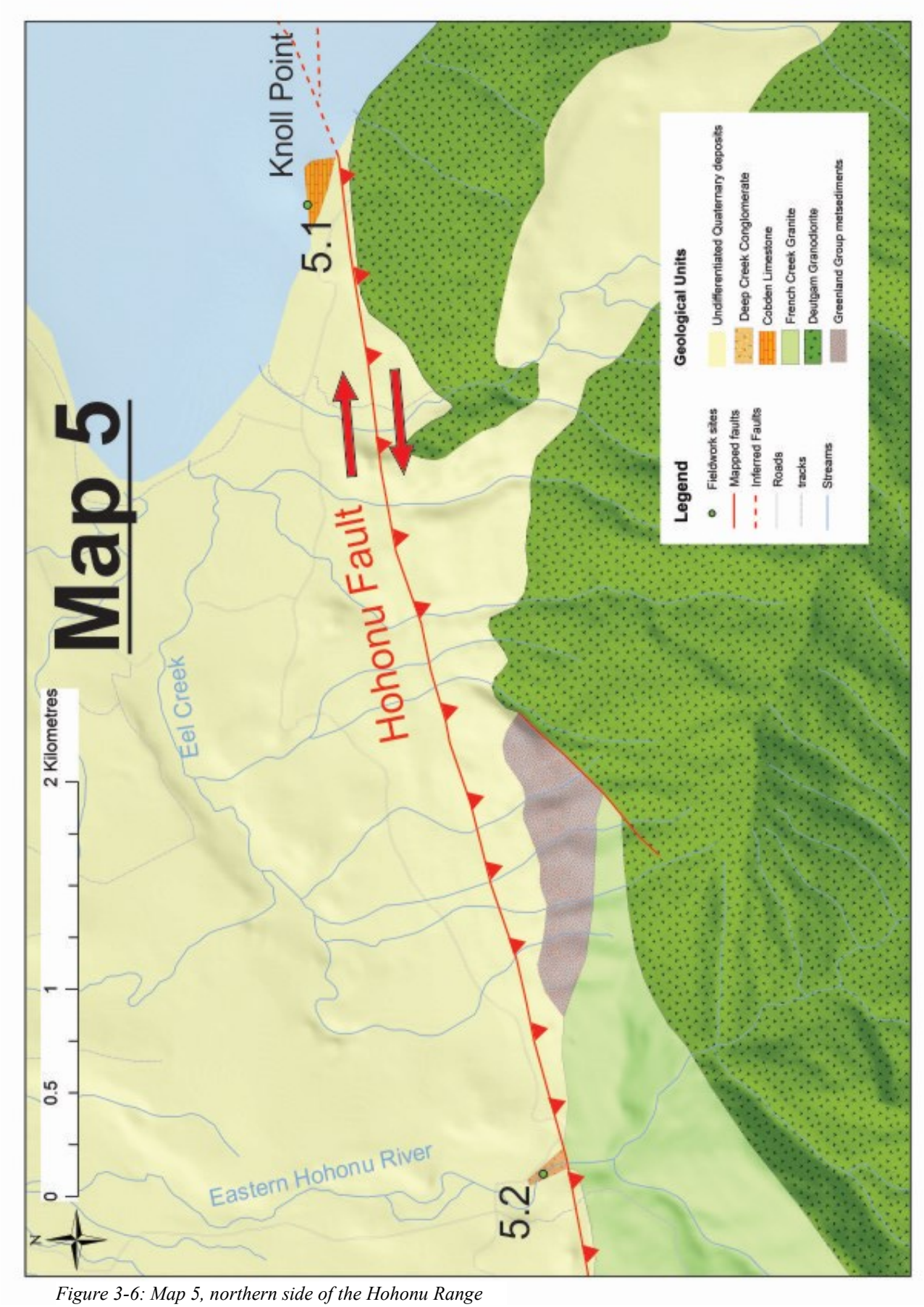

Figure 3-6: Map 5, northern side of the Hohonu Range

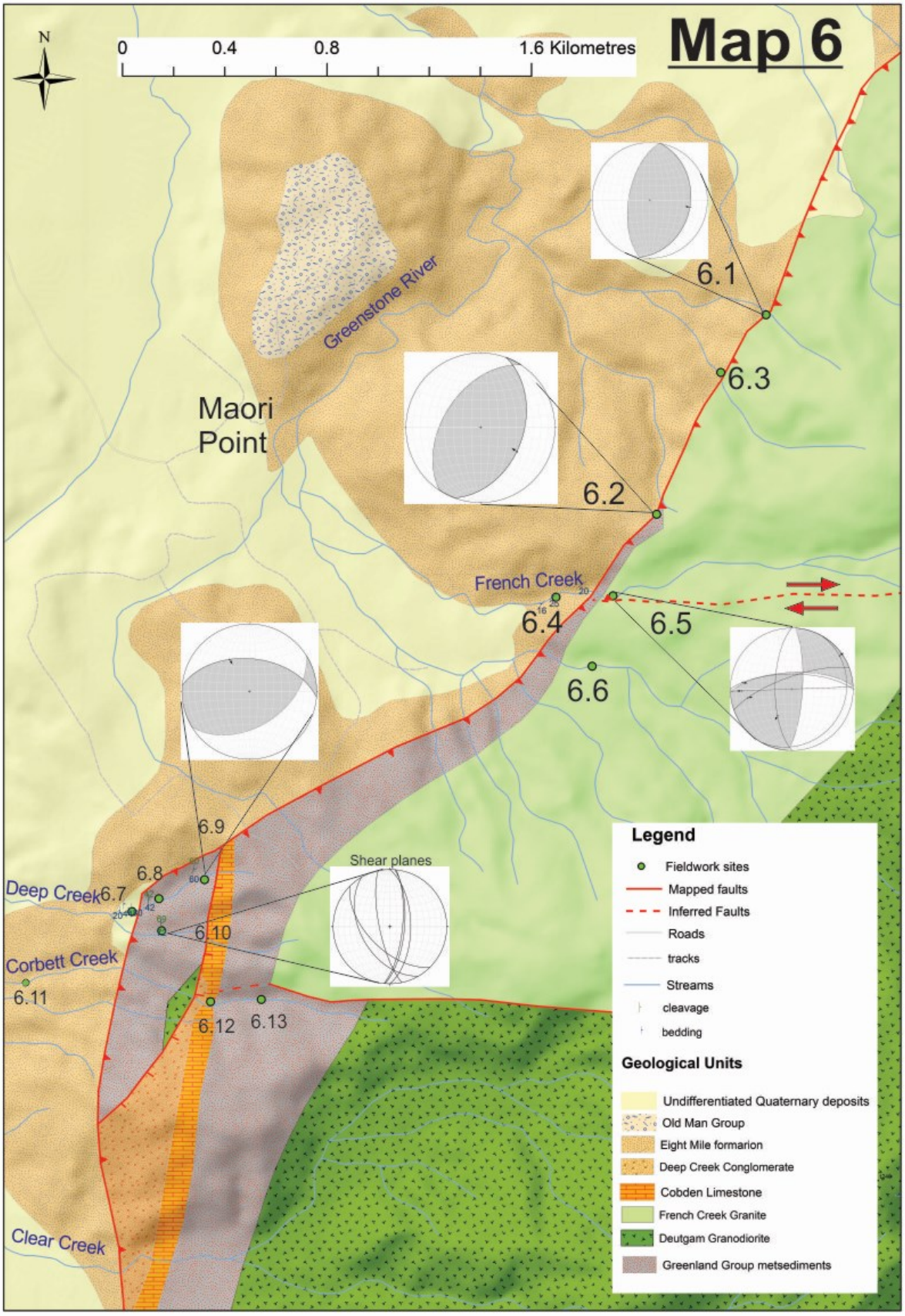

Figure 3-7: Map 6, west side of the Hohonu Range

3.2 Northern Flank Mt Te Kinga (MAP 1 –Figure 3-2)

The aim of this section of fieldwork was to assess the kinematics of an inferred east-west trending fault across the northern flank of Mt Te Kinga mapped by Suggate and Waight (1999). This fault was interpreted as a steeply south-dipping range front reverse fault, named the Rocky Creek Fault, by Waight (1995). A number of different Early Cretaceous granitoid plutons have also been mapped by Waight (1995) in this part of the field area. The Rocky Creek Fault has been mapped as being the boundary to a number of these plutons. The following Early Cretaceous granitoids outcrop in this map area: Pah Point Granite, Te Kinga Monzogranite, Uncle Bay Tonalite and Jays Creek Granite (see Figure 3-2). Members of the Late Cretaceous Hohonu Dyke Swarm are also present in the area. The orientation of these were used by Waight (1995) to gain inferences of extension direction at the time of emplacement.

3.2.1 Rocky Creek

Rocky Creek was accessed by walking along the eastern shore of Lake Brunner from Te Kinga Township to the creeks outlet. The creek was followed upstream and the first suitable outcrop displaying kinematic data was found around 200m up the second tributary that comes in from the true left (site 1.1 – see Figure 3-2). A fault plane was found within a 30 cm wide shear zone with an orientation of 173/68W and striae plunging at 44° towards 341° (see Figure 3-2 for representation on stereonet). This shear zone contains very little pure fault gouge (it is present in seams <1mm thick throughout the shear zone) and hence only a small amount of movement is inferred for this shear zone. Crushed feldspar crystals across the shear zone have altered to clays. It appears that the relatively small amount of localized fault movement, coupled with the large quantities of clays being produced has enabled ductile-like shear indicators such as s-c shears and augen to form (Figure 3-8). It was from these, along with the presence of antithetic Riedel faults, that a sinistral-reverse shear sense was determined.

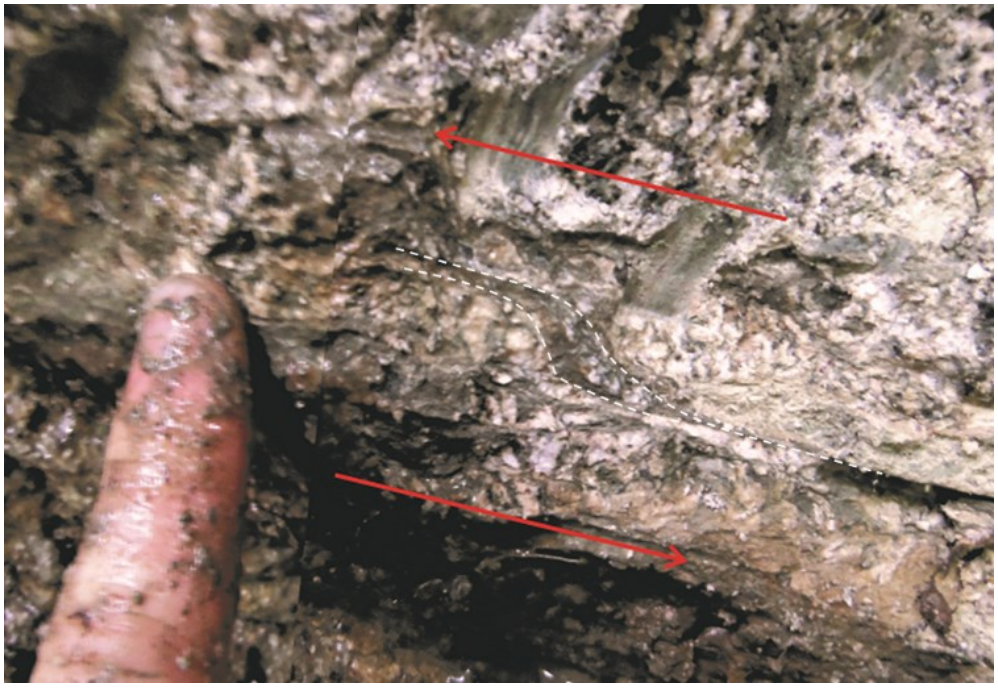

Figure 3-8: Brittle shearing in granites producing s-c and augen-type structures (site 1.1). Sense of shear shown. Finger for scale

The main creek was then followed up further, and around 100m upstream from the confluence (site 1.2 – see Figure 3-2), a >1m thick, east-west striking zone of fault breccia and gouge was found running parallel with the creek bed (Figure 3-9). The gouge material was well indurated, and because of this, a fault plane could not be exposed. Given the flat, stream-scoured plane of the outcrop, the fault was estimated as dipping anywhere between sub-vertical and 40° to the south. A measured strike of 262° for the fault is consistent with the east-west fault mapped traversing the northern flank of Mt Te Kinga by Suggate and Waight (1999). The gouge zone is bounded by a discrete linear fault plane against less brecciated granite and lamprophyre dyke in the hanging wall or south side. At least 1m of fault gouge and breccia material is exposed in the footwall of the fault.

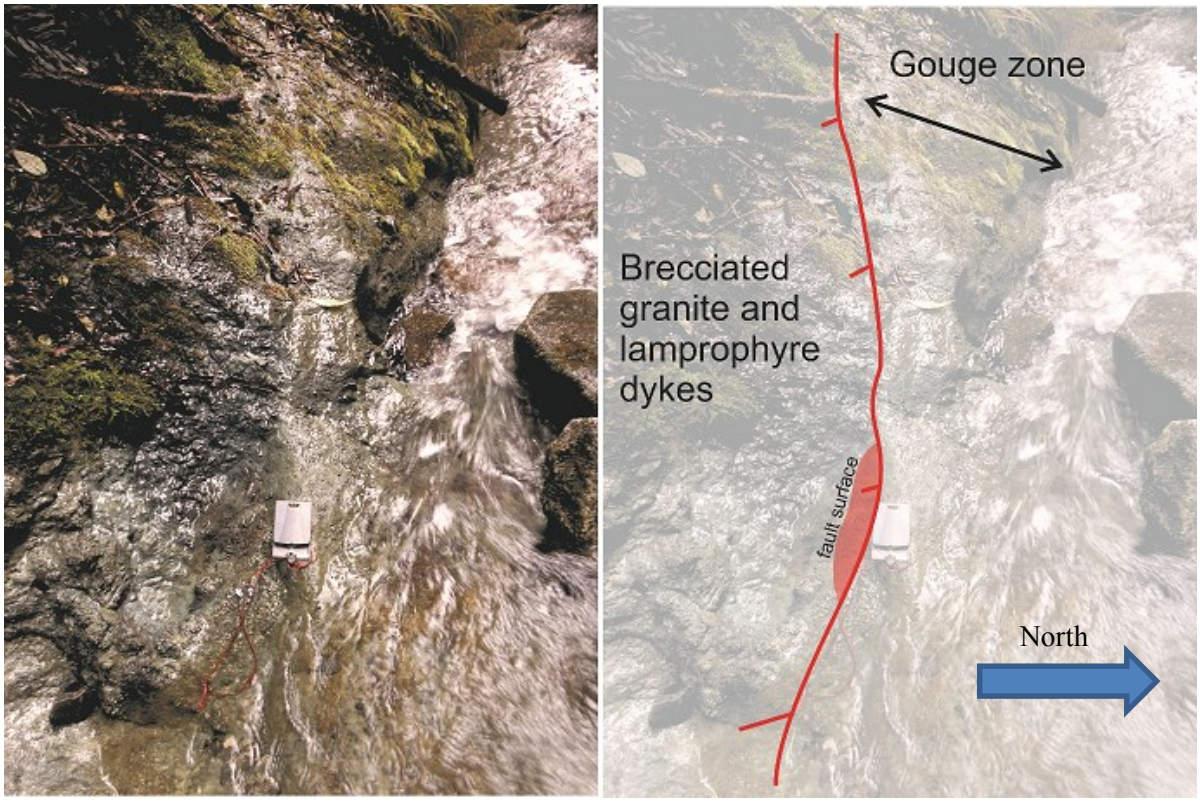

Figure 3-9: Fault outcrop facing west along the strike of the fault (site 1.2). Inferred slip sense shown. Compass for scale

Close to the top of the creek, a number of small, well scoured out gullies enter the main stream from the true right (site 1.3 –see Figure 3-2). Here, a relatively large amount of clean outcrop is exposed. Some valuable outcrop containing s-c shears within a clayey gouge zone can be found a short distance up one of these gullies. As with the first outcrop described downstream, this outcrop is interpreted as showing pseudo ductile deformation fabrics that presumably formed in semi - brittle conditions due to the large amount of clay formed in the shearing process. Again, no fault plane could be exposed, but the sub-horizontal surface of the outcrop displays an almost exactly east-west strike of the C-shears with a dextral shear sense (Figure 3-10). The dextral shear sense is important to note when considering Waight's (1995) description of the fault as follows; 'the fault plane proper is well exposed and strikes E-W, dips to the south east at between 37-47° with slickensides plunging 15-37° towards the SSW'. If Waight's measurements are correct, and the fault also has a dextral component as observed, then the fault must have a component of normal slip. The stereonet for the fault in Rocky Creek (in Figure 3-2, between sites 1 and 3) shows the first fault described, as well as a fault representing an average of Waight's measurements with an inferred dextral component of slip based on the outcrop shown in Figure 3-10. This final outcrop is relatively easily accessed by dropping down into the top of Rocky Creek from a small saddle on

the track up Mt Te Kinga. In future work it may be valuable to assess the kinematics of the shear zone at this outcrop more fully.

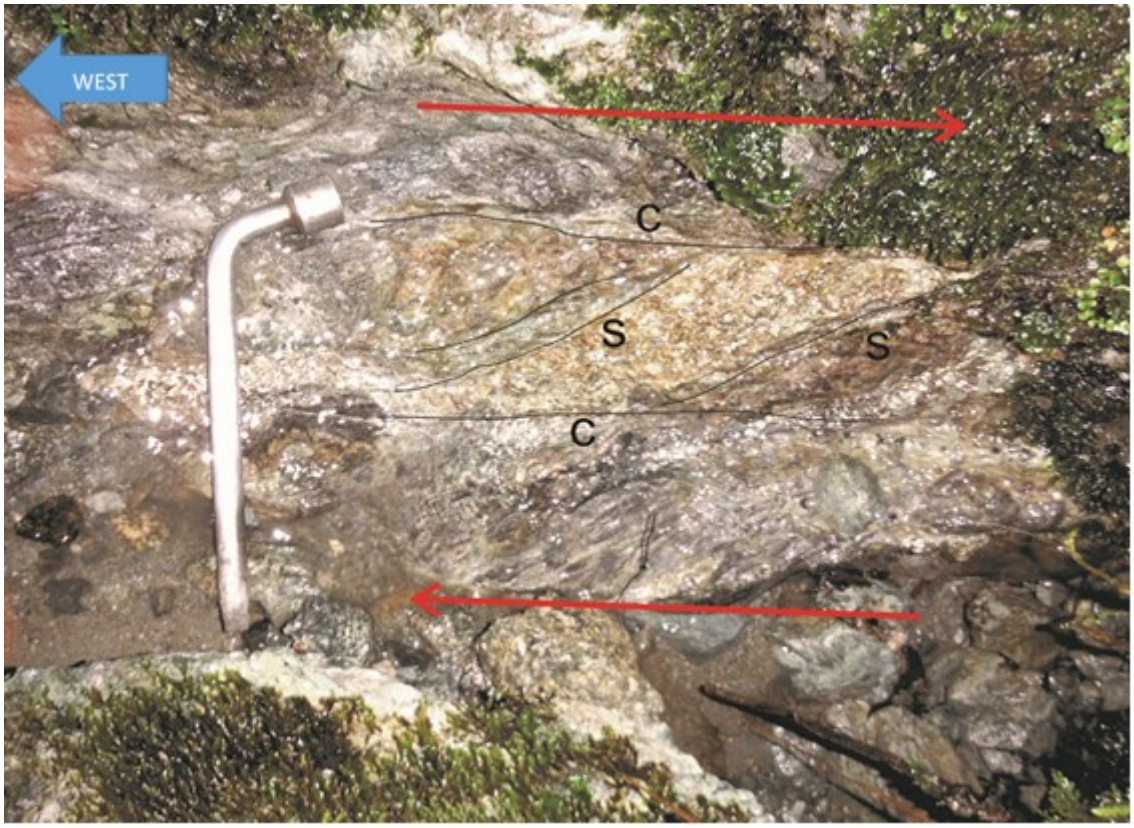

Figure 3-10: S-C shears in gouge zone near the head of Rocky Creek (site 1.3). Shear sense and orientation shown. 25cm long wheel brace for scale.

3.2.2 Jays Creek

Jays Creek was accessed by dropping down to the east from the same small saddle mentioned to access the top of Rocky Creek. A small outcrop of sheared Pah Point Granite, identified by its large pink alkali feldspar megacrysts (Suggate and Waight, 1999), is located at site 1.4 (see Figure 3-2). The fault plane exposed in the granite contains flakes of pyrite and has a dark and glassy surface which may be either fine grained cataclasite or possibly pseudotachylite (Figure 3-11). Two measurements of the kinematics of this fault are displayed in the stereonet for site 1.4 in Figure 3-2. These show the fault plane to be striking ESE-WNW and dipping between 53° and 56° to the east. Striae on the fault plane indicate a dextral-normal sense of movement.

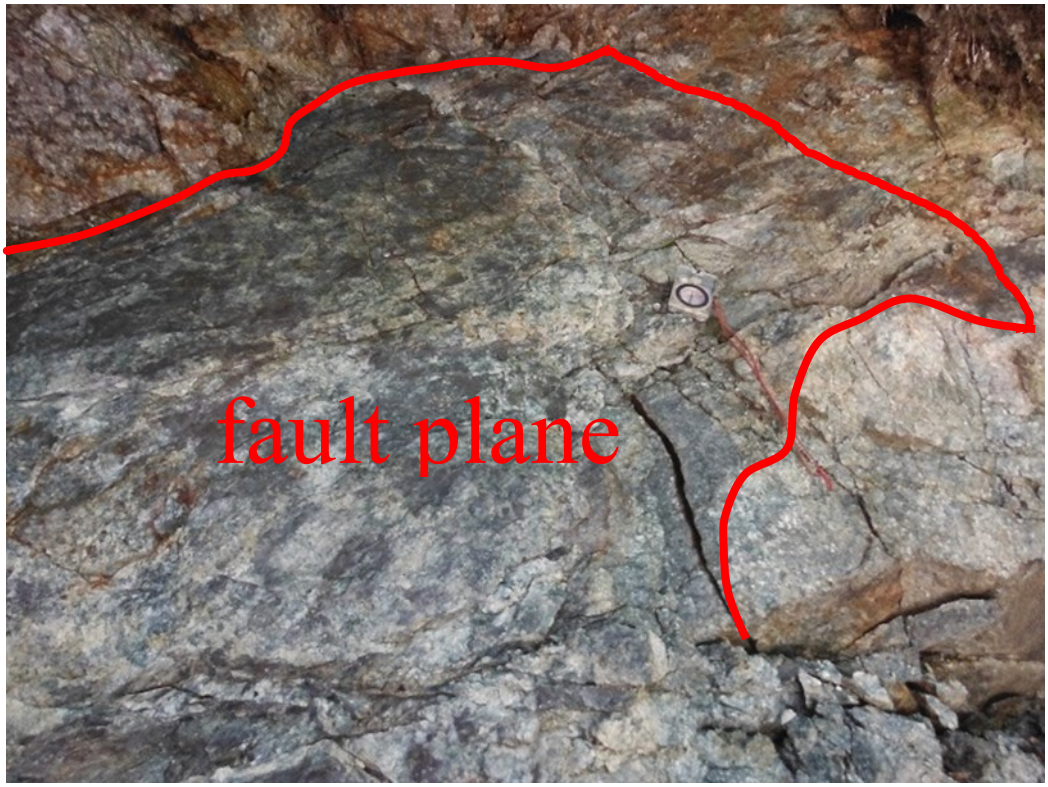

Figure 3-11: Fault plane in Jays Creek (site 1.4). Compass for scale. Photo facing north.

There is no outcrop for the next 500m upstream until the creek runs into a gorge with walls composed of Uncle Bay Tonalite (site 1.5 – see Figure 3-2). Here, the rock mass is more intact than the small outcrop further downstream and no thick shear zones were found. There is still a number of shear planes with striae that yielded good kinematic data, although they did not appear to show any prevailing shear mechanism pattern (see stereonet for site 1.5, Figure 3-2). The orientations of three 1-2m wide mafic dykes found at this site were subvertical and striking between 105° and 118°. These are very likely to be members of the Hohonu Dyke Swarm, and are striking in the characteristic ESE-WNW orientation.

Although it could not be observed, Waight (1995) assumed that the contact between Pah Point Granite and Uncle Bay Tonalite in the upper reaches of Jays Creek is an extension of the Rocky Creek Fault. Based on the Suggate and Waight (1999) map, this is a faulted relationship that continues across the northern flank of Mt Te Kinga where Uncle Bay Tonalite is juxtaposed against Pah Point Granite. Given the greater amount of deformation that has occurred in the Pah Point Granite outcrop, it would appear that the fault is present beneath Quaternary cover a short distance upstream from this outcrop. The 500m long absence of outcrop within the creek bed may be explained by glacial scouring out of the fault scarp, followed by its infilling with Quaternary glacial sediment during the last glacial period.

3.2.3 **Wallace Creek**

Wallace Creek was accessed by sidling across from Jays Creek to a point a short distance upstream of site 1.7. Around 400m upstream from where it was entered, the creek comes down over an impassable waterfall (site 1.6 – see Figure 3-2). The basement rock into which this waterfall has cut is hornfelsic Greenland Group. This outcrop is part of a mostly inferred, 2-3 km long, c. 100m wide, linear slice of Greenland Group mapped by Suggate and Waight (1999) that extends from the lower parts of Wallace Creek up to the ridge top just to the northwest of Mt Te Kinga. A c. 150m long stretch of almost continuous basement outcrop occurs downstream from the waterfall. Within c. 30m of the waterfall, Greenland Group grades into a grey equigranular granitoid (inferred to be Uncle Bay Tonalite) by way of a tectonically re-activated intrusive contact. This intrusive boundary zone rock appears as 'pods' of hornfelsic Greenland Group intermingled with pegmatite and granite 'pods', with small amounts of shearing having taken place on the 'pod' boundaries. In the outcrop extending further downstream, Uncle Bay Tonalite is cut by number of slickensided joints as well as mafic and pegmatite dykes (Figure 3-12). Because no persistent, through-going shear planes were observed, no kinematic data were recorded for site 1.6.

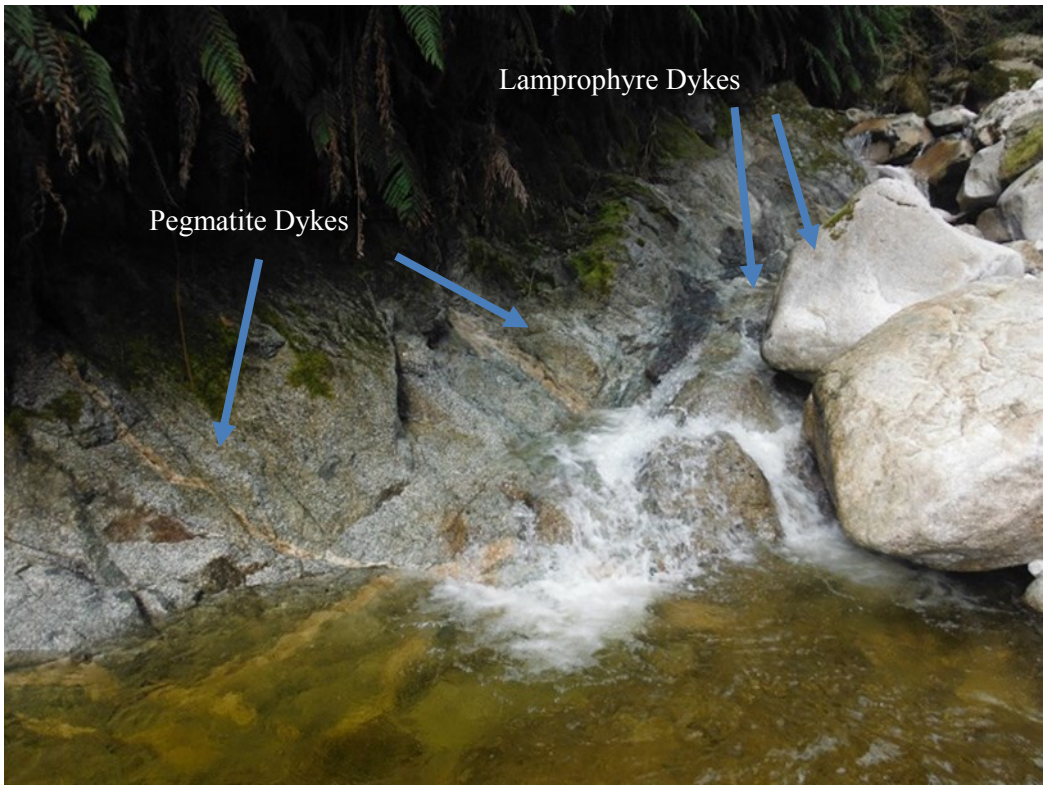

Figure 3-12: Uncle Bay Tonalite, with cutting pegmatite and lamprophyre dykes, c. 100m downstream from site 1.6.

Downstream of the outcrop below the waterfall, there is a stretch of c. 400m of streambed before basement rock is again exposed at another, smaller waterfall. Here, there is a subvertical, north-south trending fault contact between the Uncle Bay Tonalite upstream and hornfelsic Greenland Group downstream (Figure 3-13, site 1.7 – see Figure 3-2). This shear zone is c. 50cm wide and is comprised mostly of fault breccia with thin (<3cm) clay gouge fault planes throughout. Slickensides showed the fault to have a large strike slip component, and observations of s-c shears on a horizontal cross section of the fault showed a sinistral sense of slip.

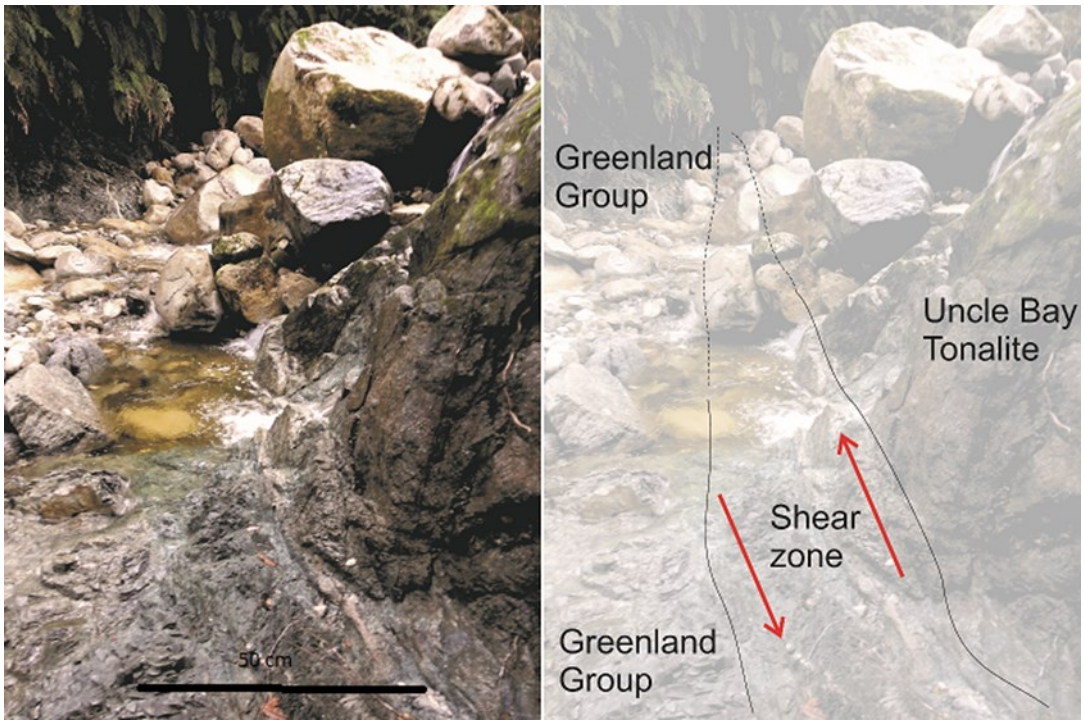

Figure 3-13: Tectonically activated contact between Uncle Bay Tonalite and Greenland Group (site 1.7). Photo looking south.

Around 200m further downstream a prominent fault outcrops on both sides of the creek (site 1.8 – see Figure 3-2). The fault juxtaposed Greenland Group on the upstream side with rock on downstream side that is interpreted to be part of the gradational intrusive boundary zone between the Uncle Bay Tonalite and the Greenland Group similar to that described at site 1.6. On the true left side, the fault plane itself is exposed and has an orientation of 104/55S (Figure 3-14). Striae on the fault plane plunge at 54° towards 168°. Fault breccia and gouge in the hanging wall of the fault is over 1m thick, while the footwall of the fault is very coherent and well indurated. The fault outcrops again on the true right side of the creek, around 10m downstream from the exposure on the true left. Here, the principal slip plane has maintained a similar orientation of 106/40S. The true right outcrop exposes a cross section of the shear zone where brecciated Greenland Group is faulted over a complex of pegmatite dykes and quartz veins (Figure 3-15 and Figure 3-16). The

combination of Riedel orientations and s-c shears in the true right outcrop suggest the fault has a dextral component of slip. This is in contrast with striae on the true right outcrop which suggest that it has most recently ruptured with almost pure reverse motion.

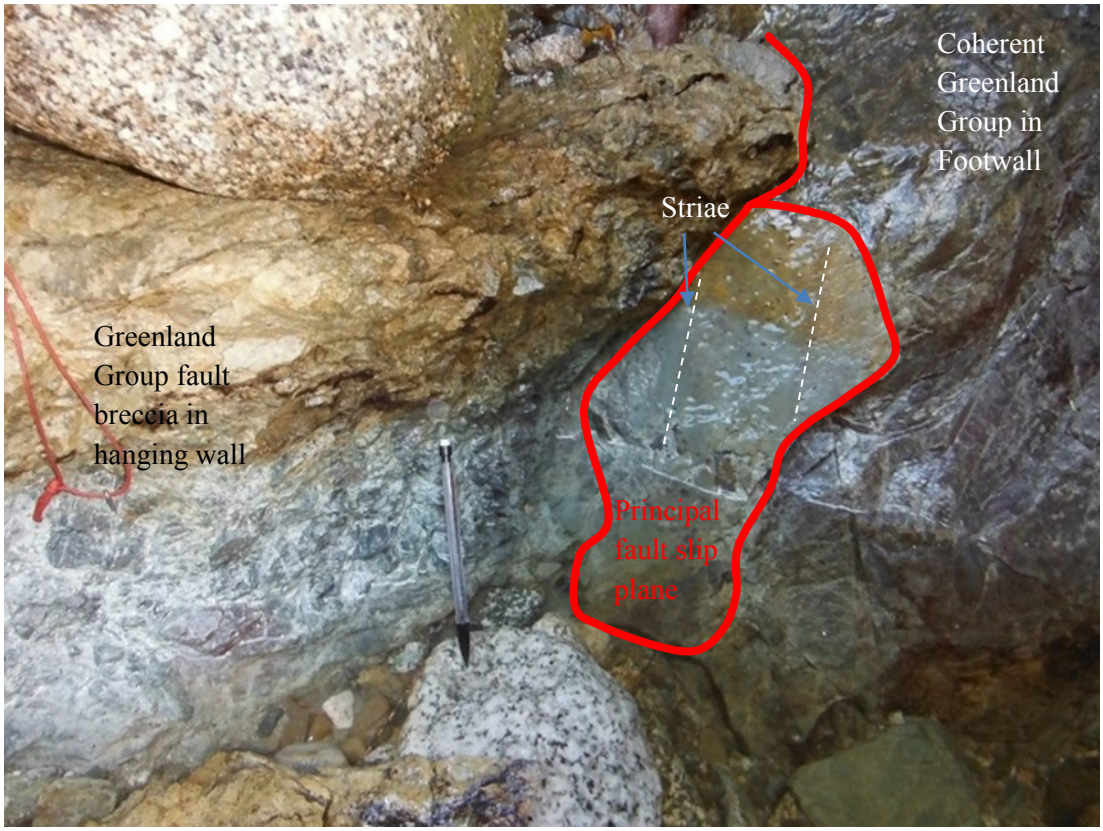

Figure 3-14: Fault plane exposed on the true left side of the creek at site 1.8. Principal slip plane exposed to the right of the pencil, fault breccia to the left. Note the coherent, undamaged Greenland Group in the footwall of the fault. Photo facing downstream or north

Another c. 200m further downstream, a 30 cm wide gouge zone within Greenland Group was found (site 1.9 – see Figure 3-2). A principal slip plane within the gouge zone was measured to have an orientation of 152/38W.

Waight (1995) states "A small exposure of brecciated Uncle Bay Tonalite at the base of Wallace Creek (K32 885399) is in fault contact with Greenland Group". This grid reference location is downstream of the last outcrop, in an area dominated by fluvial aggradation where outcrop is unlikely to be present. For this reason, the author questions the accuracy of this location, and suggests Waight is probably describing the fault at site 1.8. Other parts of Waight's description of Wallace Creek do not match with the map he produced. He also stated: "An intrusive contact between Te Kinga Monzogranite and Greenland Group is exposed at the base of a waterfall (K32 876400) and several intrusive sheets of Te Kinga Monzogranite cut the Greenland Group

Figure 3-15: Vertical section view of the fault zone on the true right side of Wallace Creek at site 1.8. Brecciated Greenland Group in the hanging wall, deformed quartz and pegmatite veins intruding Greenland group in the footwall. Camera case for scale. Photo facing east

Figure 3-16: Plan-view of same fault outcrop displayed in figure 3.8. Camera case for scale. Note the prominent Riedel shear below principal slip plane indicating dextral component of slip. Photo facing south

immediately downstream of this contact". This description matches the location and sounds similar to that of the small waterfall at site1.7, but the contact observed during this study has been reactivated as a N-S trending fault where the granitoid is on the west side, and Greenland Group on the east. Waight (1995) mapped Uncle Bay Tonalite, not Te Kinga Monzogranite as contacting with Greenland Group at this location. It is suggested here that there is an error in assignment of the rock type in Waight's description as the granitoid in contact with Greenland Group at site 1.7 is likely to be Uncle Bay Tonalite due to its overall colour being more grey than white. Intrusive sheets that fit the description of Te Kinga Monzogranite are present downstream of the contact.

Part of the objective for visiting Wallace Creek was to determine if the NE-SW trending 'slice' of Greenland Group mapped by Suggate and Waight (1999) is tectonically controlled. During the visit to the creek made during this study, the mapped contact with Te Kinga Monzogranite at the eastern side of the linear Greenland Group 'slice' was not observed, therefore, making conjecture on the contact as a potential fault is impossible. The contact with Uncle Bay Tonalite at the western side of the mapped 'slice', is described above as a tectonically re-activated intrusive one. The tectonic activation that has occurred on the western contact is inferred to be pre-Kaikoura Orogeny, as it appears to have formed in semi-ductile conditions, possibly close to the time the Uncle Bay Tonalite was emplaced.

3.2.4 Rotomanu Quarry

A visit was made to a quarry in a small hill of Te Kinga Monzogranite situated c. 1.5 km west of Rotomanu (site 1.10 – see Figure 3-2). A number of thin shear planes were observed, with two kinematic measurements from the most significant of these being displayed on the stereonet for the site shown in fFigure 3-2. Mason (1990) described a "knife sharp" contact between Uncle Bay Tonalite and Te Kinga Monzogranite at this location. This was not observed during this study and is likely to have been removed by quarrying.

3.3 Bell Hill (Map 2 – Figure 3.3)

Bell Hill is a large outcropping area of Greenland Group. The bedding of Greenland Group rocks in the southern Paparoa Range are described as isoclinally folded with a penetrating cleavage sub-parrallel to the axial planes of the folds (Nathan 1978a). Observations during this study show the bedding in Greenland group rocks at Bell Hill to form long wavelength, open folds. A consequence of this is that cleavage orientation and cleavage – bedding angular relationships are more consistent over broader areas. This makes it easier to constrain two important tectonic

components: Firstly, the degree of offset on a fault by observing the juxtaposition of the different modes cleavage and bedding orientation on either side of the fault. Secondly, the sense of shear, by observing how cleavage fabric has been bent or folded adjacent to the fault zone. These were both important techniques primarily employed in the Bell Hill part of the field area.

3.3.1 Area behind Bell Hill Retreat

In the area between Bell Hill Retreat and the lower section of Deep Creek there is an area that has been extensively worked over in gold mining operations, leaving a relatively large amount of Greenland Group bedrock exposed. Access is provided by an overgrown 4WD track that winds its way up through these workings onto a high terrace on the northwest flank of Bell Hill.

Where a small stream comes out at the bush edge, at the bottom of the workings, the Greenland Group bedrock is particularly well exposed (site 2.1). Here, bedding dips moderately, and cleavage, steeply towards the southeast. A diffuse tectonic re-activation of cleavage and bedding planes has occurred in this outcrop with reverse sense of shear (Figure 3-17). In the upstream section of the outcrop, more discrete gouge zones were exposed. Well exposed striae (Figure 3-18) show that one of the gouge zones has a clear dextral-reverse sense of slip.

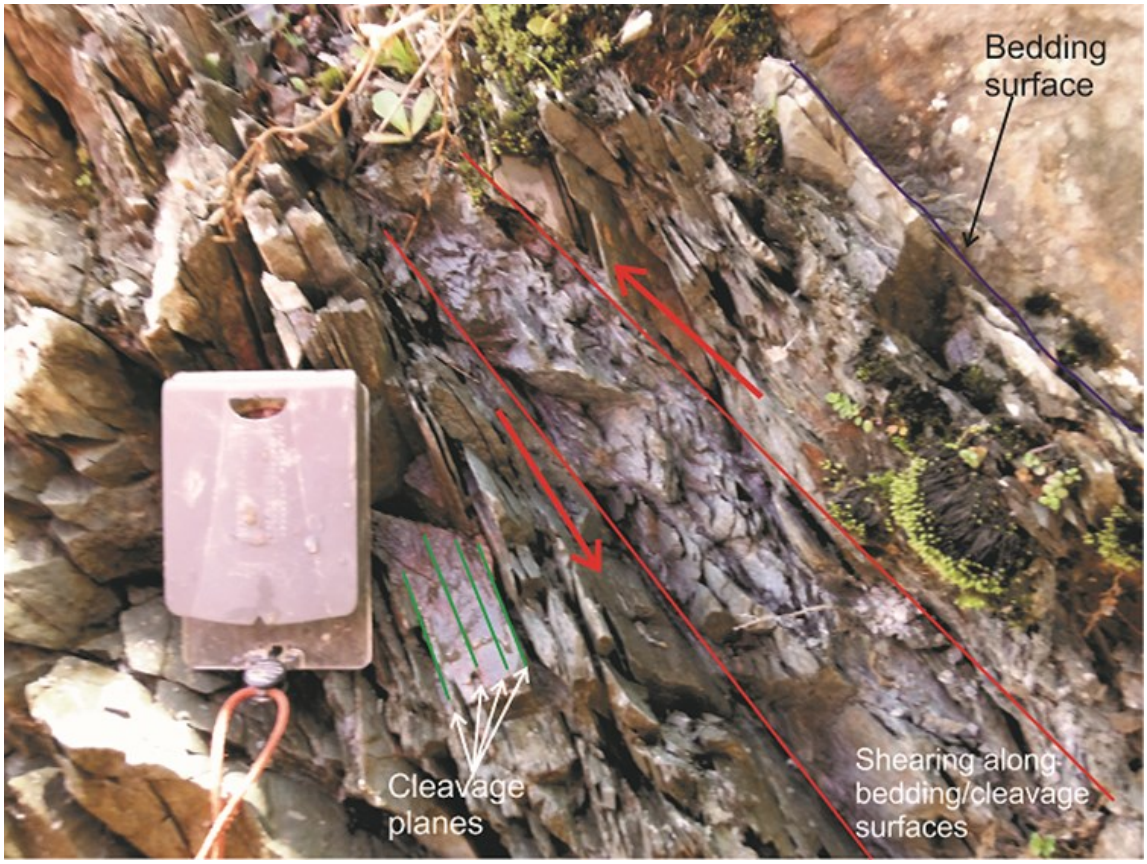

Figure 3-17: Outcrop at site 2.1 showing reactivation of cleavage and bedding as shear planes. Compass for scale. Photo facing north.

Figure 3-18: Fault plane at site 2.1 showing a clear dextral-reverse sense of slip. Pen for scale. Photo facing east.

Directly downstream from site 2.1, the stream cuts sideways along a man-made terrace for c. 10m, before cutting down into the bedrock again to make a small waterfall (site 2.2). This waterfall cuts directly across the cleavage and bedding fabric by exploiting a plane of weakness provided by a sub-vertical E-W trending fault with a discrete gouge zone 5-10 cm wide. Measurements of striae and observations of bedding offsets on Riedel shears (Figure 3-19) indicate a dextral sense of slip for the fault. At this outcrop, both bedding and cleavage are slightly steeper than at site 2.1, with cleavage being more subvertical, but still with a NE-SW strike. Tectonic reactivation of bedding and cleavage planes is less prevalent in this outcrop. This is likely to be associated with the bedding and cleavage being less optimally oriented for activation as reverse –shears, although the cause-effect relationship is uncertain: has tectonic re-activation occurred *because* the fabric in the rock mass is optimally oriented, *or* has the fabric become optimally oriented *due* to shearing of the rock mass?

Figure 3-19: Fault zone at site 2.2 showing antithetic and synthetic Riedel shears, the principal stress direction associated with movement on the fault zone is shown with green arrows. Downstream is west.

Upstream of site 2.1, the naturally formed gully of the stream can be followed up for c. 300m towards where it intersects the track again directly above site 2.3. There is an almost continuous outcrop of varying quality along this stretch of the stream. As a whole, the rock mass in this section is relatively deformed and is cut by numerous small shears and gouge zones. A number of shear plane orientations and their kinematics were recorded. Many of these are N-S trending, east-dipping reverse faults with both dextral and sinistral components. These faults are sub-parallel to, and likely to be controlled by the bedding orientation. There are also a number of steeply dipping to sub-vertical strike slip faults. Most of these are NE-SW striking dextral faults, with one subvertical NNW-SSE striking sinistral fault. At the start of this stretch, bedding orientation changes from its NE-SW strike at site 2.1 to be more N-S, still dipping moderately to the east.

Upstream from this point, the small number of bedding planes identified, consistently kept that orientation. A larger number of cleavage plane orientations were recorded, ranging in strike from NNE to ENE and moderate to sub-vertical in dip. The greater concentration of shear zones is likely to be responsible for the relatively large variance in cleavage orientation over this small stretch of creek.

Directly below where the stream described above is cut by the track, there is a waterfall exposing a significant gouge zone (site 2.3). The gouge zone is c. 3m wide, with other shears present within c. 5m of the hanging wall of the gouge zone. The orientation of most of the fault planes measured is N-S striking, moderately dipping to the east. This is close to that of the bedding recorded nearby which suggests that the structure is controlled by the bedding orientation. The overall kinematics obtained from the striae showed the fault to have a pure-reverse sense of slip. However, there are a few, less significant striated planes where the orientation and sense of slip are considerably different. These are interpreted to have formed in response to rupturing on nearby faults, possibly inducing anomalous slip movements within the gouge zone.

Site 2.4 is a waterfall draining into true right of the head of a deep man-made gully produced during the gold mining process. It is an outcrop of moderately deformed Greenland Group where the cleavage appears to be tectonically re-activated. A singular measurement of the cleavage orientation shows it to strike ENE-WSW and dip moderately towards the southeast. Five striated planes were measured. Three of these have similar orientation to the cleavage and a predominantly reverse sense of slip. These are likely to have developed from re-activated cleavage planes. The other two striated planes measured were sub-vertical, striking NE-SW and had a predominantly dextral sense of slip.

Site 2.5 is an outcrop on the true left side of the head of the large man-made gully described above. Here, both cleavage and bedding have been rotated from their typical orientation so that the bedding is sub-horizontal, and the cleavage dips shallowly to moderately to the NE. This is interpreted to have happened as a result of bending of the rock mass adjacent to a significant fault. A complex fault zone is also exposed at this location. Two striated planes suggest that the fault zone has a reverse sense of slip. However, these were not good representations of the whole fault zone and the overall orientation and kinematics remain uncertain.

3.3.2 Jones Creek

Access to the upper reaches of Jones Creek is by a 4WD track that leads up the ridge to the north, and then drops into the creek above a gorge section where there are abandoned gold workings. Along the 4WD track that accesses the upper section of the creek, there a few small outcrops in

which cleavage measurements were taken and were typically striking NE-SW and dipping between 50° and 70° to the SE.

At a more recent part of the workings where the track intersects the creek, there is a pit dug in highly altered, weathered and fractured greywacke that exposes what is named here as the Jones Creek Fault Zone (site 2.6). The west side of the pit (Figure 3-20) exposes two fault strands that strike ESE and dip steeply to the south. The northern fault strand truncates, with a south-up sense of slip, a fluvial sand and pebble lens lying within a colluvial wedge (Figure 3-21). The southern fault strand offsets, with a south-down sense of slip, an overlying unconformity with Quaternary boulders and gravel. Striae on the southern strand show a sinistral-normal sense of slip. No obvious striae were observed on the northern strand on this side of the pit. On the eastern side of the pit, the northern strand was exposed again. Here, exposed striae and a clayey s-c fabric show the fault to have a reverse-sinistral sense of slip (Figure 3-22). This is consistent with the reverse offset of the fluvial lense on the same fault strand on the western side of the pit. The both normal and reverse sense of faulting is a common feature of strike-slip faults, and forms as bends in the fault produce pop-up and drop-down structures. This fault zone is one of the most important discovered during the fieldwork during this study as it undoubtedly proves that there has been active faulting during the Quaternary. It also shows that range front deformation that has occurred during the Quaternary isn't purely thrusting, and involves a component of strike-slip deformation.

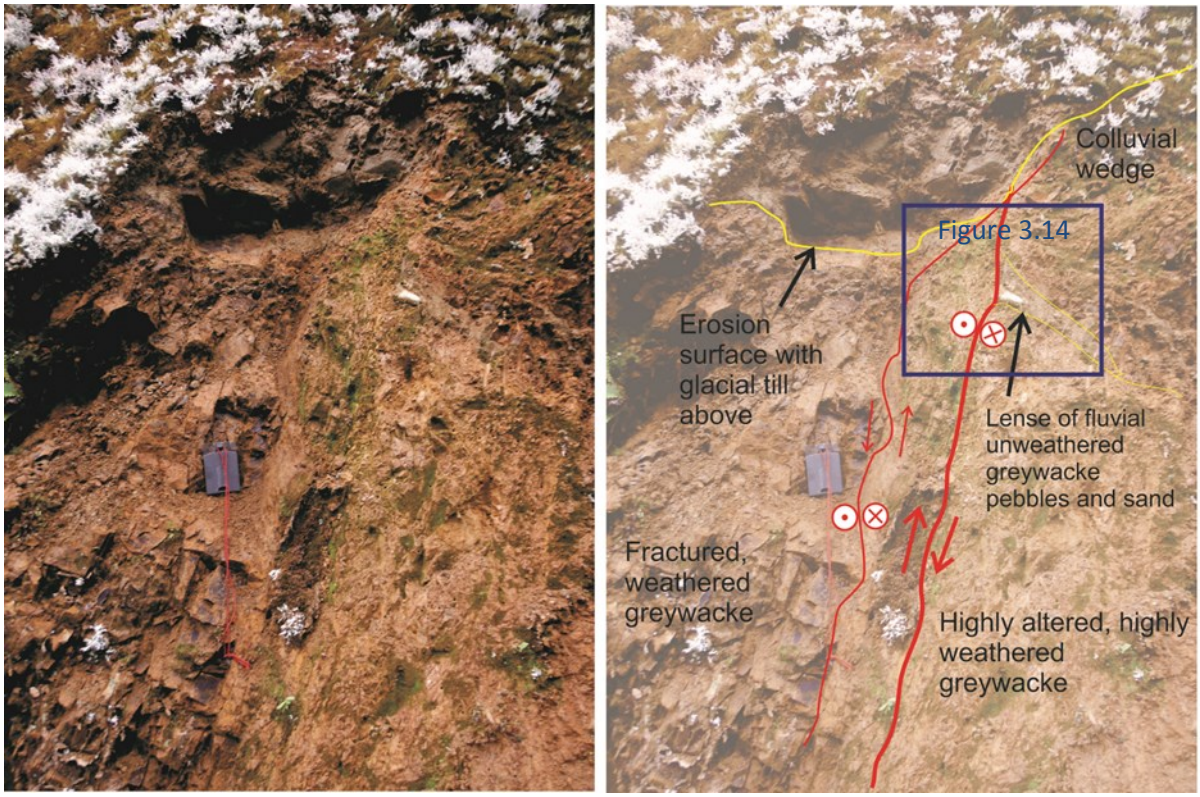

Figure 3-20: Looking at the western side of the pit where the fault was exposed at site 2.6. A lens of fluvial sediment is truncated by a fault plane. Compass for scale.Photo is facing west.

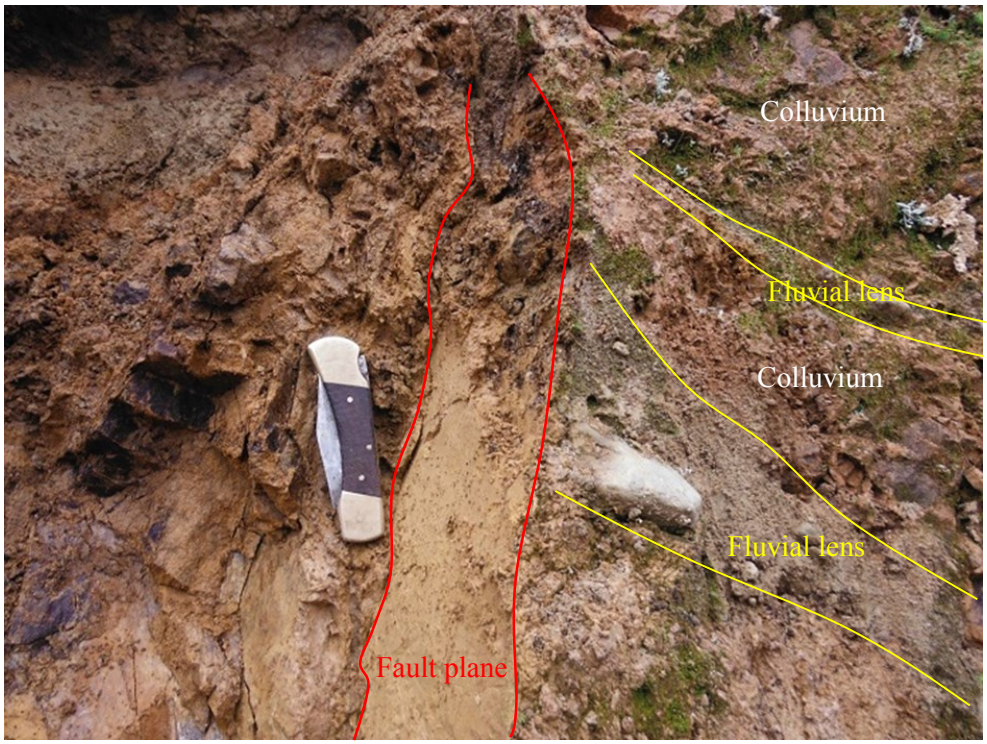

Figure 3-21: Close up of northern fault strand on eastern side of the pit, truncating a lens of fluvial sediment. Pocket knife for scale. Photo is facing west.

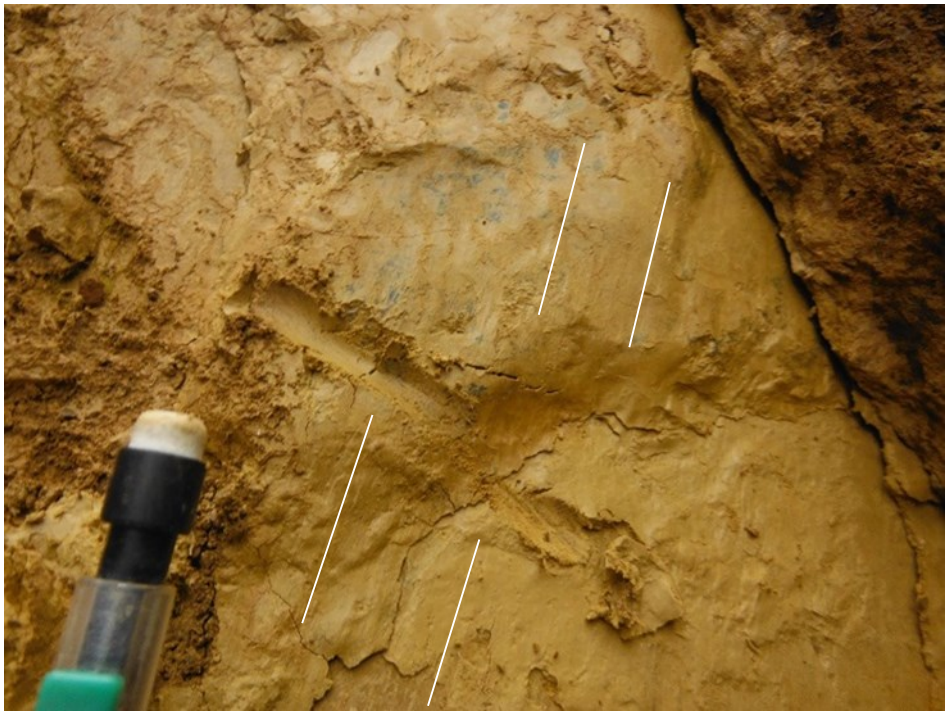

Figure 3-22: Close up of northern fault strand on western side of the pit at site 2.6, showing a reverse-sinistral sense of slip. Striae orientations shown with white lines. End of pencil for scale. Photo is facing north.

In general, the rock mass for the upper section of Jones Creek was moderately deformed with a number of thin (<3cm) shear planes and an apparent tectonic re-activation of the cleavage which often left bedding difficult to distinguish. A major shear zone, consisting of a gouge and damage zone around 5m wide was found at the most upstream part of the creek visited (site 2.8, figure 3.16). A plane of dark grey clay that marked the principal slip plane was measured to be striking at 121° and dipping at 56° to the southwest. The sense of slip on the fault was constrained by observing how cleavage in the argillite had rotated in the hanging wall of the fault. The typical cleavage measured in the area was dipping between 50-70° to the southeast. In the footwall, the cleavage has bent upwards to an angle of 70-90° to the southeast. In the hanging wall, there is a progressive change in the orientation of the cleavage away from the fault. Starting c.15m into the hanging wall, the cleavage has progressively shallowing SE dips to become almost flat lying, then, continuing to rotate, it dips progressively more steeply northwest as it converged with the fault. As can be seen on the stereonet for this site on Figure 3.3, these measurements show that the fault has bent the cleavage into an antiform, with a fold axis trending at c. 040° and plunging at around 10°. The cleavage is folded in a way that is consistent with a reverse sense of movement on the fault. Also plotted on the stereonet are striations found on cleavage planes in the hanging wall which trend at 336° (Figure 3-24). It is likely that these formed during the flexural slip that would have

occurred between the cleavage planes as they were folded. No clear evidence was found to indicate whether there was any strike slip component of movement on the fault, however, pure reverse slip on a fault plane dipping as steep as 56° requires particular mechanical conditions and is mechanically unlikely (Sibson, 2009), and a strike-slip component is possible.

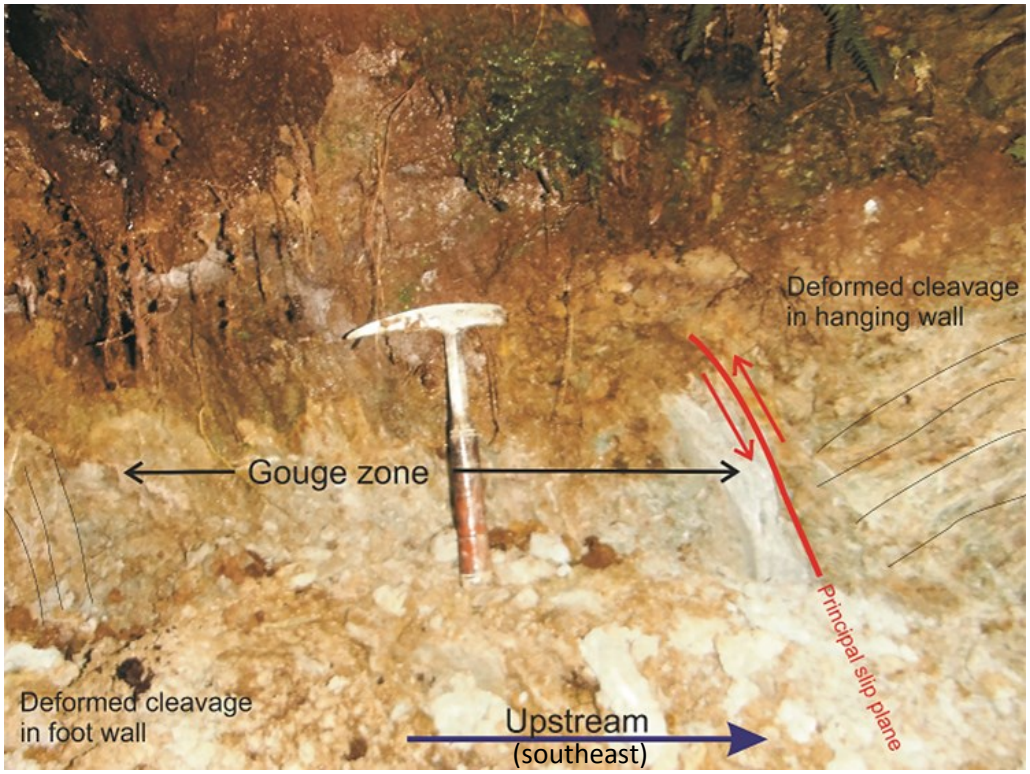

Figure 3-23: Gouge zone at site 2.8 showing the approximate orientation of the cleavage in the immediate footwall and hanging wall of the gouge zone. Hammer for scale.

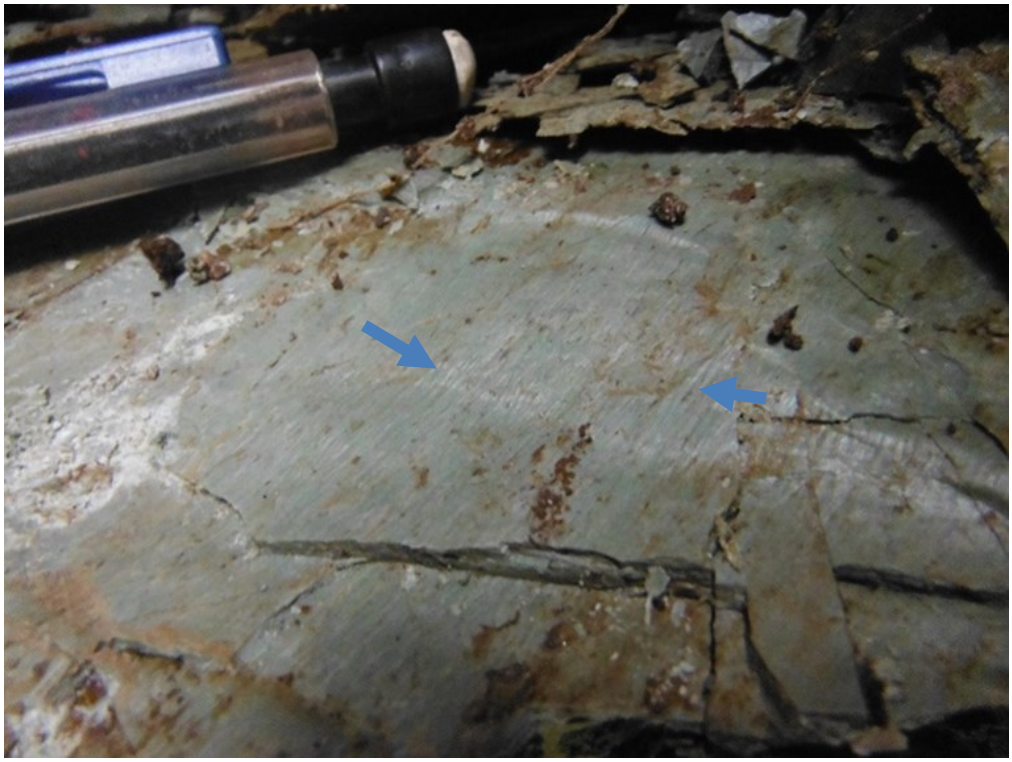

Figure 3-24: Striae showing movement on cleavage planes in hanging wall of fault at site 2.8

Figure 3-25: An example of undeformed Greenland Group bedding dipping to the southeast in the gorge section downstream of the workings in Jones Creek. Hammer on boulder at centre for scale, upstream to the right, photo facing northeast.

Downstream from the workings, there is a section of the creek where the bedrock becomes relatively coherent and forms a steep creek bed with a number of small waterfalls. Here, both bedding and cleavage is undeformed, striking sub parallel with each other at between 025°and 50°. Bedding dips at between 22° and 48° to the SE and cleavage, between 60° to the SE and vertical (Figure 3-25).

In the bottom, flatter, section of the creek extending c. 500m upstream from the road bridge, the Greenland Group outcrop is more deformed than the gorge section directly above. Tectonically reactivated cleavage and bedding planes were observed, but no significant gouge zones were found. An outcrop about 150m upstream from the road was very well indurated, pyrite-rich, silicified greywacke.

Cleavage orientation measurements were taken at regular intervals throughout the Jones Creek section. In general, the cleavage consistently remained striking roughly NE-SW with dips ranging from moderate to sub-vertical towards the southeast (see cleavage stereonet for upper Jones Creek in Figure 3.3), although there are a few locations where faults have locally reoriented the cleavage. A change to this typical orientation occurs in the bottom, c. 500m long flat section of the creek. Here the cleavage consistently dips moderately to steeply towards the NW (see cleavage stereonet for lower Jones Creek in Figure 3.3). This, along with a general greater degree of deformation of the rock mass for this section suggests a fault is crossed by the creek at the bottom of the gorge. In the lower section of the creek, topographic contrasts of c. 50 vertical metres between the flat terrace on the true left and the extended ridge on the true right may be tectonically controlled. For this reason, a fault is inferred to be present trending sub-parallel to the lower section of the creek.

3.3.3 Deep Creek

The outcrops found in the lower section of Deep Creek (before it straightens out into a NW-SE trend) were of relatively undeformed beds of Greenland Group. They exhibit cleavage orientations with a NE strike and a steep to vertical dip towards the southeast. Of the Greenland Group outcrops observed in the upper, SE trending section, almost all were on the true right bank of the creek. All of the true right outcrops were relatively undeformed, and no gouge zones were recorded. This contrasts considerably with the true left side of the creek where significant brittle deformation has taken place on the singular outcrop observed (site 2.9). Given the incoherent nature of the outcrop at site 2.9, it is possible that the reason no other outcrop occurs on this side of the creek is because the bedrock is highly deformed and has been eroded.

The highly fractured rock, fault breccia and gouge at site 2.9 exhibits what appears to be clayey s-c shears with a top to the west sense (Figure 3-26). Rough orientations of both the S and C shear

planes were recorded (see stereonet for site in Figure 3.3). No localised principal slip plane was exposed and it is uncertain whether the s-c shears represent the overall kinematics of the fault zone. The unconsolidated nature of the s-c sheared fault breccia suggests it formed very close to the surface. It is inferred to be part of a fault that has splayed out into a shallow angle thrust structure in order to utilise the topographic low of the creek bed. It is uncertain what the orientation or slip sense of the controlling fault is, however, the straight, NE trend of the upper section of Deep Creek has the potential to be controlled by a significant fault structure. The presence of the heavily deformed basement at site 2.9, and the relative lack of outcrop all along the SW side of straight, upper section of the creek support this hypothesis.

Figure 3-26: Fault breccia and clay gouge showing an S-C shear pattern at site 2.9. Hammer for scale, upstream or southeast, left.

For the c.2km lower section of Deep Creek up to site 2.10, bedding orientation measurements consistently show a moderate to shallow dip to the SE. A significant change to this occurs at site 2.10 where bedding orientation measurements clearly show folding around a NE plunging axis. In outcrop, over a lateral distance of c.25m heading upstream, the bedding rotates from its typical orientation as described above, to an E-W striking, north dipping orientation (Figure 3-27), and therefore forms a NE plunging syncline structure. 10m further upstream from this point, the bedding orientation rotates back again along the same NE plunging axis to dip shallowly to the NE, forming an anticline structure. The bedding then stays in this NE dipping orientation for at

least 150 m further upstream. This folding doesn't appear to affect the cleavage orientation a large amount, and has an axis sub-parallel to it. This strongly suggests the cleavage formation and folding occurred diachronously, during the same tectonic event.

Figure 3-27: Section of north dipping bedding c. 15m east of syncline axis at site 2.10. Note cleavage refraction in argillite. Hammer for scale. Right is upstream or south east.

Cleavage along the length of Deep Creek was reasonably consistent in orientation, typically striking NE-SW with dips ranging from sub-vertical to steeply dipping to the SE. Anomalous cleavage orientations were recorded at two locations. The first being directly above the clayey gouge zone at site 2.9 where the cleavage strikes around E-W and dips to the south. The second was up a tributary on the true right at the head of Deep Creek, where cleavage strikes N-S, and dips steeply to the east. A gap of c. 400m separates the second location from other observed, therefore the difference in cleavage orientation may be attributed to a broad warping of the basement rocks rather than a discrete, significant fault structure.

3.3.4 Sam Creek

Heading up Sam Creek, the first outcrop of Greenland Group starts about 200m upstream from the road bridge. Here, it continues as regular outcrops of interbedded argillite and greywacke adjacent to the creek for around 500m. At the top of this stretch, a massive, undeformed, well indurated >15m thick bed of greywacke forms the walls of a 30m long gorge. Above the gorge, the bedrock

returns to being interbedded argillite and greywacke for a distance of around 30m before being covered by Quaternary sediments with outcrop not appearing again for over 2km upstream.

Most of the outcrop found in the bottom section of Sam Creek is relatively un-sheared and appears to be unaffected by faulting. However, cleavage measurements made at regular intervals along the length of the creek where outcrop occurs reveal a sharp change in average orientation coinciding with an 80m long section of no outcrop (site 2.14). Downstream of this point, cleavage has an orientation that ranges in strike between E-W and SE-NW and dips relatively shallowly to the north. Upstream of this point, the average cleavage has a markedly different orientation with strikes N-S to NE-SW and dips close to vertical (see Figure 3.3). It is likely the presence of a major fault is responsible for this dramatic change in cleavage orientation. In the downstream outcrop that bounds the gap where the cleavage changes, a fault with a dark grey clay slip plane, with an orientation of 067/72NW and striae raking at 6^{o} NE was exposed. This is taken as an indicator that the major fault that changes the cleavage orientation is almost pure strike-slip.

Around 100m downstream from the gorge, and bounding the upstream side of the gap where the cleavage changes, there is an outcrop of undeformed Greenland Group clearly showing cleavage and bedding (Figure 3-28). Here, bedding dips moderately to the east, and cleavage, steeply, both strike approximately north-south. Directly upstream, the outcrop changes to a broad, deformed zone where the rock mass is cut by numerous shears (site 2.15). There is no clay gouge or cataclasite in these shears, and it is possible that they formed in semi- ductile conditions deeper in the crust. The surrounding cleavage has a similar orientation to the individual shears, and it is likely that the shear zone has formed through activation of the cleavage structure. It is possible that these shears formed during a deformation episode prior to or earlier in the Kaikoura Orogeny. This shear zone probably represents a localized area where cleavage has been re-activated as a shear zone.

Figure 3-28: Undeformed cleavage and bedding directly upstream of the inferred fault that changes the cleavage orientation at site 2.14. Hammer for scale. Right is upstream, photo facing north.

Heading up the true right tributary, Greenland Group outcrop begins where the creek bed intersects the NE trending base of the hill slope. From this point to around 400m upstream, outcrops were found at regular intervals. In general the rock mass was moderately deformed with a number of shear zones found.

As with the bottom of Sam Creek, cleavage measurements were taken at regular intervals along the length of the creek. The cleavage orientation showed several abrupt and clear changes that were coincident with observed shear zones. Starting from the highest point reached in the creek, heading downstream, cleavage in the first 50 m of outcrop is N-S striking, dipping moderately to the east. A shear zone is then crossed that has an orientation of 084/85S with striae plunging at 30^{o} towards 258^{o} (Site 2.11). Only the rock on the north side of the shear plane is exposed and it is relatively intact undeformed, although cleavage bends upon convergence with the shear plane in a way that suggests dextral movement. The southern side of this fault plane is assumed to be much more damaged by the faulting as that is likely to be the reason it has eroded away.

Downstream of the fault described above, the cleavage still strikes roughly N-S, but changes to dip shallowly-moderately to the west. Outcrops showing cleavage with this orientation continue for c. 230m. Within this stretch, a number of shear zones were found, predominantly with east-west strikes. One of these yielded good kinematic data and has both a similar plane, and striae

orientation as site 2.11. Observation of Riedel plane orientation and the bending of cleavage suggested it also has a dextral slip sense. The kinematics for this fault have been added to the stereonet for site 2.11.

Below the stretch of the creek described above, there was a c.20 m stretch where the cleavage changed again to dip steeply to the east before a zone of intensely deformed rock was encountered (site 2.12). The argillite cleavage has been crumpled and bent in a complex and erratic fashion, making it very hard, if not impossible to identify the sense of shear (Figure 3-29). No principal slip zone was exposed, but the general nature of the deformed rock suggested the plane of deformation was subvertical. The changing in cleavage orientation over a c. 20m distance either side of the shear zone suggests that it is a significant structure. Below the fault described above, the cleavage orientation changes again to dip moderately towards the northwest and this continues for the remaining c. 140m of outcrop.

Figure 3-29: Chaotic deformation showing no clear shear sense or principal slip plane at site 2.12. Hammer for scale, photo facing south.

Heading up the true left tributary of Sam Creek, Greenland group outcrop was first encountered at site 2.13. The small amount of kinematic data collected from this outcrop showed a NNE-SSW trending thrust. There was regular outcrop of moderately deformed Greenland Group from this point, to about 1km upstream, where a decision to turn back was made. The aim of this trip was to locate the outcrop of the Granite Hill Fault, but this was not found. There is a large amount of data in the form of kinematics on a number of small gouge zones observed, as well as bedding and cleavage orientations that could have been gathered from this stretch, but there wasn't enough time to do so.

3.4 Unnamed hill to the Northwest of Lake Ahaura (Map 3, Figure 3-4)

This area was visited for the reason that it is mapped as Greenland Group basement in the Greymouth QMap (Nathan et al, 2002). It was therefore likely to yield kinematic data that may provide a valuable link to the style of Neogene deformation further north.

Access to this area is from the eastern end of a forestry track that approaches the southern base of the hill. From here there is a 1.5 km walk eastwards through the bush, until the creek that drains the last significant catchment on the southern side of the hill is intersected. The first outcrop found where the stream comes out at the base of the hill is a complex of sheared and deformed greywacke overlain by Quaternary gravels that tilt between 15^{o} and 30^{o} to the south (Site 3.1). The first fault observed has a strike ranging between 290^{o} and 300^{o} and a dip between 63^{o} and 80^{o} to the north with striae that dip at 47^{o} towards 100^{o}. It has hard, un-sheared Greenland Group on the SW side of the fault, a gouge zone that varies in thickness between 5cm and >40cm, and rock on the NE side of the fault that is much more deformed and damaged than the other side. The large >40 cm pod of gouge is located at the point at which a second gouge zone is truncated by the one just described. This second gouge zone is in the more deformed NE side of the original fault, is 10cm thick, and has an orientation of 028/39E. Exposed directly beneath the second, more shallowly dipping gouge zone is a zone of folded cleaved Greenland Group (Figure 3-30). It appears that the cleavage fabric has folded in response to movement on the overhead shear zone with north striking sub-vertical cleavage being bent to dip shallowly to the NE over a vertical distance of c. 50cm. The bending direction of the cleavage strongly suggests the overhead gouge zone is a thrust fault. This outcrop is interpreted as showing a sinistral – reverse fault with thrusting occurring on its northeast side.

Figure 3-30: Bending of cleavage in response to overhead thrust at site 3.1. Hammer for scale.

Figure 3-31: Hand sample of pyrite – rich fault gouge at site 3.2.

Heading further upstream, no outcrop was found until around 100m downstream from where the creek splits into two main tributaries. Here, there is a 1m or wider zone of puggy fault gouge and highly fractured rock (site 3.2). A fault plane of dark grey clay was exposed, with coherent, but oxidised Greenland Group greywacke in the footwall of the shear zone. The orientation of the fault plane had a strike between 036º and 040º and a dip that varied between 55º and 79º to the northwest. The pug in the hanging wall (NW side) of the shear zone was very rich in pyrite (Figure 3-31).

The confluence in the creek marks where outcrop of a pink, fine grained, equigranular foliated granite (Figure 3-32) begins. This granite is not mapped on the Greymouth Qmap (Nathan et al., 2002), and it is uncertain what suite it belongs to. Analysis of a hand sample shows the granite contains quartz, alkali feldspar, plagioclase, and muscovite, and small crystals of biotite. The rock mass only occasionally fractured along foliation planes where alignment of muscovite crystals provide a plane of weakness. One such foliation plane was measured and has an orientation of 094/50S. Stream sediments in the true left branch contain about 80% granite and 20% greywacke, indicating that the granite makes up most, if not all of the bedrock for its catchment.

Figure 3-32: Hand sample of foliated granite near site 3.3. Note exposed foliation plane top right.

Heading up the true right tributary of the creek, the granite outcrop continues, with the creek appearing to follow a shear plane in the granite that strikes at 148° (Site 3.3). Kinematic measurements around this shear plane indicate that it may be a sinistral strike-slip fault (see stereonet for site 3.3). Basement rocks outcrop in the true right tributary for c. 350m upstream from the confluence. Most of this outcrop is the foliated granite, but there are some <20m long sections of hornfelsed Greenland Group that are interpreted to be xenoliths within the granite body. A 15m long section towards the top of where basement outcrops in the creek (c. 30m downstream from site 3.4), showed what is interpreted to be a semi-ductile shear zone. The original rock mass appeared to have been highly silicified to the point where the protolith was impossible to identify, while being crossed by numerous < 1mm seams of what appeared to be fine grained cataclasite. At the upstream end of the basement outcrop there is an unconformity which is overlain by medium to fine-grained, yellow brown, quartz-rich sand at least 10m thick (site 3.4). Although this sediment has a similar appearance to the Eight Mile Formation which is found elsewhere in the field area, no glauconite or forams were in hand specimen, and therefore is interpreted to be a Pleistocene glacial lake deposit.

3.5 Neogene sedimentary sequence across the Grey Valley Trough and Paparoa Inversion Zone (Map 4, Figure 3-5)

This section of fieldwork was undertaken primarily for the purpose of understanding the palaeo-environmental changes that occurred across the Paparoa Inversion Zone and Grey Valley Trough around the time of the Late Miocene Unconformity. This was done with the aim of understanding the tectonic setting that has caused these palaeo-environmental changes.

3.5.1 Deep Creek gorge near Kotuku

2-3km north of Kotuku, Deep Creek forms a gorge that has cut into Miocene interbedded conglomerate and sandstone (site 4.1). This is the type locality for the Deep Creek Conglomerate, the basal member across the Kotuku Anticline area of the Eight Mile Formation, within the Blue Bottom Group (Suggate & Waight, 1999). This site was visited during this study, and can be accessed by walking c. 300m upstream from the Deep Creek road bridge. As can be seen in the outcrop in Figure 3-33, the strata consist of sub-horizontal, 0.2 to 1.5 m thick beds of pebble conglomerate separated by >2m thick bands of, grey or light yellow-brown fine sandstone. A notable feature is the sharp boundaries between the conglomerate beds and the sandstone.

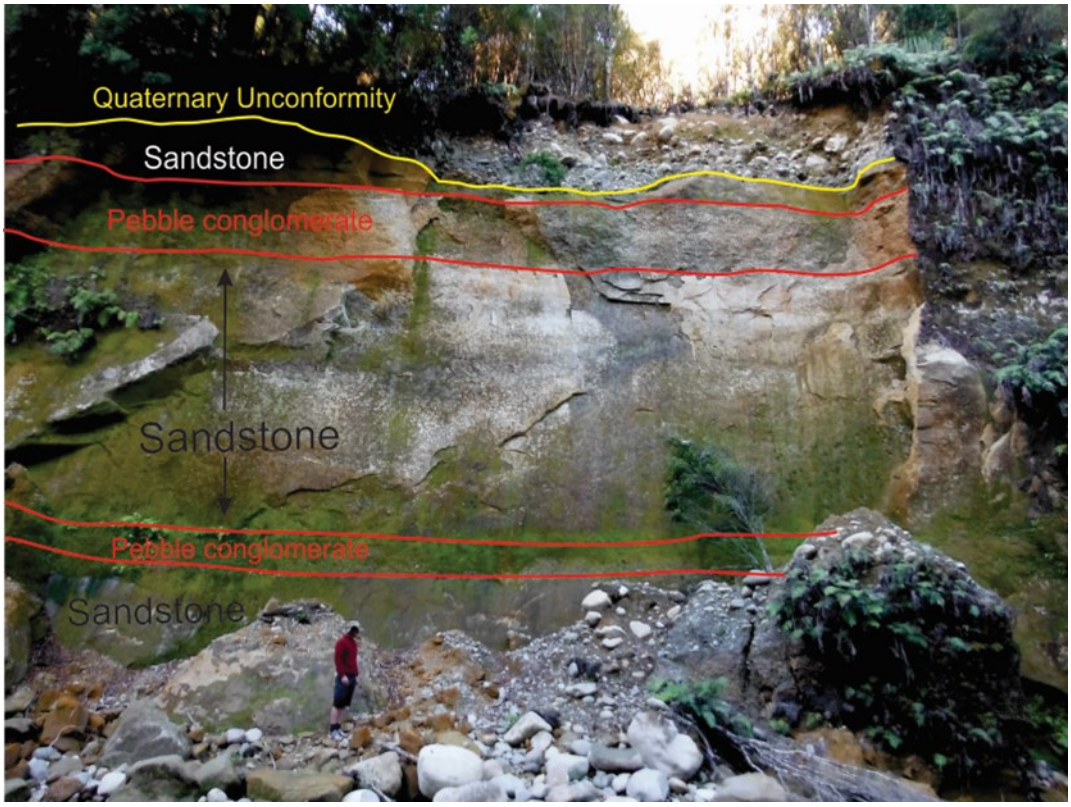

Figure 3-33: Deep Creek Conglomerate at Deep Creek Gorge. Upstream or north, left

The discrete beds of pebble conglomerate are moderately indurated, well-sorted, and clast-supported with a fine sand matrix (Figure 3-34). One of the larger beds (1.5m thick) appears to be reverse-graded. Sand cross beds were observed in the conglomerate beds, indicating the beds were formed by deposition as opposed to being lag deposits. The pebble clasts are no larger than 4cm, well rounded with clast compositions estimated as 50% greywacke, 35% granite, 10% chert and 5% Quartz. The sand that comprises both the thick bands separating, and the matrix of the conglomerate is composed of quartz, mica, lithics and 1-2% glauconite. Parts of the sand had pods of what appeared to be pure iron oxide on the walls of the gorge. These are likely to be produced by large amounts of iron rich minerals dissolving into the pore fluids of the sandstone (probably from glauconite). This iron then oxidises when exposed to air as the fluid seeps out of the walls of the gorge. The depositional environment that produced the well sorted conglomerate beds is inferred here to be one of a relatively constant, strong shallow water current with a high degree of sediment input, as well as subsidence. Suggate and Waight (1999) describe the Deep Creek Conglomerate as a near shore marine deposit.

Figure 3-34: Close up of deep creek conglomerate.

Heading NW along the road from the Deep Creek Bridge, there is a road cut that exposes well indurated, slightly calcareous, glauconitic, fine grained grey sandstone (site 4.2). It is possible that this unit is stratigraphically above the conglomerate beds found in the gorge, but it cannot be demonstrated by field relationships. An increased glauconite and calcareous content is interpreted to represent a period of slower rates of sedimentation compared to that of the conglomerates found in the Deep Creek Gorge. No previous documentation or interpretation of depositional environment for this outcrop could be found.

3.5.2 **Road cutting 2km east of Moana**

In this road cutting there is a 3-4m high outcrop consisting of a light grey, medium grained sandstone with thin beds of conglomerate towards the top and massive, poorly sorted, conglomerate at the base (site 4.3, Figure 3-35). The conglomerate is matrix supported with rounded clasts, up to 30cm in size and composed of granite and greywacke. Imprecise

measurements on the orientation of the thin gravel beds towards the top showed them to be striking NE to ENE and dipping 35º to 55º to the northwest. Three en-echelon, c. 2mm thick clayey shear planes were observed. These have an average orientation of 118/48 NE with striae plunging at 46° towards 019º. It is uncertain whether the fault planes formed prior, during or after the beds were rotated. Assuming the fault planes have not been rotated, the observation that they down-step between the en-echelon strands when heading up-dip, as well as the rake of the striae, suggests they have formed under reverse-faulting movement. This outcrop was identified by Suggate and Waight (1999) as being Deep Creek Conglomerate. Fieldwork observations undertaken in this study show the sediments at this outcrop to be different in character to all other outcrop and borehole descriptions. All other descriptions of the Deep Creek conglomerate show it to have a strictly pebble or smaller clast size, whereas the road cutting outcrop described here has up to boulder sized clasts. This, along with the difference in induration and colour of the sandstone, as well as the location in the Moana Syncline, suggests the assignment of this outcrop as Deep Creek Conglomerate needs to be reconsidered, and it is suggested here that the stratigraphic position of the sediments in this outcrop may be close to the regressive boundary between the upper part of the Eight Mile Formation and the Old Man Group and probably Upper Pliocene in age. If these sediments are as young as Upper Pliocene, the re-orientation of their bedding and the presence of crosscutting shear zones provides a younger age for the deformation of the area.

Figure 3-35: Outcrop in road cut, 2km east of Moana. Note thin, en-echelon shear planes running from the top left, above the hammer head, and down to the bottom right.

3.5.3 **Callaghans Road**

A visit was made during this study to the Callaghans area in order to observe a representative section of the Callaghans Greensand. Kennett (1966) described the type section of the Callaghans Greensand exposed at Callaghans Creek as "extremely difficult" to access as also confirmed during this study. However, Callaghans Road, which has probably been cut and widened since Kennet's description, exposes sections of the basal Eight Mile and top Stillwater formations. A c. 3m high section across the Tongaporutuan unconformity and Callaghans Greensand has been exposed by a road cut in the headwaters of Maori Gully (Figure 3-36). Sharp bedding planes were not observed, but the irregular unconformity appeared to be sub-horizontal. The lower 1.5 m of the outcrop is grey calcareous siltstone containing 1-2% glauconite and is interpreted to be the top of the Stillwater Mudstone. The upper 90cm of this unit is bioturbated, with the bioturbation becoming more intense in the 50cm below the overlying unconformity. *Thalassanoides* burrows in the upper part of the unit are filled with greensand composed of up to 80% glauconite. Above the sharp burrowed contact that marks the unconformity, there is a 15cm thick bed of fine-grained muddy, bioturbated greensand, with compositions ranging from 50 to 80% glauconite (Figure 3-37). This unit contained quartz and lithic pebbles as well as phosphate nodules. Above this unit there is a rapidly grading contact into 1.5m of very fine sandstone, composed of c. 15 % glauconite and containing bivalve fossils.

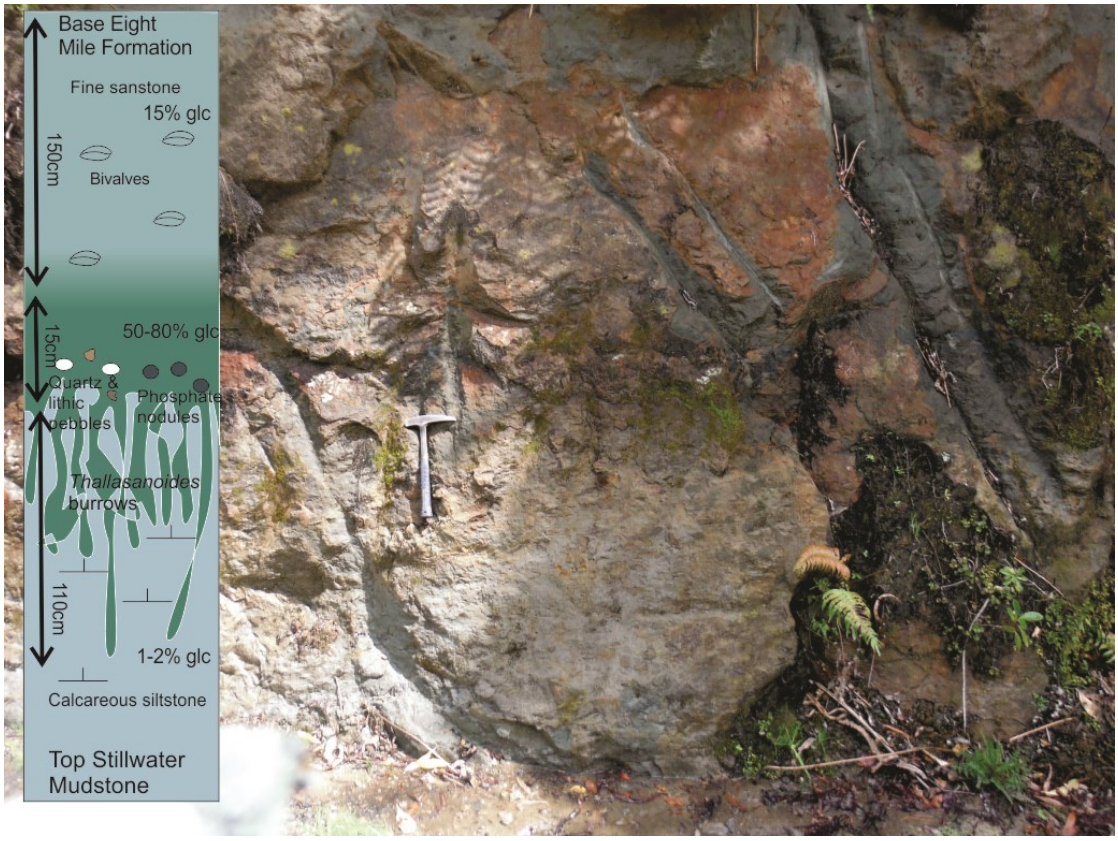

Figure 3-36: Section of the Tongaporutuan unconformity exposed at site 4.4. Hammer sits at the top of the Stillwater Mudstone.

Figure 3-37: Burrowed contact at site 4.4. Note the concentrated glauconite sand overlying the contact and infilling the burrows.

Around 5m above the unconformity just described is a c. 1m thick very well indurated bed of black sandstone that weathered orange on its exposed margins (Figure 3-38). This bed is evidently much more resistant to erosion than the sediments above and below it, and as a result it has formed a waterfall. Thin sections were created from this material (Figure 3-39) and are dominantly composed of glauconite and quartz with some opaque minerals that are inferred to be magnetite. The feathery texture within some of the glauconite suggests that it has undergone chloritization. This is a process that can occur during catagenesis at temperatures greater than 100°C (cf. Ivanovskaya et al 2003). This is a chemical process that can have a by-product of producing magnetite (Pers. Comm. Oze, 2014). An alternative way in which the magnetite may have concentrated in the sediment is through reworking, and preferential transport of lighter grains. Suggate and Waight (1999) describe the Callaghans Greensand as a shallow water deposit, although far away from any shore line. The greensand is likely to have deposited on a marine high where currents were likely to be strong, and able to concentrate the magnetite.

Figure 3-38: An eroded part of glauconite and iron oxide rich bed c. 5m above the unconformity. Finger for scale.

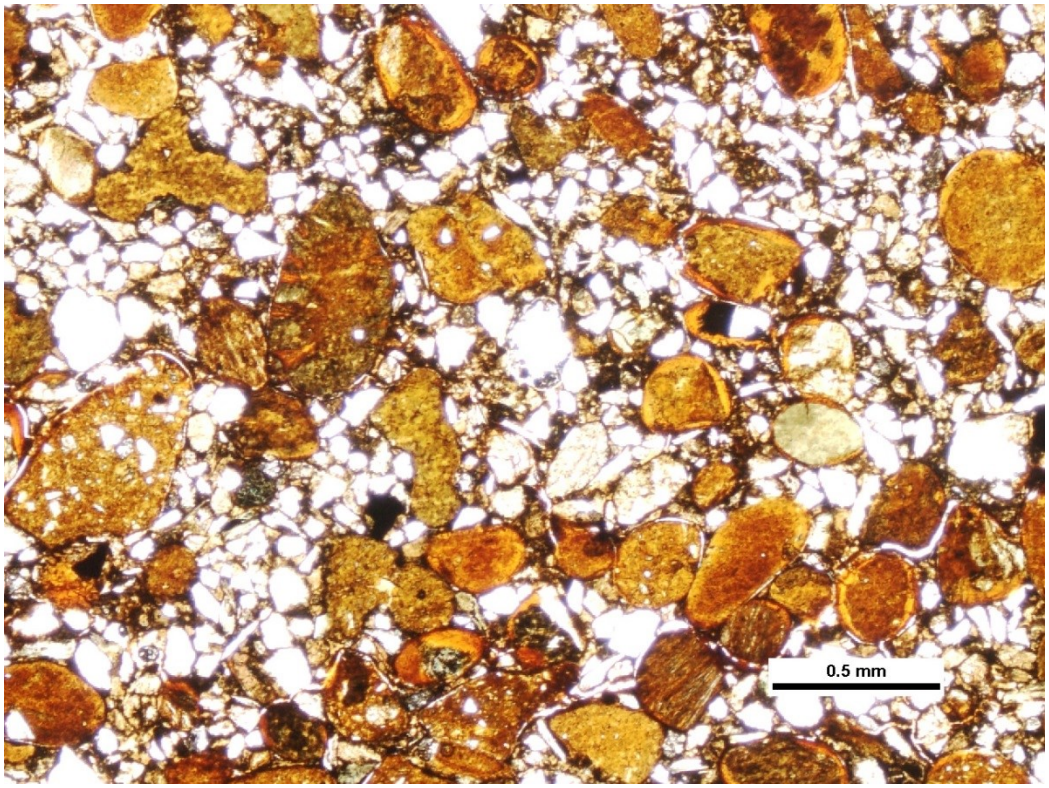

Figure 3-39: Thin section of glauconite-rich sandstone. Opaque minerals are likely to be magnetite.

3.5.4 Other Callaghans Greensand Outcrops visited

Lower Stillwater Creek (site 4.5) and an outcrop on the East side of the lower Taramakau River (site 4.6) are other areas visited during this study where Callaghans Greensand is mapped by Suggate and Waight (1999). In both of these locations, the sediments weren't as well exposed as the ones at the road cut on Callaghans Road. Probably due to the poor exposure, no obvious unconformity, or hard, heavy mineral layer was observed at either locality, although elevated concentrations of glauconite of up to 10% were present. It is possible that closer observations of the sediments in these localities would have yielded a distinction between the Stillwater Mudstone below the unconformity and that of the Eight Mile Formation above.

3.6 North Side of the Hohonu Range (Map 5, Figure 3-6)

This area was visited with the purpose of understanding the tectonic processes that have allowed Oligocene and Early Miocene sediments to be exposed directly adjacent the basin-bounding Hohonu Fault. A further aim was to understand whether the deposition of the sediments at site 5.2 was somehow related to activity on the Hohonu Fault itself or due to prior tectonic activity.

3.6.1 Knoll Point

Site 5.1 was on the shore of Knoll Point which is a block of Oligocene limestone that was mapped by Suggate and Waight (1999) and described by Wellman (1950). The limestone is very hard, veined with calcite and containing occasional pink bands. Some slickensided joints were observed, but due to the small amount of outcrop examined, kinematic data were gathered from only two of these. This was considered to be too small an amount of data to gain inferences on the overall kinematics of the site. The nature of the contact with the granite that comprises the adjacent flank of the Hohonu Range is uncertain because it is covered by an area of swamp and dense forest.

3.6.2 Eastern Hohonu River

Around 250 metres upstream from the bridge over the Eastern Hohonu River on the Kumara-Mitchells road, two outcrops on opposing sides of the river can be found (site 5.2). These are mapped by Suggate and Waight (1999) as Inangahua Formation, and the conglomerate exposed there was interpreted as being part of the Hohonu Conglomerate Member within that formation.

On the true right of the river there is a massive, clast supported, well indurated, poorly sorted boulder conglomerate (Figure 3-40). Clasts are up to 20cm in size, sub-angular to sub-rounded and mostly granite and greywacke with less common siltstone clasts. There is a bed of medium sandstone within the conglomerate which is also well indurated, and, upon hand specimen

inspection, is quartz-rich and contains biotite, muscovite and lithic grains. The sandstone bed thickens from 50cm to 1m over a distance of 7m. Bedding dips at c. 5° to the northwest. A fault plane with a normal offset and an orientation of 032/46NW cuts the sandstone (shown on Figure 3-40).

Figure 3-40: Conglomerate and sandstone, thought to be part of the Hohonu Conglomerate Member, Inangahua Formation outcropping on the true right of the river at site 5.2. Small normal fault with c. 10cm offset, with an orientation of 032/46NW shown with arrows. Downstream (north) to the left.

The outcrop on the true left of the river (Figure 3-41) is a calcareous mudstone containing blocks of calcareous sandstone, small clasts of coal, and rounded to angular clasts of granite, greywacke and argillite (Figure 3-42). Given the downstream dip of the true right conglomerate beds and the fact that the true left mudstone is slightly upstream, it appears that the latter is stratigraphically below the former, although this is uncertain. The outcrop has undergone both soft sediment and brittle deformation. Soft sediment deformation includes what appear to be zones where coarser sediment has been injected into what was originally a homogeneous mudstone. Brittle deformation includes calcite veins that are present throughout the rock mass which often contained slickensides. Kinematic data were gathered from these, but this was considered to be to small an amount of data to gain inferences on the overall kinematics of the site. This outcrop is interpreted as being a bed of mudstone within or beneath the Hohonu Conglomerate that has been deformed by the weight of overlying sediment.

Figure 3-41: Calcareous mudstone thought to be part of the Inangahua Formation outcropping on the true right of the river at site 5.2. Downstream (north) to the right.

Figure 3-42: Close up of outcrop above. Showing granite, coal, argillite, greywacke and calcareous sandstone clasts.

The Fossil Record Electronic Database (www.fred.org.nz) has two samples that have been analysed from at or near this site. One was identified as about Waitakian in age, the other was found to be probably Altonian. These ages are consistent with Suggate and Waight (1999) tentative assignment as the Hohonu Conglomerate Member of the Inangahua Formation (see Figure 2-2).

Roughly 200m upstream, the Eastern Hohonu River passes into a gorge where the walls are composed of fairly undeformed granite. The only shearing that was observed was on a number of thin (>1cm), usually subhorizontal planes. These are interpreted as being exfoliation joints associated with exhumation of the rock mass on which a small amount of shearing had taken place.

3.7 West Side of the Hohonu Range (Map 6 - Figure 3-7)

3.7.1 True right tributary of the Greenstone River, around 1.5 km downstream from Maori Point

The principal aim of visiting this creek during this study was to observe the only recorded outcrop of the Hohonu fault, where French Creek Granite thrusts over the Eight Mile Formation, as described by Wellman (1950). Both the nature of the footwall sediments and the deformation in hanging wall granites are also described. Notably, on visiting the creek, two outcrops of the fault were discovered.

In the main bed of the Greenstone River, there are river-cut outcrops of Eight Mile Formation up to 30 metres high. These are mostly composed of flat lying, massive, moderately to poorly sorted medium to coarse oxidised yellow-orange sandstone, with boulder conglomerate beds typically ~50cm thick and spaced typically every 10 metres within the sandstone. The clasts are rounded and ranging from pebbles to 30cm in size.

From the main tributary creek, a total of 4 second order tributaries were followed to where granite was over-thrusting Eight Mile Formation, only at two of which was the Hohonu Fault contact itself exposed. The Eight Mile Formation is quite coherent, forming vertical-sided gullies and gorges. Occasional beds of pebble to boulder conglomerate are present, these were useful for measuring bedding dip which ranged from being flat lying to dipping shallowly (<10°) to the northwest. In general the formation here was much the same as that in the main Greenstone River, consisting of massive, fine to coarse grained sandstone. The sandstone contained common (roughly every 10m) thin (<50cm) beds of very poorly sorted conglomerate with clasts ranging from granule to 20cm boulders. The clasts were mostly granite with smaller amounts of gneiss and greywacke. The granite and gneiss clasts were rounded to sub-rounded and the greywacke, sub-angular. Notably, none of the granite clasts found anywhere in the sandstone were the easily distinguishable French Creek Granite. Although no fossils were encountered in outcrop, a boulder of conglomerate was found as float in the creek bed which contained abundant bivalve shells. Occasionally, well rounded, very hard granite boulders up to 2 m in diameter were found isolated within the sandstone. As well as these, 2 boulders of similar description, but much larger (>5m across) were found jammed into the gorges cut into the sandstone. Seeing as the catchment for the creek drained hills only composed of the relatively crumbly French Creek Granite, these massive boulders must have been eroded out of the surrounding Eight Mile Formation. This fact has important implications in understanding the depositional environment of the Eight Mile Formation at this location which will be discussed later.

Observation of the Google Earth satellite photos of this area show the surface intersection of the Hohonu Fault to be represented to some extent as a lineament of slips in adjacent creek beds. This is because the granite in the hanging wall of the fault has been intensively pulverised, making it much weaker than the Eight Mile Formation it thrusts over. As previously mentioned, two exposures of the Hohonu Fault were observed in this study. The northern outcrop appeared to match the description by Wellman (1950). Up until now, Wellman's outcrop has been the only outcrop of the fault found, and as discussed in Wellman's report and by Nathan (1978b), important assumptions about the broader nature (including the overall fault dip) have relied solely on information gathered from this single outcrop.

The Northern exposure consisted of a large active slip within the pulverised granite coming down on both sides of the gully just before it entered a gorge, the walls of which were composed of Eight Mile Formation (site 6.1). At the downstream edge of the slip, the principal slip plane was exposed as a 5mm thick layer of dark grey clay directly on top of un-sheared Pliocene sandstone (Figure 3-43). It was difficult to expose an extensive representative sample of the slip plane, but measurements taken on the small amount of the slip plane that was exposed had a strike that varied between 340° and 40° and a dip that varied between 25-35° towards the east. No obvious striae were found. Above the dark grey clay layer there was at least 1m thick layer of white clay gouge containing small angular pieces of French Creek Granite. This graded upwards into over 10m of highly fractured granite with pods of white clay fault gouge. Wellman (1950) commented on the presence of a 30cm thick band of "black pug" separating the sandstone from the pulverised granite. Black clay was witnessed at the site, but it was situated in a 10cm band within the sandstone 2m below the fault zone. If this is fault zone material, its presence within the sandstone can be explained by a back thrust within the sandstone. Microfauna was obtained and dated from this black pug by Wellman (1950) who assigned it as probably Altonian in age. This is taken as evidence that Early Miocene sediments are truncated by the Hohonu Fault at some level down-dip on the fault (Wellman, 1950).

Figure 3-43: Northern exposure of Hohonu fault at site 6.1. Fault plane in photo has an orientation of 340/30E. Compass for scale.

The southern exposure of the Hohonu Fault was in a slip with a smaller area exposed (site 6.2). The material found in the hanging wall of the fault was similar to that in the northern fault exposure: a >1m thick band of white, granite-derived clay fault gouge was present directly above the principal slip zone which consisted of a dark grey clay. The principal slip plane was exposed and kinematic measurements were taken (Figure 3-44). The fault plane had a strike of 200°, and dipped at 42° to the East. Striae were plunging at 41° towards 112° with a rake of 80°. This supports the interpretation that the fault in this location has pure reverse kinematics. A key difference in the southern fault exposure was that between the fault plane and the underlying, undeformed Pliocene sandstone, there was 1m band of breccia composed purely of angular Greenland Group clasts no more than 1cm in size. The important implication of this is that, at least local to this strand of the fault, Greenland Group rocks were unroofed before the French Creek Granite was exposed.

Figure 3-44: Southern exposure of Hohonu Fault at site 6.2. Fault plane in photo has an orientation of 200/42E. Compass for scale.

In one of the tributaries where the fault was not exposed, in the area between outcrops of granite and Eight Mile Formation, a NNE trending linear zone of Quaternary, very poorly sorted, angular debris-flow deposits with clasts up to 1m in diameter was present (site 6.3). These were interpreted as being emplaced in a channel that was eroded out along the fault zone due to the relative weakness of the gouge material. Very little solid French Creek Granite outcrop was encountered above the fault zone, and therefore it was impossible to undertake any comprehensive kinematic measurements.

3.7.2 French Creek and Greenstone River

This area provided important field data of which no account had been found in previous literature. Outcrop of what is interpreted to upper Eight Mile Formation begins around 700m upstream from

the outlet of the creek. The first outcrop is light yellow-brown medium grained sandstone with 10-20 cm thick, pebble-cobble conglomerate beds. 250m further upstream, there is outcrop of light yellow-brown to orange-brown laminated medium grained sandstone which overlies a very poorly sorted conglomerate with clast size ranging from boulder to pebble and from well-rounded to angular. The laminated sandstone is dipping at around 15° to the northwest and have thin (<5mm) layers of dark grey clay on which there are slickensides trending down-dip (no striae measurements were taken).

Starting around 10m upstream of the last outcrop described, there are a number of outcrops along a 200m stretch of the creek that appear to be 1-2 m thick channel deposits of greywacke breccia lying within the sands and conglomerates (Figure 3-45, site 6.4). The breccia closely resembles fault breccia found elsewhere in the area. The contacts with the surrounding sand and conglomerate tend to be sharp towards the base of the channels, with the contact becoming progressively more gradational moving towards the top. The contacts, which are interpreted to be the channel walls, were sub vertical, and even appeared to undercut into the surrounding sediment. The periphery of the channels tend to be composed of coarser clasts (up to 5cm) relative to the centre of the flows which resembled clay-rich fault gouge with no fragments larger than 1cm. The interpretation is that they were discrete, marine debris-flow deposits coming off an active submarine fault scarp. No close observations were made, but it appears that the reworked gouge had a protolith of Greenland Group (when only granite is found in the hanging wall of the other side of the fault, at this location).

Figure 3-45: Greenland Group Breccia channel deposits at site 6.4. Upstream to the left.

Within this stretch of the creek where the breccia channel deposits were found, there is also an outcrop of well indurated granite boulder conglomerate, where an intervening sandstone bed, dipping at c. 30º to the northwest, has been offset across an sub-horizontal detachment fault with a top to the northwest sense (Figure 3-46).

Figure 3-46: Sub-horizontal detachment fault in French Creek c. 100m upstream from site 6.4. Downstream (northwest) to the right.

Around 100m upstream of the last sandstone and conglomerate, outcrop of French Creek Granite begins, indicating that the Hohonu Fault has been crossed. Two main shear zones were found within the granite, one of which was sub-vertical, striking east-west and appeared to have a dextral slip sense (see stereonet for site 6.5). No significantly wide gouge zone was observed, but this may have been eroded by the creek. The other was sub-vertical, trending NW, with a gouge zone thickness that tapered from around 40 cm wide towards the base to around 10cm towards the top. No conclusions were made on the sense of slip within this gouge zone due to poor preservation of striae.

The main Greenstone River bed was also explored with the hope of finding the fault and the surrounding rocks exposed. The only outcrop found was a relatively undeformed, dark grey, porphyritic dolerite with orange oxidised bands (site 6.6). This outcrop is interpreted as being part of a dyke of the Hohonu Dyke Swarm that is intruding into the French Creek Granite

3.7.3 **Deep Creek**

Heading up Deep Creek, Neogene sediments begin to outcrop in the riverbed at a point about 700m upstream from the road bridge. From here to a point around 700m upstream where the stream splits into two tributaries, there were regular outcrops of what was interpreted to be upper Eight Mile Formation. This sediment is typically comprised of medium to coarse, well-sorted, light yellow-brown sandstone containing regular < .5m thick conglomerate beds. The conglomerates has clast sizes that range to up to 30cm and compositions of granite, gneiss and greywacke. Cross bedding in the sandstone and conglomerate beds are common.

For the first 100m or so heading up the true right tributary of the creek, there are regular outcrops of what is interpreted to be a tectonically deformed glaciofluvial deposit. This deposit is generally very poorly sorted, medium to coarse sands and cobble conglomerates, grey in colour, and composed of granite, schist, greywacke and gneiss clasts. A number of small folds (<1m in scale) and change in the strike and dip of bedding was observed, with the last outcrop before outcrop of basement showing the beds tipped vertical, younging to the west (Figure 3-47, site 6.7).

Figure 3-47: Glaciofluvial deposits tipped on end directly downstream of the Hohonu Fault at site 6.7.

The first basement outcrop in the true right tributary occurs around 100 m upstream of the confluence and is relatively coherent and undeformed Greenland Group greywacke (site 6.8). Here, a number of shear zones were observed, although no kinematic data were gathered from

them. Over the next 100 m upstream the greywacke becomes increasingly fractured and gouged, and more easily erodible forming many slips on the valley sides. The last of these slips occur near the head of the valley, beyond which, the creek is too small and overgrown to continue. These last slips were composed of a lot of a lot of puggy and finely gouged material. On the slip on the south side of the valley, a shear plane defined by a clay gouge layer was exposed and its kinematics were measured (see stereonet for site 6.9, Figure 3-7). This slip also had large blocks (up to 1m) of light orange-brown calcareous sandstone scattered across its surface. These appeared to be sourced from somewhere uphill on the forest covered ridgeline to the south, however, no outcrop was observed.

Heading up the true left tributary, Greywacke outcrop begins, again, about 100m upstream from the confluence. The creek in this catchment was a bit more confined and vegetated and a relatively small amount of recent erosion has taken place. There were regular outcrops showing up to 1m wide gouge zones, although no kinematic data were gathered from them. An outcrop at site 6.10 (Figure 3-48) shows how the difference in strength of the sandstone and argillite beds affect the nature of shearing in the rock mass. The sandstone bed has broken into large rotating blocks, while the weaker argillite bed that was adjacent deformed more plastically, and controls the orientation of a significant shear plane. The orientations of these shears that are controlled by the bedding can be seen in the stereonet for site 6.10 (Figure 3-7).

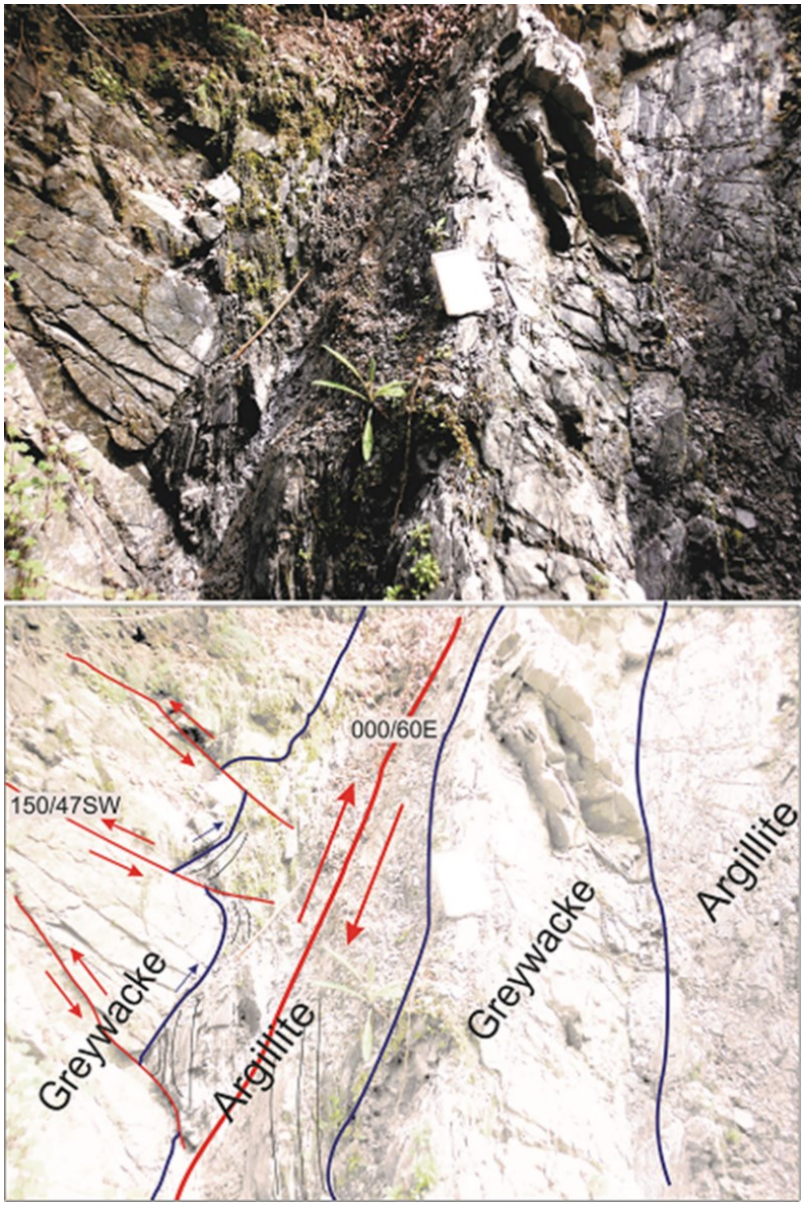

Figure 3-48: Tectonic activation of argillite beds with consequential block faulting of greywacke beds at site 6.10. Notebook for scale.

3.7.4 Corbett Creek

This is the creek referred to as Deep Creek by Wellman, 1950. In the same work he described in detail an infaulted wedge of Tertiary limestone, mudstone and conglomerate within basement greywacke and granite on either side. This site was visited during this study in order to try to constrain the timing and kinematics of the fault that bounds this infaulted wedge.

The sequence of outcrops observed along this creek was complex and difficult to interpret. Heading up from the base of the creek, the first outcrops observed were Upper Blue Bottom

sandstone and conglomerate gently dipping to the west. The last of the Upper Blue Bottom outcrops was located around 400m upstream from the end of open farmland (site 6.11).

Greywacke outcrop was found around 60m upstream from this point, indicating a contact; likely a fault, had been crossed. Highly fractured and cataclasised greywacke continues for around 250m upstream. For a large portion of this stretch of the creek, the rock mass is intensely sheared, gouged and hydrothermally altered. The heavily gouged material is coloured purple and green. There are also zones of fine white clay. No dominant shear planes were found within this zone, therefore making it impossible to get any sense of the general fault orientation or sense of shear.

This is followed by a zone of granite about 100 m long. This section of the rock mass had a number of more discrete shears, although no kinematic data were recorded from these. The upstream boundary of the granite is an exposed fault contact with conglomerate and mudstone. This fault is marked on the map (Figure 3-7) directly downstream from site 6.12. The fault has a gouge zone around 30cm wide, and had a measured strike and dip of 055/73 SE. Given that the beds upstream of the fault have been re-oriented to sub-vertical (Hamil, 1972), it is possible that the fault has been re-oriented also.

Upstream of the fault, there is a zone about 50m long of conglomerate, sandstone and mudstone. This unit has been heavily sheared and no clear bedding orientation has been preserved.. It contains mostly granite clasts, but also mudstone, greywacke, coal and limestone. A fault plane within the sheared material has a strike of 080/85S, although no sense of movement could be determined. This fault appears to bring well indurated, well rounded conglomerate on the downstream side up against more poorly indurated and highly deformed muds, sands and angular conglomerate on the upstream side.

Above the conglomerate, sandstone and mudstone there is a 20 m section of very hard, grey, calcite veined limestone (site 6.12). This limestone is fairly rich in biotite, and contains some quartz grains which were interpreted to come from a distal eroding granite source. Subvertical NNE-SSW striking stylolite planes were found, but it was unclear whether these were inherited from bedding or maximum compression planes (i.e. like cleavage). Both the upstream and downstream contacts were obscured, with the upstream contact being covered by a recent landslip. Both Wellman (1950) and Hamil (1972) reported observing the upstream contact and noted a limestone cemented pebble conglomerate with clasts almost purely composed of Greenland Group on an unconformable contact with Greenland Group. This observation, along with others Hamil (1972) made on the grading of sandy beds within the limestone indicate that the younging direction of the sequence is undoubtedly downstream.

Greenland Group outcrop was followed up the creek for around 150m. A number of thin (<10cm) shear zones were observed and measured (site 6.13), with none appearing to be structurally important. As has been observed at Bell Hill, the orientations of these shear planes appeared to be determined by the pre-existing bedding and cleavage fabric. The amount of shearing observed in this Greenland Group outcrop was, in general, considerably less than that observed in the outcrop downstream of the in-faulted tertiary limestone and conglomerate.

3.7.5 Clear Creek

A visit to this locality was not made during this study, although a number of previous workers have described a thicker, but poorly exposed continuation of the in-faulted limestone and conglomerate sequence seen in Corbett Creek. Here, the western edge of the Early Miocene conglomerate and mudstone that overlies the limestone is mapped by Suggate and Waight (1999) as coming into direct fault contact with the Pliocene Eight Mile Formation beds.

3.7.6 Previous palaeontological ages of sediments found across the western Hohonu Map

The Fossil Record Electronic Database (www.fred.org.nz) was consulted for previous work done on the palaeontological ages of both the in-faulted sediments in Deep, Corbett and Clear creeks and the Eight Mile Formation sediments in the footwall of the fault across the northwest margin of the Hohonu Range. The in-faulted mudstone conglomerate has been assigned an age with faunal assemblages as Waitakian-Otaian, with another age as possibly Altonian. These ages are consistent with the assignment of the Hohonu Conglomerate being a member of the Inangahua Formation (Suggate and Waight, 1999). The Eight Mile Formation only has ages from the Greenstone River, here, faunal assemblages show it to be Waitotaran or Late Pliocene in age.

3.8 Summary of fieldwork

3.8.1 Mapping major fault structures

Fieldwork completed during this study was not sufficient to comprehensively map the positions, orientations and kinematics of the most significant faults (those with offsets in the order of hundreds of metres) in the hangingwall of the Hohonu Fault. This was partially due to a lack of time, the difficult terrain of the field area, and also due to the fact that the most significant fault zones are also the most erodible and/or covered with Quaternary sediment. However, the data that were gathered did enable suggestions to be made as to the potential position of significant faults. This was done by noting significant changes in the general degrees of deformation of the rock mass and changes in cleavage and/or bedding orientation. For Bell Hill (Figure 3.3), cleavage

maintained the broadly the same orientation across the area (see Figure 3-49), and localised deviations from this can be attributed to faulting. The overall sense of movement on these inferred major faults is constrained from the kinematics collected from nearby smaller shear planes that are interpreted to have formed in the stress field associated with movement on the adjacent major fault. It is accepted here that it is necessary to measure a considerable number of these shear planes adjacent to a major fault zone in order to get a statistically robust estimate of the overall sense of movement. This is especially the case in Greenland Group rocks where deformation is more diffuse, and not so much of an issue in granitic rocks where shearing is more localised along specific fault zones. In most cases, with the exception of the outcrop near Bell Hill Retreat, only 1-5 kinematic measurements were taken for many of the major shear zones. For this reason, the sense of movement inferred for many of the mapped faults should be treated with caution.

3.8.2 Bedding and cleavage orientations in the Bell Hill area

Density plots of both bedding and cleavage poles were created for the entire Bell Hill area (Figure 3-49). Both bedding and cleavage show a NE-SW strike, with a clear prevailing SE dip direction. Cleavage tends to range from sub vertical to steeply dipping to the southeast. Bedding tends to dip moderately to the southeast. The western side of Bell Hill is strongly represented in this plot, as more measurements were taken there. Despite this, fieldwork conducted during this study suggests cleavage striking within the NE-SW quadrant is persistent throughout the Greenland Group outcrop in the Bell Hill area. It is also likely that bedding continues to be folded in broad-wavelength, open folds with axes sub-parallel to cleavage (i.e. oriented NE-SW) across the Bell Hill area.

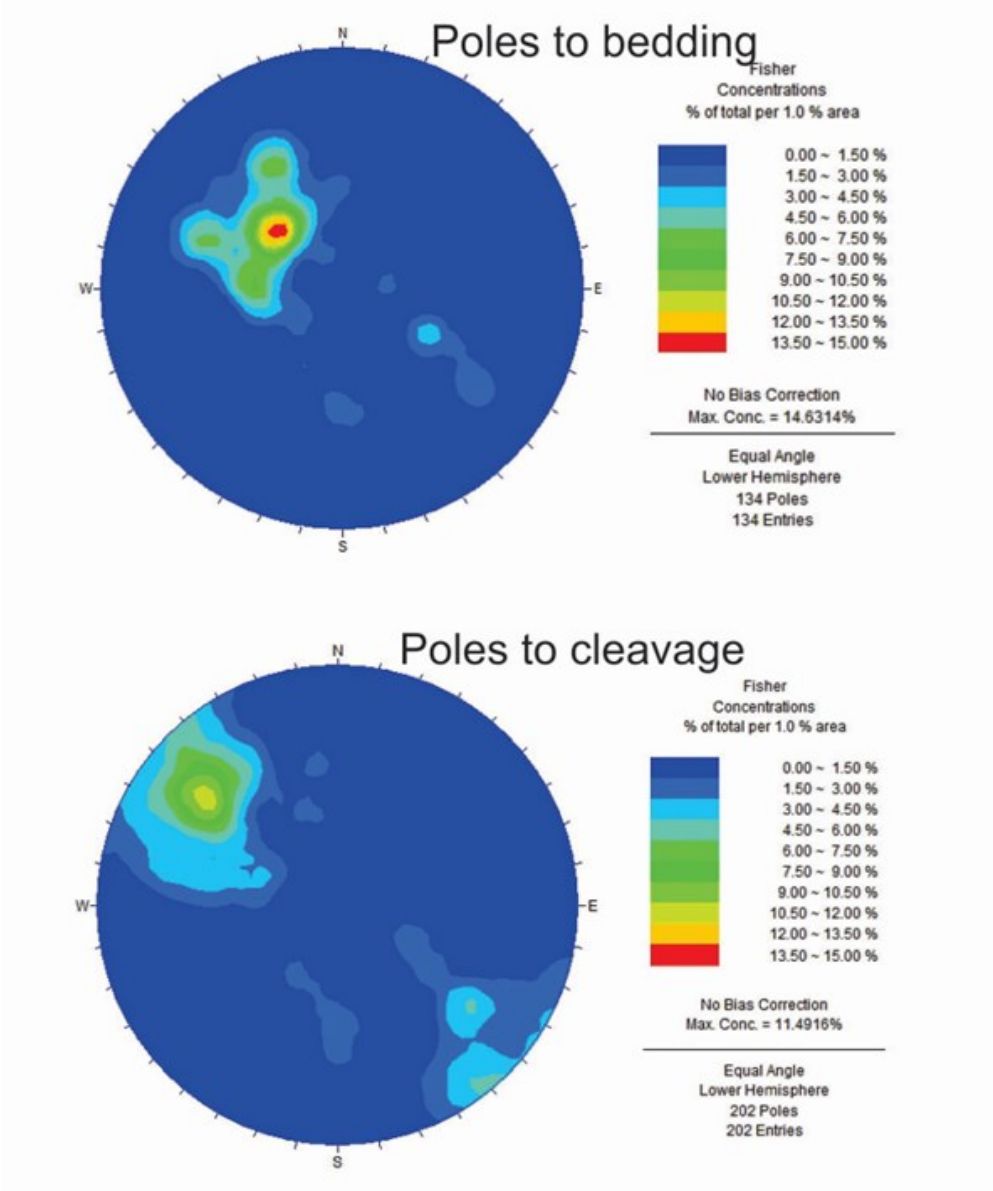

Figure 3-49: Fisher concentration density plots for both cleavage and bedding for the entire Bell Hill area. The plots are lower hemisphere, equal angle projections. These plots show that both cleavage and bedding show a clear tendency to strike NE-SW

3.8.3 **Determining timing of fault activity**

A core problem faced when analysing the fieldwork data was constraining the time of activity of the main faults. Most of the faults observed were within the basement rocks and can only be directly constrained in age as being younger than the cleavage formation in the Greenland Group, or younger than the age of intrusion for the Cretaceous granitoids depending on which of these two rock types they cut through. This is unhelpful given that a number of different tectonic episodes have occurred in the study area since these events have taken place.

Waight (1995) provided evidence suggesting that c. 9km of exhumation occurred across the Hohonu Block during the Cretaceous extensional episode (see Figure 3-50). This is likely to have been the point in time the rock mass crossed the brittle-ductile transition and fault breccias and cataclasites began to form (cf. Sibson, 1977). It is therefore assumed that fault breccias and cataclasite zones found across the Hohonu Block during this study formed during or since the Cretaceous extensional episode. The principal interest of this study was to determine the deformation that has occurred in the study area since Alpine Fault inception. For this reason, faults that appeared to be the youngest were of most importance. A "younger" age of faulting is potentially inferred by the relative incoherency of their fault gouge (for example at site 2.9) because the lack of coherence may indicate that they were formed relatively close to the surface in a tectonically uplifting zone. There is also the possibility that alteration and weathering of older fault zone rocks due to exposure at the surface may cause them to become incoherent. The majority of faults observed in the field area were of this nature. Other zones of fault gouge and breccia such as sites 1.2 and 1.8 on the Rocky Creek Fault (see Figure 3-2) were much more cohesive which suggests that they have been exhumed from greater depth since the fault last ruptured. It is therefore possible that this fault was active at any time since the Late Cretaceous. Relatively rare shear zones such as site 2.15 in the lower reaches of Sam Creek and site 3.3 on the unnamed hill northwest of Lake Ahaura, show ductile deformation and they may have formed either early in the Cretaceous extensional phase or before that time. Evidence for fault activity in the Quaternary is shown at site 2.6 (Figure 3.3). This gives some clue on deformation in the Bell Hill area being recent.

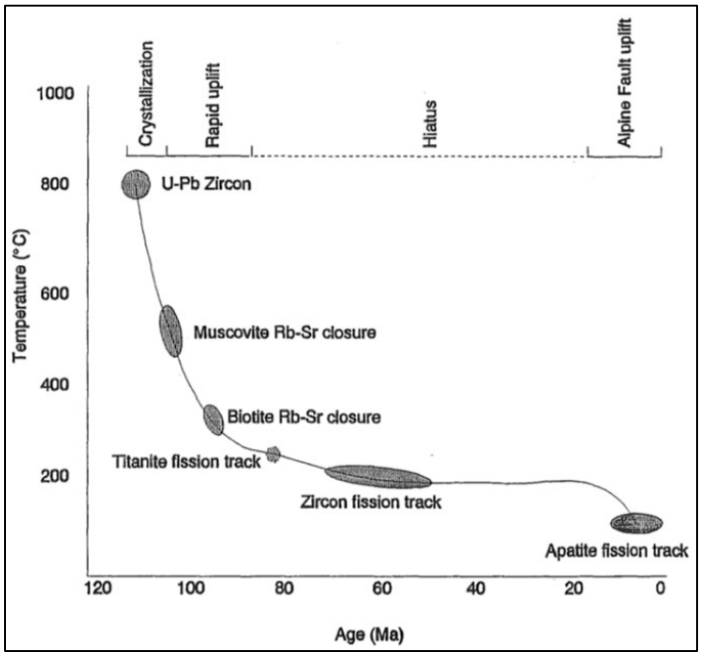

Figure 3-50: Uplift history across the Hohonu Range (from Waight, 1995).

3.8.4 The stress field in which faulting has occured

Agglomeration of all kinematic data collected for the Bell Hill area was undertaken through linked-Bingham analysis in the Faultkin software. This showed that the primary mechanism of deformation is reverse faulting under a S_{Hmax} of c. 120° (Figure 3-51). This is consistent with the regional compilation by Townend et al. (2012) showing a highly uniform S_{Hmax} averaging c.115° across most of the South Island.

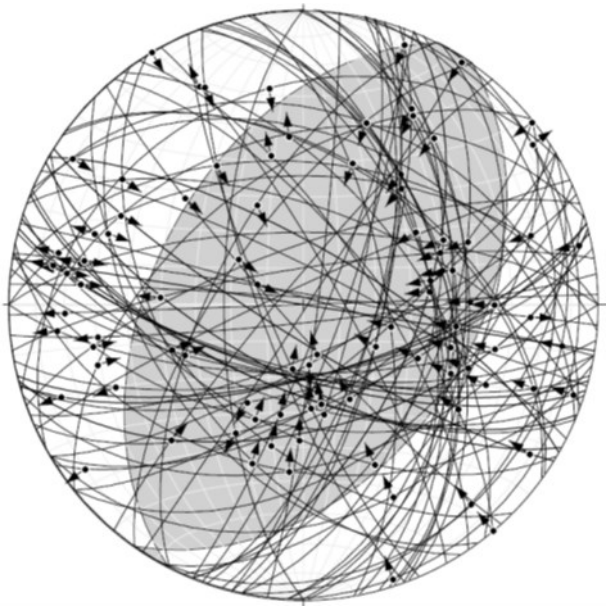

Figure 3-51: agglomerate of all kinematic data recorded in the bell hill area. Linked Bingham solution is plotted behind showing thrust faulting perpendicular to a maximum principal stress orientated at c.120°.

3.8.5 Summary of general kinematics of faults

Diffuse reactivation of cleavage as shear surfaces has been observed in Greenland Group outcrop across Bell Hill and on the western Side of the Hohonu Range. This occurs where the cleavage is well oriented for activation in the current stress field (cf. Sibson, 2009). Cleavage reactivation is possibly an important component of deformation of the bedrock at a large scale.

The localised faulting observed could be summarised into three main modes of deformation. These were:

1) North to northeast striking, west dipping thrust faults as seen at sites 2.1, 2.3, 2.4, 2.4, 2.13 on the Bell Hill map (Figure 3.3), and sites 6.1 and 6.2, which is the principal slip plane of the Hohonu Fault on the western side of the Hohonu Range (Figure 3-7)
2) WNW to WSW striking dextral strike slip faults as seen at sites 1.3 and 1.8 on the Rocky Creek Fault (Figure 3 2), at sites 2.2, 2.11 and 2.14 in the Bell Hill area (Figure 3.3), and at site 6.5 on the western side of the Hohonu Range.

3) WNW to NNW striking sinistral faults as seen at site 2.6 in the Bell Hill area (Figure 3.3), and at site 3.3 on the unnamed hill to the northeast (Figure 3-4). Based on the sharp, NW trending linear topographic boundary along the southwest margin of the Hohonu Range (see, and the sinistral offset of the rangefront compared to the front of the adjacent Mt Turiwhate, a major sinistral fault is inferred here also.

Figure 3-52: Google Earth image of the inferred sinistral fault across the southwest margin of the Hohonu Range. Fault position is indicated with arrows.

3.8.6 Sedimentation across the Grey Valley Trough and Paparoa Inversion Zone after the Late Miocene unconformity

Inspection of the sediments overlying the Late Miocene unconformity underlined the strong contrasts in depositional environment between the Paparoa Inversion Zone and Grey Valley Trough. The Deep Creek Conglomerate is thought to have been deposited in a near-shore setting where there were strong currents could sort the sediment into its bi-modal grain size. It appears that rapid subsidence was occurring in the Grey Valley Trough directly after the formation of the unconformity, providing accomodation space in which the Deep Creek Conglomerate, and later, the remaining Eight Mile Formation could deposit. This is in contrast to the Callaghans Greensand (the basal member of the Eight Mile Formation in the Paparoa Inversion Zone) which was deposited in a shallow water setting, starved of sediment input (Suggate and Waight, 1999). In this study, the presence of a high concentration of magnetite in the Callaghans Greensand is also questioned, and as to whether it was chemically derived in situ of sorted through current action. It

is inferred here that the Paparoa Inversion Zone was a seafloor high probably with strong currents flowing across it, enabling magnetite to concentrate. The Deep Creek Conglomerate in the Grey Valley Trough is interpreted by Suggate and Waight (1999) as showing the first evidence of uplift of the Southern Alps Orogen with the appearance of schist clasts. No schist clasts were observed in the Deep Creek Conglomerate during this study, and it is therefore inferred that at the time of deposition of this unit (Late Miocene) the schists were a very small proportion of the sediment being eroded and transported into the Grey Valley Trough.

3.8.7 Incorporation of pre-existing structures and sediments into the Hohonu fault Zone

The presence of small Oligocene and Early Miocene outcrops directly adjacent to the Hohonu Fault on the northern side of the Hohonu Range (Figure 3-6) is important given that the Hohonu Fault is commonly considered to be a shallowly dipping range front thrust (Wellman, 1950). There are two possible explanations for why these older sediments are present at the surface of the thrust front:

1) The original, un-eroded surface of the hanging wall of the fault is exposed on which pre-fault sediments are still present, or;
2) The fault is actually steeply dipping to vertical at this point, (possibly because of strike slip components), and blocks of pre-fault sediment have been entrained into the fault zone along flower-structure faults.

The in-faulted wedge of Tertiary sediments found in the headwaters of Deep Creek on the western side of the Hohonu Range (Figure 3-7) presents a complex history for the development of the Hohonu Range thrust. The observed angular relationship between the fault plane on the downstream side of the Oligocene and Early Miocene inlier and adjacent bedding planes, suggests that the fault was originally a west dipping thrust fault. It is, at least in this locality, interpreted that this reoriented through becoming involved in the hangingwall of the east-dipping Hohonu Fault. The possible implication is that the Hohonu Thrust developed at a later stage and cross cut an Early Miocene west-dipping thrust zone.

CHAPTER 4. MAPPING STRUCTURES, AND CREATION AND RETRODEFORMATION OF GEOLOGICAL CROSS SECTIONS USING MOVE.

4.1 Introduction

The main aim of this chapter is to provide a regional structural synthesis of the study area by incorporating open source borehole and seismic data, published surface data from geological maps, aeromagnetic data, and observations gathered during fieldwork. The main outputs of this are: (1) a tectonic map that shows the structures that occur across the study area and their context in the present tectonic setting (displayed in Figure 4-1); and (2) two balanced and restored cross sections that display the Neogene tectonic evolution of the study area (the traces of these are also in Figure 4-1). The primary tool used to produce these outputs is Midland Valley's MOVE software (under academic license to the University of Canterbury). This is a structural geology computer program that allows input of data into a 3D model where it can be displayed in 3D, section view or map view. Cross sections created in this programme can then be balanced and restored using fault movement, folding and decompaction algorithms.

Revised fault map of the study area

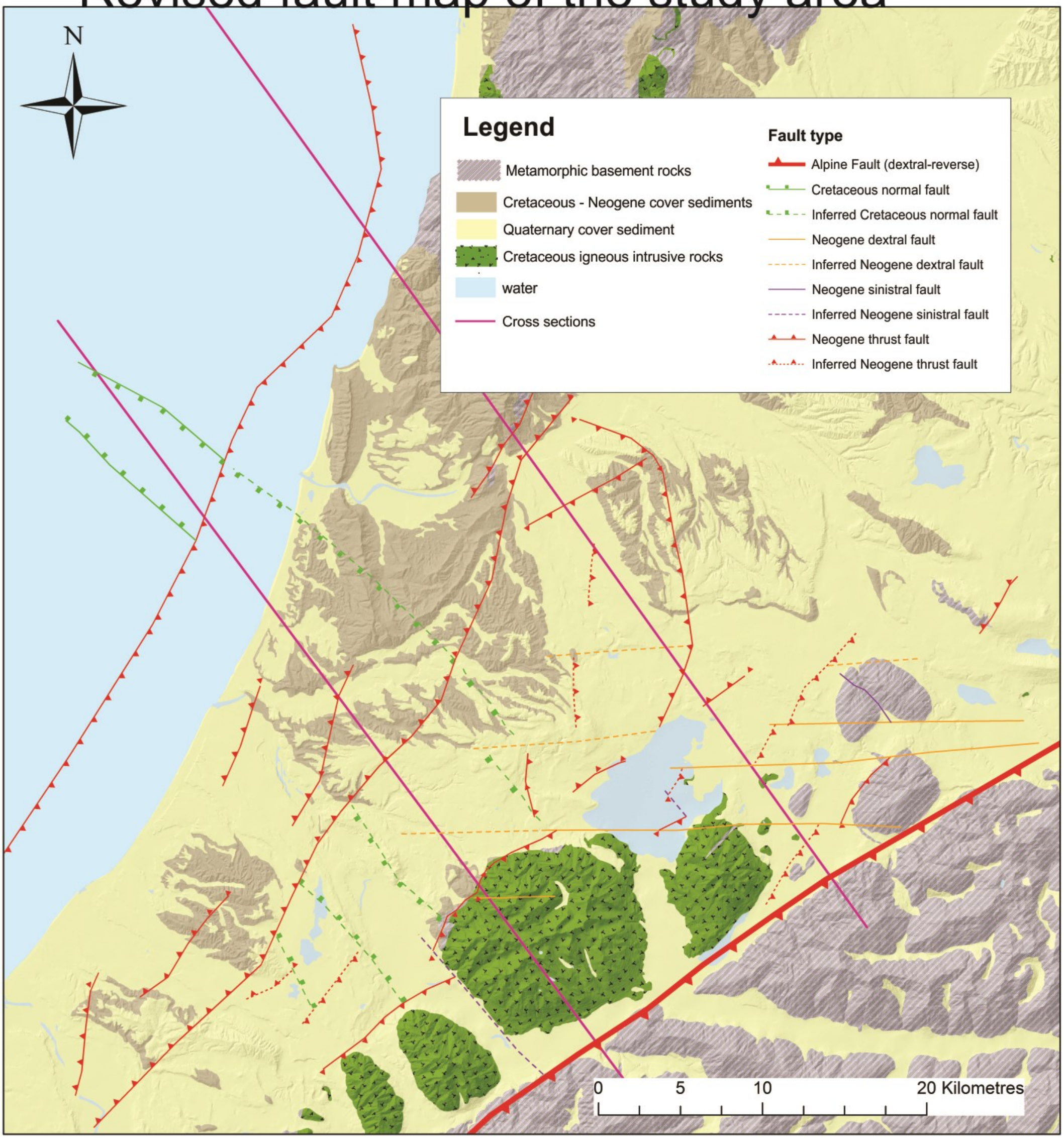

Figure 4-1: Tectonic map that summarises the structures identified during analysis of field observation, seismic profiles and aeromagnetic data

4.2 Inputs into the Move Model and their sources of error

4.2.1 Surface data

Surface data incorporated into the model includes where sedimentary contacts and faults are mapped at the surface, as well as bedding dips. Small-scale published maps by Suggate and Waight (1999) (1:50000) and Nathan (1978) (1: 63360), enabled relatively detailed surface data to be obtained for most of the study area. The Greymouth QMap (Nathan et al, 2002) covered the remainder of the study area at a 1:250000 scale. Georeferenced scans of these maps were put into the model which was set up with the same projection and geodetic datum as the QMaps (NZGD1949). Specifically for the Greymouth map by Nathan (1978), the coordinate system was different to the model, making georeferencing more difficult. The positions of contacts and faults were used by matching them with those on the QMap to make a best-fit georeferenced map. The maximum error associated with these georeferencing issues is c.200m.

Once georeferenced, all of faults, sedimentary contacts and bedding dip data from the maps were digitised. Small editions to the locations of some of the contacts and faults were made based on fieldwork observations. Many of the Cenozoic contacts mapped are at least partially obscured by overlying Quaternary sediment units as, for example, in the case of the contact between the top Stillwater Mudstone and the Callaghans Greensand. Projections of the contacts were made across the overlying Quaternary sediments, linking the mapped Cenozoic contacts. For the Callaghans Greensand and to some extent the Deep Creek Conglomerate, obscured bounding contacts were validated using the aeromagnetic data (see Figure 4-6). Once digitised in the correct geographic location, the surface data were then projected onto a 15m digital elevation model of the area to give their location in 3D space. A map view screenshot example of contact and bedding dip data within the MOVE program can be seen in figure 4.1

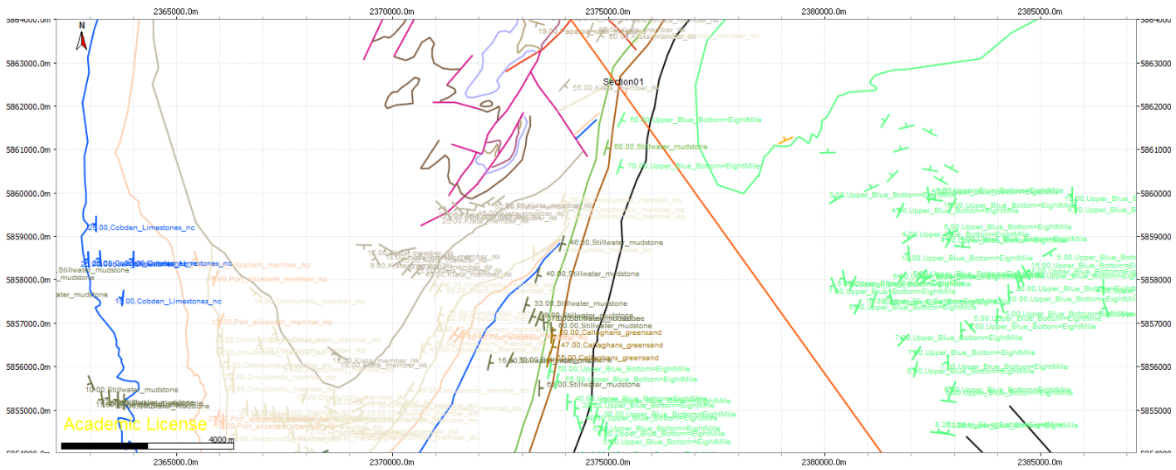

Figure 4-2: Surface contact and dip data displayed in map view in MOVE.

4.2.2 **Borehole Data**

To insert wells into the model, the geographic location, and the depth relative to sea level of the horizons in the well at that location were required. An important error associated with the input of well data was the certainty of the geographic location. Sources for grid references of well locations in the study area included a list of boreholes presented by Suggate and Waight (1999), and well completion reports from the New Zealand Petroleum and Minerals website (www.nzpam.govt.nz). In a number of cases, the grid references for individual wells varied considerably (sometimes by over 1km). If this was the case, the well completion report location was considered to be the most valid and was used. Another source of error in the well data was the variance in interpretation of the depth and classification of horizons in the wells. A number of small changes were made to the interpretations by Suggate and Waight (1999). These changes have been incorporated into the well data for this study. Picks for some of the gradational boundaries such as the one between the Inangahua Formation and the Stillwater Mudstone were inserted into the model. Because of their nature, the picked elevations of these horizons were treated with a high margin of error when tying with seismic profiles. The wells have been projected into the model assuming no deviation from the vertical. For some of the wells deviations data are not available. However, considering the scale of the model, any error in horizon depths associated with the deviation of the well tracks would be negligible. Figure 4-3 shows the locations of the boreholes in the study area that have been used for the model. The list of boreholes with grid referenced location and horizon elevations is given in Figure 4-4.

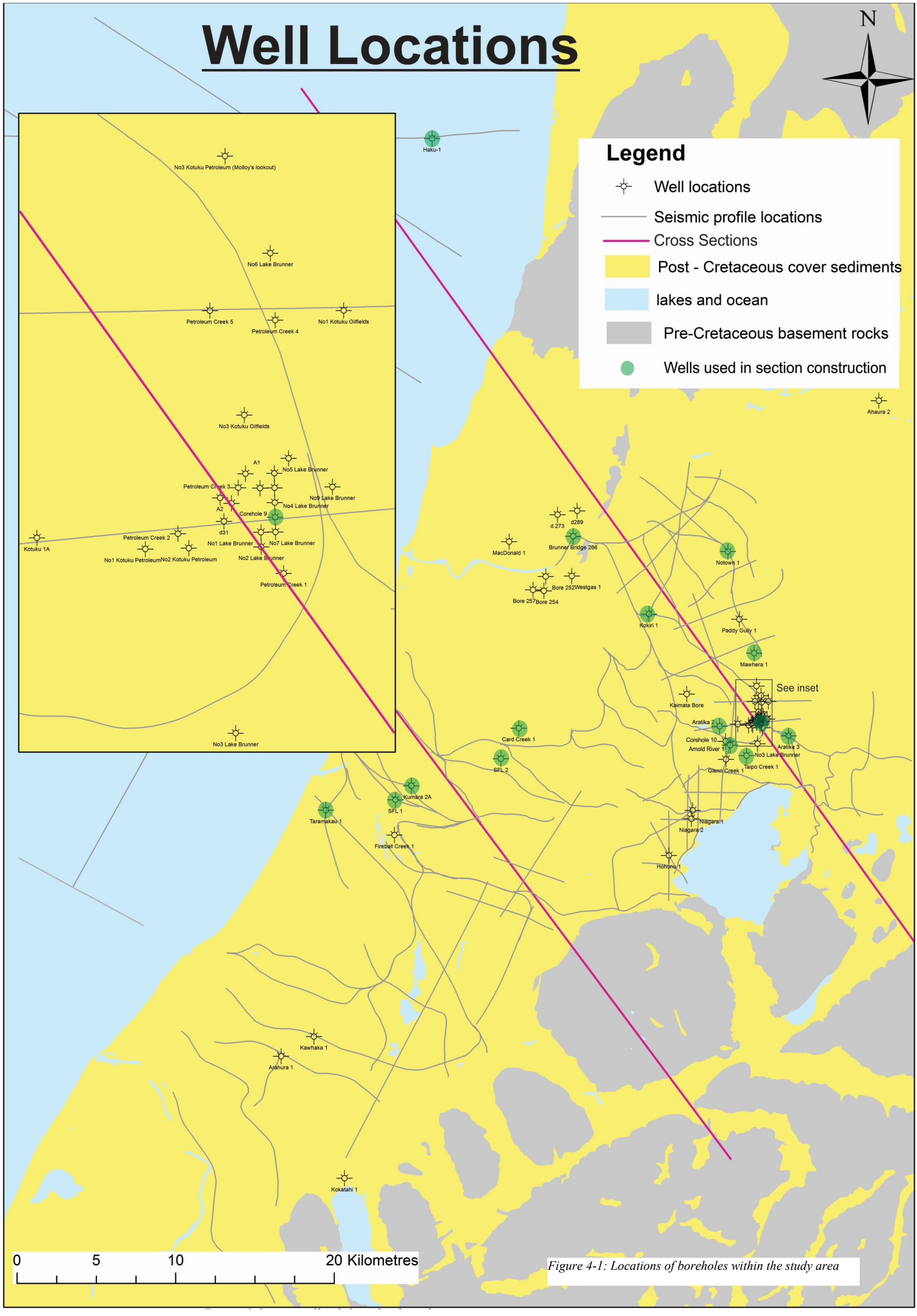

Figure 4-1: Locations of boreholes within the study area

	Grid reference (NZGD 2000)		Horizon tops																				
well	East	North	KB	q	be	ben	bec	bed	bs	bi	nc	rkp	rko	rkk	ri	rm	br	ap	ph	g	TD		
North Section																							
Haku-1	2363238	5887598	30		-245				-890	-1202	-1426	-1486		-1539						-1623	-1638		
Brunner Bridge 266	2372113	5862495	18														18	-26		-595	-598		
Kokiri-1	2376886	5857391	53	47	-31	-472			-992	-2427	-3149									-3150	-3180		
Notown-1	2381861	5861346	81	81	76	-721			-852	-1753	-1973						-2006			-2028	-2034		
Mawhera-1	2383511	5854923	251	251	244			-79		-173	-242						-290	-376			-446		
Aratika-2	2381344	5850507	91	83	80			39	-122	-454	-484						-534	-575		-701	-1058		
Corehole 9	2383985	5850863	98	98					78	54	-23						-68			-103	-140		
Arnold River-1	2382004	5849313	93	93					-105	-205	-387						-429	-493			-617		
Taipo Creek -1	2383044	5848655	124	124					-153	-380	-492						-526			-536	-555		
Aratika-3	2385691	5849907	118	113	13			-192	-395	-1082	-1592									-1593	-1611		
South Section																							
Taramakau-1	2356507	5845023	36	31	9		-43		-55		-786	-881		-939			-1689		-1887	-1977	-2093		
SFL-1	2360902	5845865	75								75	-107	-192	-578	-1544		-1567				-1588		
Kumara-2	2361897	5846751	71	69					67		7	-182	-337	-654	-1584		-1601	-1684			-1700		
Card Creek 1	2368679	5850382	66						64		-198	-336	-489	-899	-1089		-1093	-1152			-1276		
SFL-2	2367547	5848262	122						122		-381	-418	-498								-786		

Figure 4-2: Table showing horizon elevations in metres above sea level for all wells used in construction of cross sections. Shorthand for units are used (refer to Figure 2-2). Locations of wells can be seen in Figure 4-1.

4.2.3 Seismic Profiles

New Zealand Petroleum and Minerals enables access to effectively all of the seismic data available for the study area in processed, reprocessed and migrated form. For some seismic data, 2 or 3 different forms of the migrated profiles are available. If this was the case, the most recently processed of these were used in the model. The geographic traces of the available seismic lines are shown in Figure 4-5.

Many of the lines analysed for this study were available by order from New Zealand Petroleum and Minerals as seg-y files. Files of this form were put directly into the model, appearing as a vertical section along the profile's trace with time as the vertical dimension. The only alteration that had to be made (specifically for the onshore data) was for the profiles to be moved vertically in order to align them with the sea-level datum. This was done by looking at already sea-level-aligned profile images available in petroleum reports and matching the two-way-time of significant reflectors at specific locations. Alignment with the sea level datum is necessary for the depth conversion process which will be described later.

Some of the important profiles such as line 8 offshore were not available as seg-y files, although images of them were present as enclosures in petroleum reports. If this was the case (as with the area offshore Greymouth) a vertical image of the profile was imported onto a vertical section along the profile's geographic trace. This was done by: firstly, georeferencing shotpoint maps of the profiles that are available in the petroleum reports. Secondly, a section trace was created along the trace of the profile. Thirdly, a vertical image of the profile was then imported onto the section. Fourthly, this image was then stretched so that it's shot point locations matched with the map, and it's time scale matched with that of the model. Some of the onshore profiles had very irregular traces (eg. PR75-87-505). For these, a simplified, more direct section trace was created, and the location of the vertical image of the profile on the section was more approximate. This is likely to have been a significant source of error (up to c. 1km) in the northeast part of the seismic grid, where the method had to be used most.

Quality of seismic lines ranged from good to poor, with some lines basically uninterpretable. Two factors may have affected this – rugged topography and intense faulting in some localities – smaller, better quality lines done more recently by Ocean Harvest International Ltd (2008) near the Niagara wells suggest that the poor quality from previous lines is mainly due to the inadequate shot hole depth.

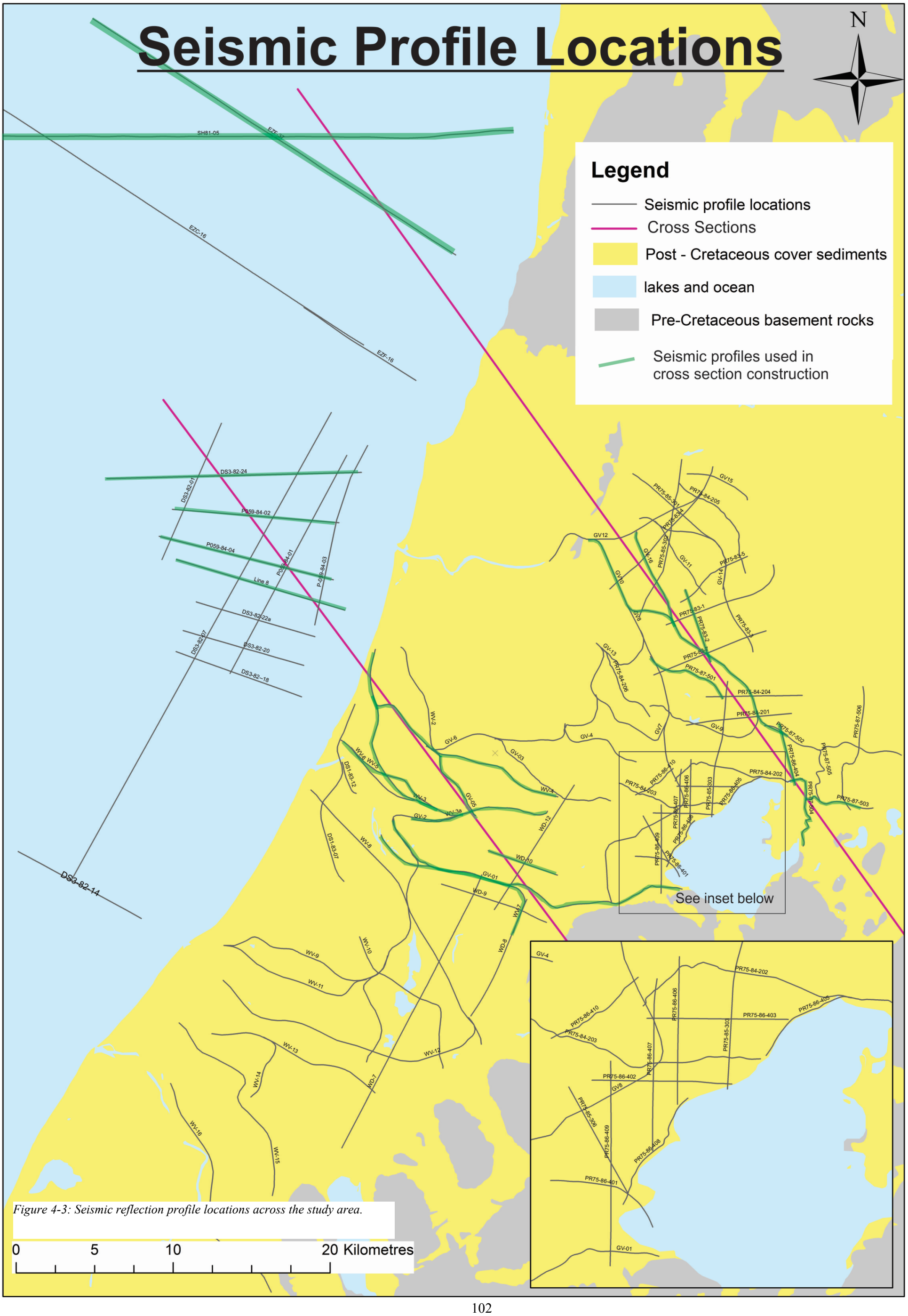

Figure 4-3: Seismic reflection profile locations across the study area.

4.2.4 **Aeromagnetic Data**

The aeromagnetic data used in the model are from New Zealand Petroleum and Minerals as part of a recently released (2013) dataset from an airborne magnetic survey across a large portion of the West Coast region (cf. Vidanovitch, 2013). A number of different magnetic grids derived from the raw data were provided in the dataset. Of these, the grid that was found most useful to map potential structures and important stratigraphic horizons in the study area was the basic levelled total magnetic intensity as displayed in figure 4.4. This grid showed the changes in magnetic susceptibility of the sediments across the Paparoa Inversion Zone and Grey Valley Trough, as well as showing up the broad changes from the underlying basement. Other derivative grids are often used for delineating fault structures, but the total magnetic intensity still shows the truncation of magnetic anomalies required to locate a fault. The grid is available as a georeferenced raster file, so it was easily imported directly into the Move model.

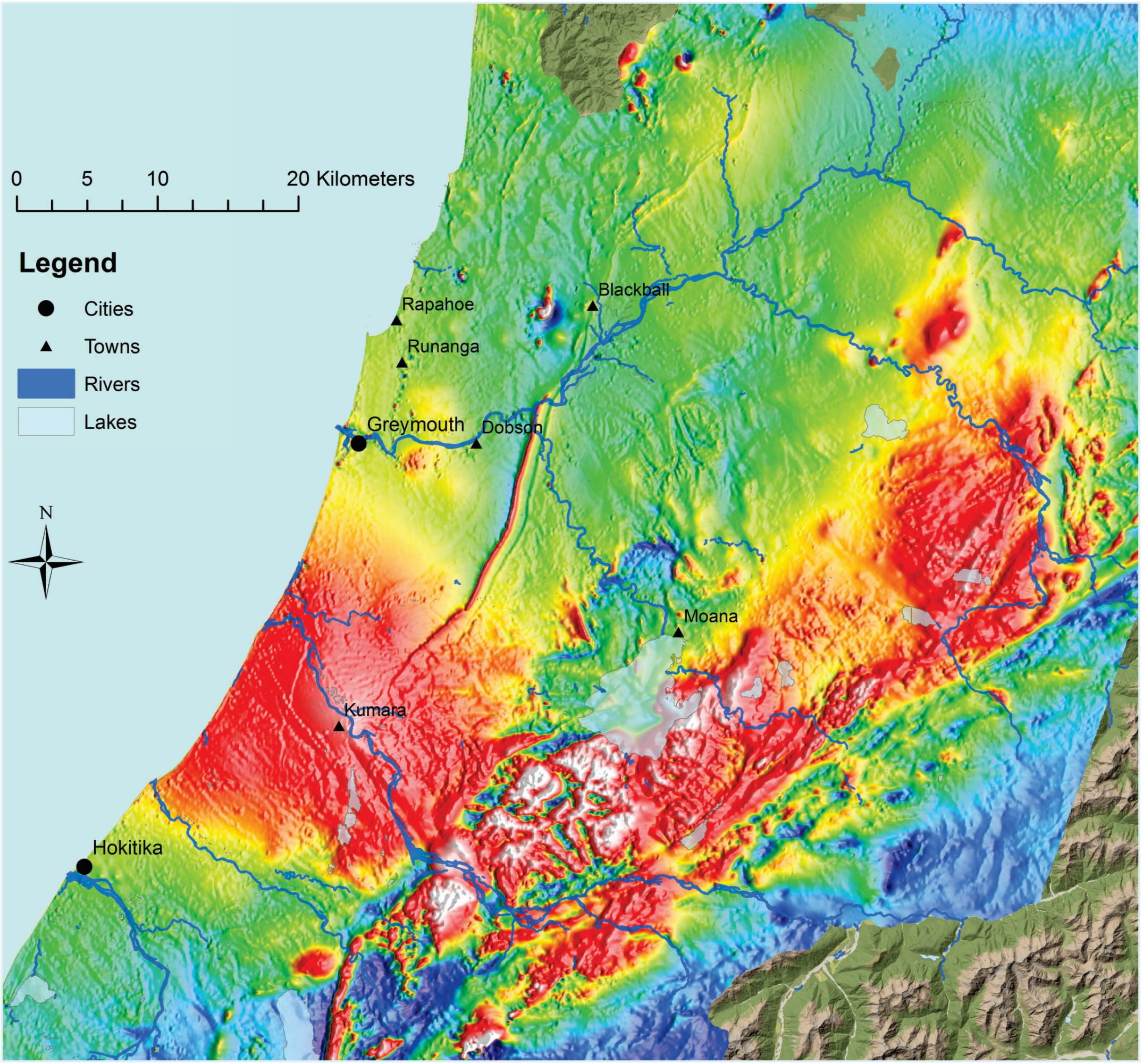

Figure 4-6: Uninterpreted aeromagnetic data of the study area. Sourced from New Zealand Petroleum and Minerals

4.3 Mapping Faults across the Seismic Grid

4.3.1 Methods

For this part of the study, the entire seismic grid across the study area (Figure 4-5) was interpreted for the purpose of determining the extent and nature of discrete fault structures (as seen in Figure 4-1). Using horizons in wells (Figure 4-4) as guides for reflector identification, some linking of horizons around the seismic grid was undertaken for the purpose of identifying the timing of activity on faults. However, a comprehensive interpretation and identification of horizons throughout the grid was deemed impossible given the poor quality of a number of the profiles.

Structures were mapped by plotting the location of the truncation of key reflectors (such as the top Cobden horizon) across the seismic grid (see Figure 4-8 for example). Structures that were intersected 3 or more times in different locations by seismic profiles were mapped with certainty and were represented with a solid line. Structures crossed only 1 or 2 times, or possibly more, but with poor quality profiles, were mapped as inferred and represented with a dotted line.

Faults were classified by three criteria: size, type of fault and kinematics. Faults were classified as major and mapped with a broader line if the vertical movement on the fault was greater than c. 300 m. Faults with smaller vertical offsets were classified as minor and marked with a thinner line. The fault types identified were normal, reverse, possible strike slip and reflector-bending structures where an up and a down side were also identified. Possible strike slip faults were identified thanks to the truncation or warping of reflectors across sub-vertical zones of separation, possibly in connection with the presence of flower structures. The different groups of faulting identified by orientation and kinematics were NNE-SSW directed extension (represented in lime green), WNW-ESE directed extension (represented in blue), and WNW-ESE directed compression (represented in red). Each of these groups of faults are thought to have developed in separate tectonic regimes, these being the Late Cretaceous extensional, Paleogene extensional, and Neogene compressional regimes.

In poor quality profiles, often only the bending of reflectors was mapped. In this case, the inflection points of significant reflectors were traced with the up and down sides marked. Due to the basement reflectors usually being of very poor quality or non-existent, the structure that controls the bending of the overlying strata is very difficult to constrain.

4.3.2 Results

A number of unpublished petroleum reports have already mapped the structures in the study area across the seismic grid (Buchan, 1997, Booth, 2008, Haskell, 2007, Matthews, 1992 (PR1960, Haskell, 1991 PR1752, Toomath and Palmer, 1987 PR1327). These have collectively identified the major structures in the area including the Cape Foulwind Fault, Takutai Half Graben, Tansey Fault, Grey Valley Fault, Nemona Fault and Moana Fault (see Figure 4-7). In areas where the seismic quality is relatively poor, a number of different interpretations are possible. Tracing of structures through the seismic grid in this study has had the added information of the aeromagnetic data to compare it to. This has helped in providing some constraints on the uncertainties that cannot be resolved from poor quality of seismic imaging of the sub-surface structures. Described below is (1) an example of a structure mapped through the seismic grid, the Kokiri-Notown Fault, and (2) two sets of structures that have been mapped in this study that have either not been identified before or recognized to some extent, but not focused upon. These are a set of east-west trending strike slip faults that cut across the Kotuku anticline, and a series of WNW to NNW trending structures in the southern Grey Valley Trough

4.3.2.1 Kokiri-Notown Fault

This fault has been previously mapped by Buchan (1997) and Mathews (1990), and is used here as an example of a mapped fault through the seismic grid (Figure 4-8). The fault is characterised by a reverse offset of the basement reflector, and a west-verging fault propagation fold in the Neogene strata above. This fault was mapped by tracing the point at which the top Cobden Limestone reflector was truncated in the hanging wall across the seismic grid.

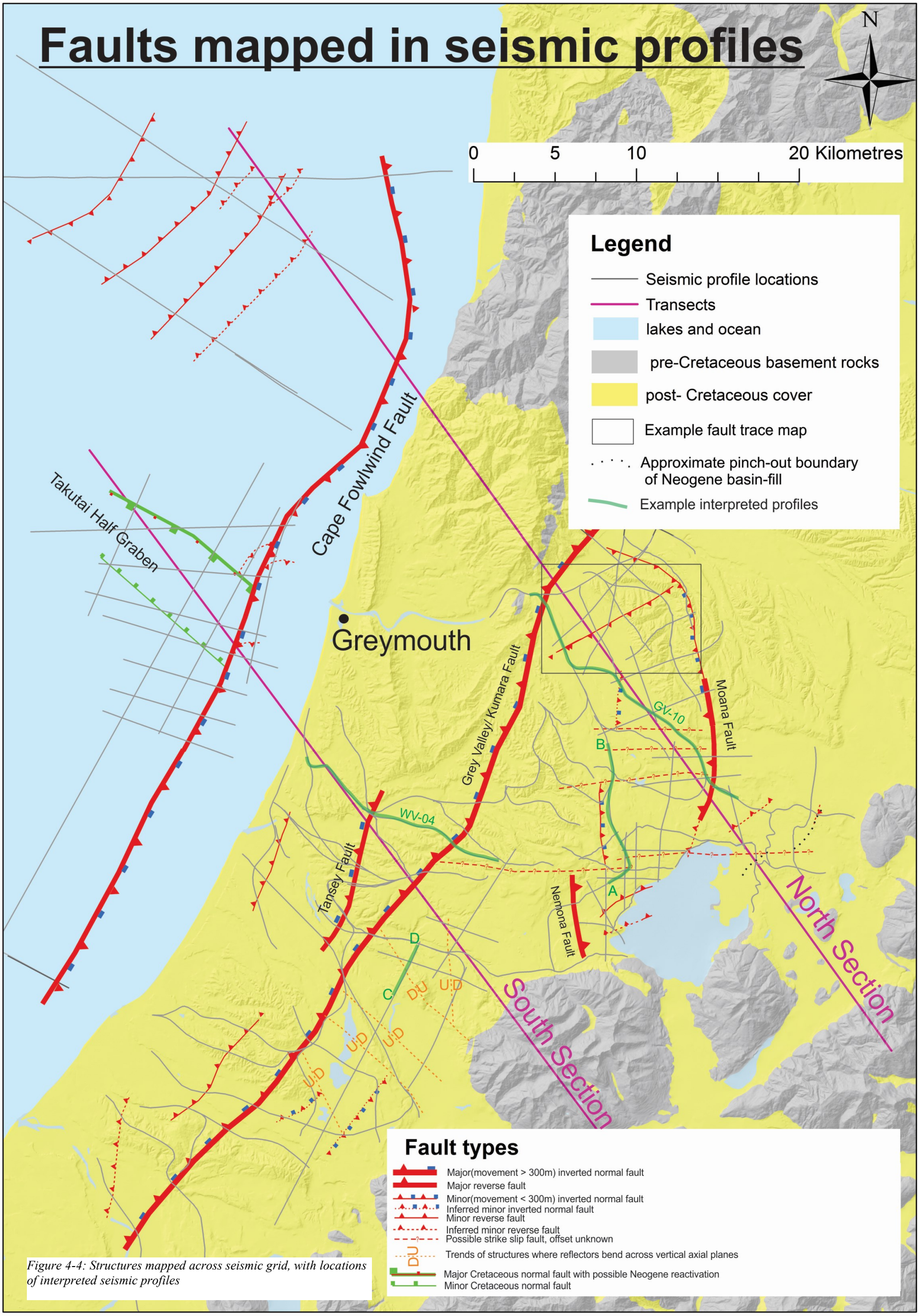

Figure 4-4: Structures mapped across seismic grid, with locations of interpreted seismic profiles

Examples of fault mapping in seismic profiles

Location map

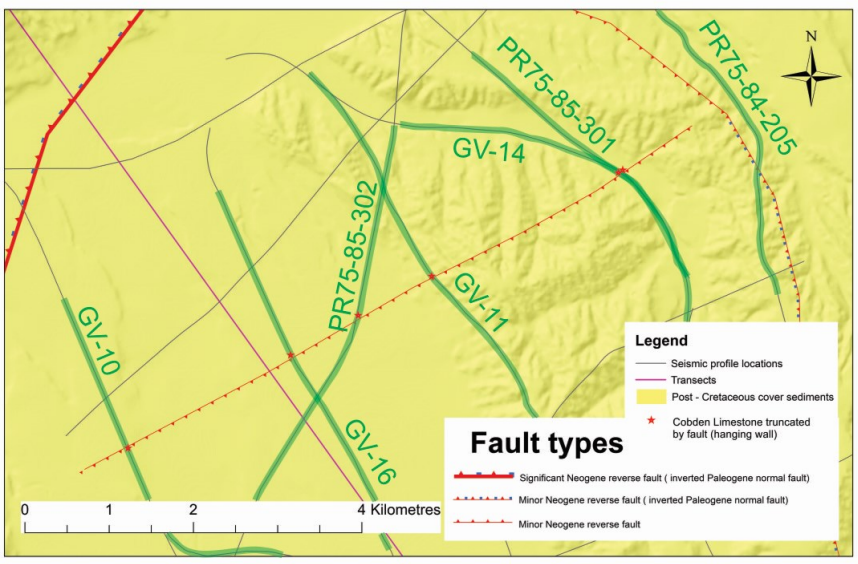

PR75-84-205

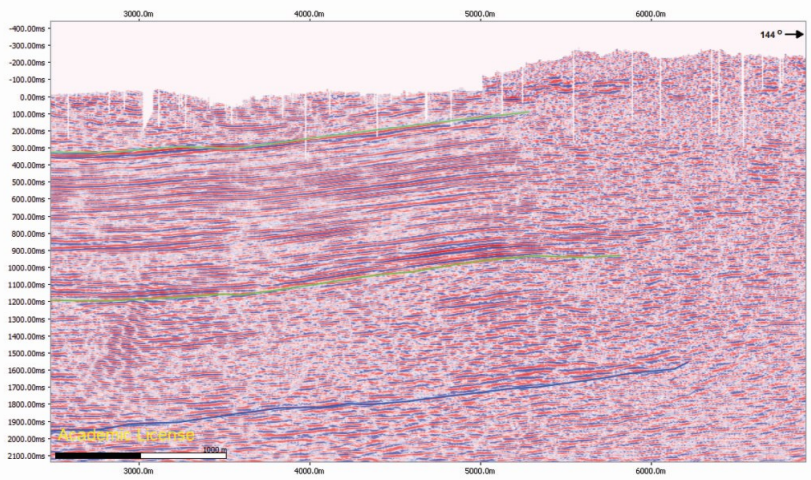

GV-10

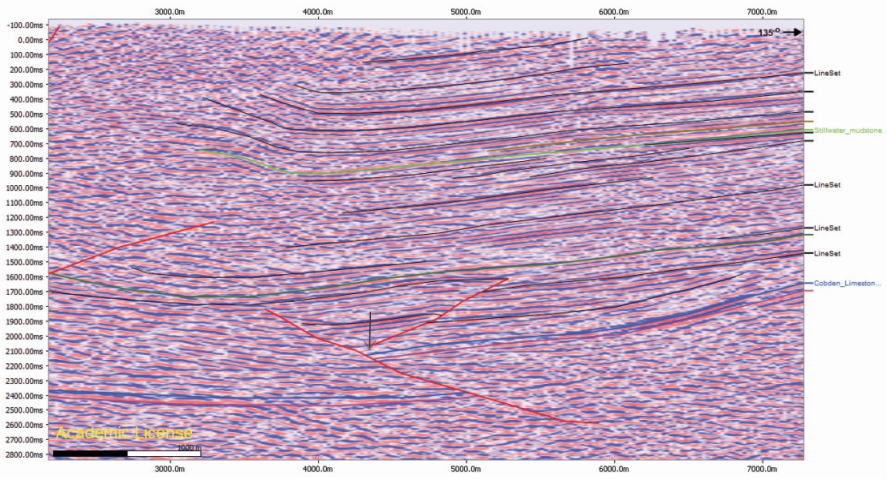

PR75-85-301

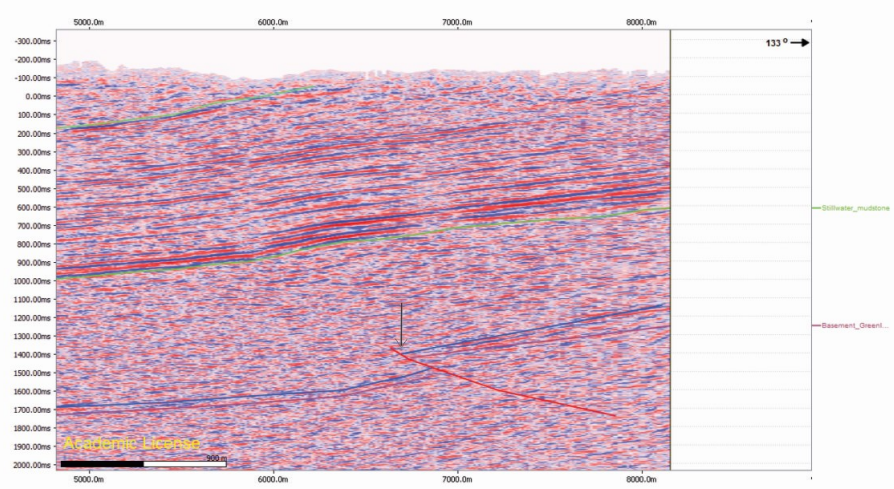

GV-16

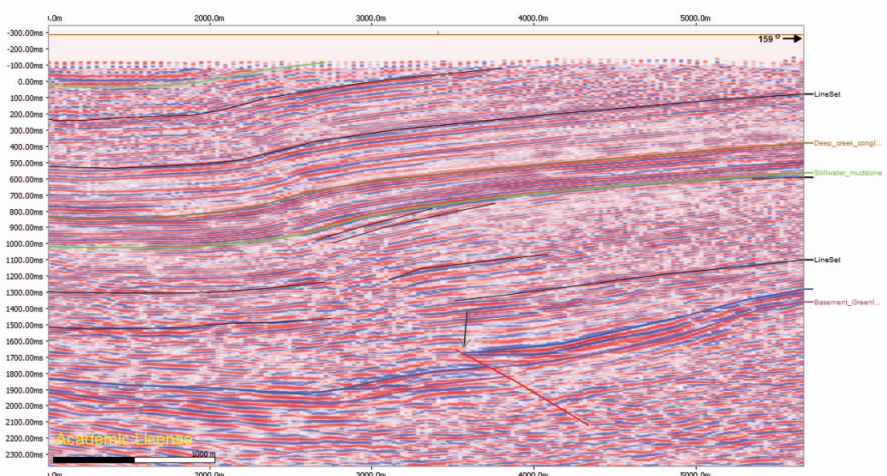

GV-14

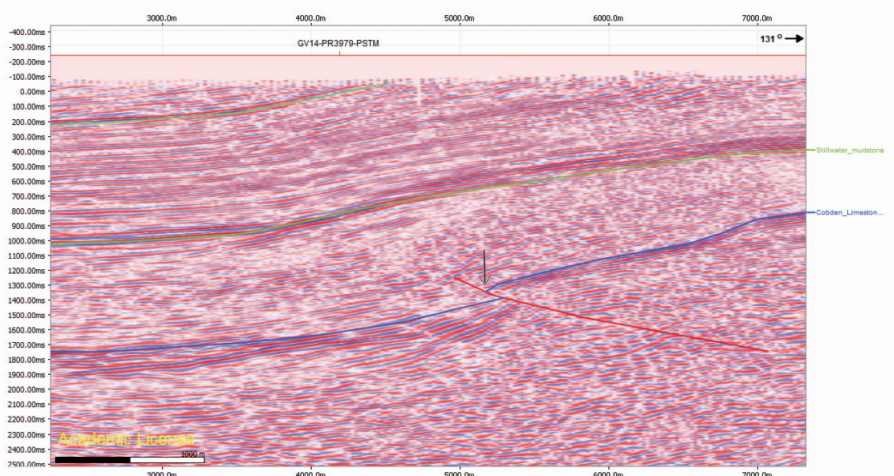

PR75-85-302

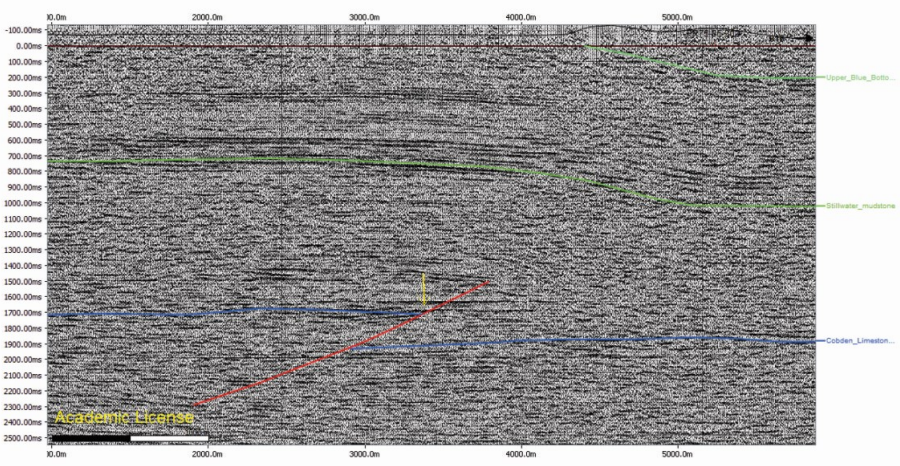

GV-11

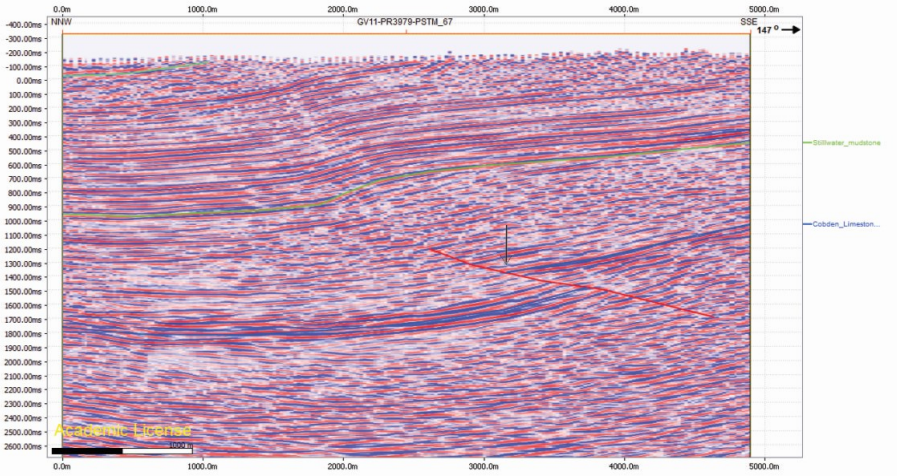

Figure 4-5: Example of tracing the Kokiri-Notown Fault across the seismic grid. The point where the top Cobden reflector is truncated in the hanging wall of the fault is marked with an arrow on each profile.

4.3.2.2 East-west strike slip faults across the Kotutu Anticline

The set of inferred east-west strike slip faults across the Kotuku anticline has been mapped as a result of integration with interpretations from the aeromagnetic data. In general, the quality of the seismic profiles in the area where these faults have been inferred is poor, often with very little continuous reflectors leaving a broad range of possibilities for interpreting the nature and orientation of structures in the area. GV08 is the best quality profile in the area. This profile shows two potential strike slip faults as sub vertical structures that offset and truncate significant reflectors (Figure 4-9). These structures coincide with east-west trending linear features interpreted in the aeromagnetic data (see Figure 4-11). Interpretation of the poor quality surrounding profiles also comply with the potential existence of east-west striking faults.

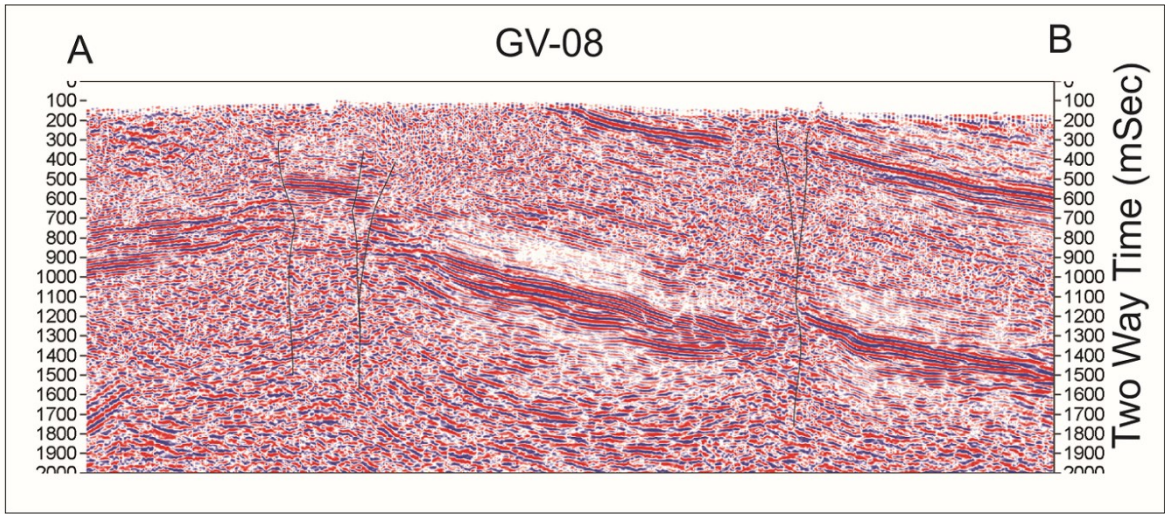

Figure 4-9: Section of GV-08 showing suspected strike slip faults that match up with east-west striking linear features on the aeromagnetic data. See figure 4.5 for section location.

4.3.2.3 Subvertical bending of reflectors through NW-SE striking axial planes in the southern Grey Valley Trough

A number of locations where reflectors bend through NW-SE striking vertical axes in the Neogene sequence were identified in the profiles of the southern Grey Valley Trough. Mostly due to the poor quality of the seismic profiles, the nature of the basement faults that are thought to control these reflector-bending structures is unknown. An important and typical example of these structures is the one intersecting Lines WD-7 and WD-9. This structure is situated at a location where the basement unconformity may be up to 5 km deep, and consists of a ESE-WNW trending, c. 1 km wide zone of gentle bending of reflectors that extends from basement levels through to the surface (see Figure 4-10). Structures of this orientation at this location were also mapped by Haskell, (1991).

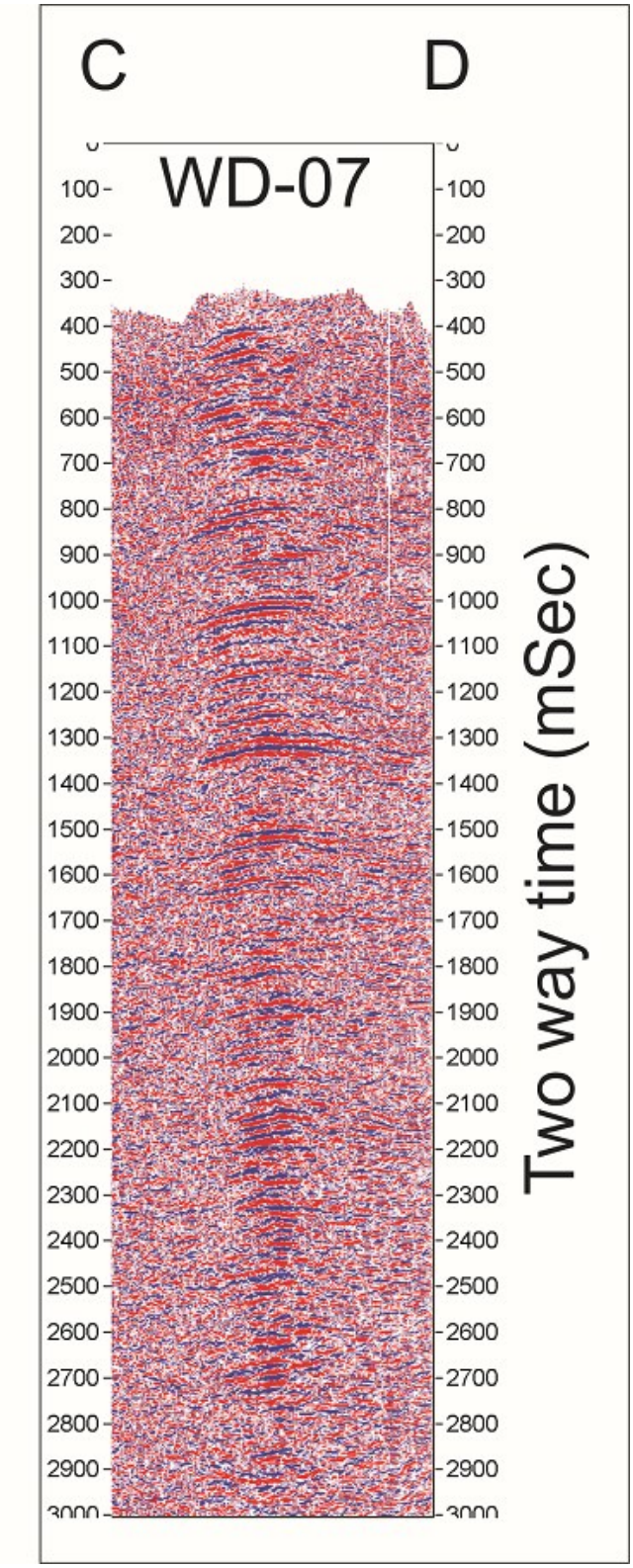

Figure 4-10. Example of bending of reflectors along a vertical axial plane from WD-07. See Figure 4.5 for section location.

4.4 Interpreting aeromagnetic data

4.4.1 Methods

The interpretation of the aeromagnetic data involved integration of information from previously published maps (Suggate and Waight, 1999, Nathan, 1978), fieldwork observations and seismic mapping. By doing this, the aeromagnetic data were used to gain information about the geology of the study area. This included gaining information on the deformation of important bedding horizons and the continuation of mapped faults beyond the seismic grid.

Linear features across the study area were mapped (see Figure 4-11). Many of these were mapped in red as faults based on three levels of certainty as follows; if they represented faults already documented in previously published maps or theses, they mere mapped with a solid line. If the interpreted faults matched observations during fieldwork or seismic interpretation, they were marked with a dashed line. If the faults were interpreted solely from the aeromagnetic data, with very little evidence of their existence otherwise, they were mapped with a dotted line. Linear features corresponding with mapped stratigraphic horizons were mapped in blue. The remaining linear features that may be associated with the existence of a fault were mapped with a black dashed line.

4.4.2 Results

4.4.2.1 Late Miocene Unconformity

Particularly within the Paparoa inversion Zone, a strong linear magnetic anomaly traces the mapped location of the Tongaporutuan unconformity almost exactly (compare Figure 2-3 with Figure 4-11). This is almost certainly produced by the Callaghans Greensand, a unit that directly overlies the unconformity at the base of the Eight Mile Formation on the Paproa Inversion Zone (see Figure 2-2, refer to section 2.3.7). This anomaly can be seen tracing along most of the eastern side of the Paparoa Inversion Zone within the study area. It appears to be faulted out at two locations (see Figure 4-11), firstly, at the northern end, just north of where it crosses the Grey River, and secondly, at the southern end where the Kumara Fault has been previously mapped (Suggate and Waight, 1999). Directly south of this point, the anomaly can be seen to trend westward as the horizon is exposed across the plunging axis of the Brunner Anticline. It then changes to trend northwards, along the western flank of the anticline. There is a significant step right just before the northern end of this part of the magnetic anomaly that can be attributed to the steep northern bank of the Taramakau River producing an apparent offset of the shallowly west-dipping horizon. The anomaly is also sharply offset on the other side of the Paparoa Inversion Zone, directly east from the point described above. This apparent dextral separation is thought to

be fault related as there is no significant topographical change at this location. Given that the horizon dips steeply to the east at this location, the fault is likely to have either a north-side-up component or a dextral component or a combination of both.

Within the Grey Valley Trough, roughly coincident with the Kotuku Anticline, there is a region of relatively low magnetic intensity sharply bounded to the north and west by relatively high magnetic intensity. Based upon well intersections, seismic data and outcrop mapped to the north of Kotuku, this boundary is interpreted to be roughly coincident with the Tongaporutuan Unconformity. In this area, the Deep Creek Conglomerate overlies the unconformity. Detailed inspection of the position of the boundary between low and high magnetic intensity with the outcrop of the formation at Deep Creek suggest that the magnetic boundary is stratigraphically directly above the Deep Creek Conglomerate. This means that the magnetic boundary mapped is probably representing the eroded margin of an anomalous bed c. 50-100m stratigraphically above the unconformity.

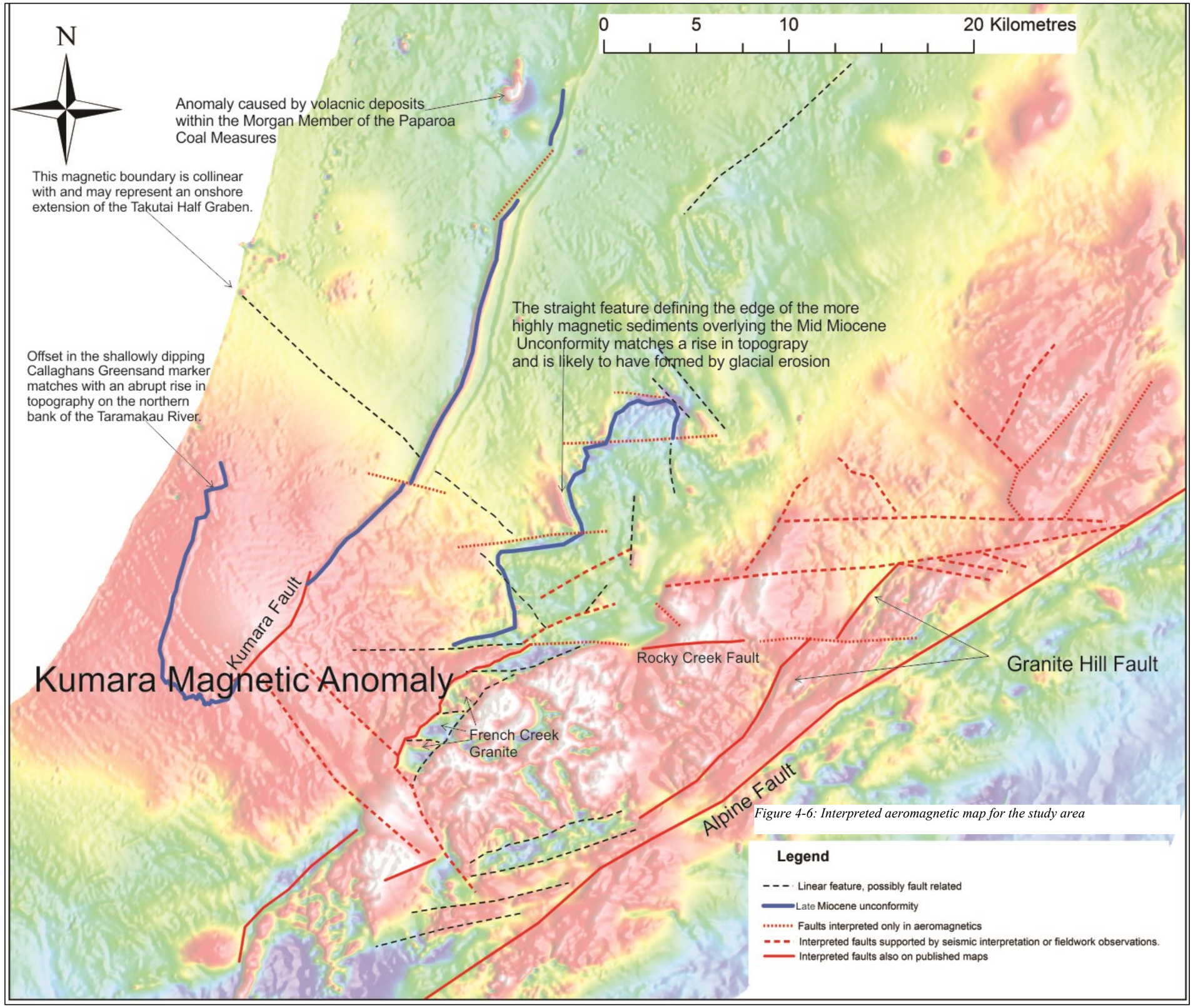

Figure 4-6: Interpreted aeromagnetic map for the study area

4.4.2.2 Broad, diffuse high magnetic intensity anomaly centred on Kumara

This broad magnetic anomaly is inferred as being caused by a highly magnetically susceptible intrusive body within the basement and will henceforth be referred to as the Kumara Magnetic Anomaly (see Figure 4-11). The magnetic susceptibilities of the basement rocks in the area were documented by Tulloch (1987). In this work, many of the granitoids in the Hohonu Range are described as having relatively high magnetic susceptibilities, this explains their high magnetic intensity in the aeromagnetic data. Tulloch suggests that the anomaly that extends from the Hohonu Range, across the Grey Valley Trough and Paparoa Inversion Zone may be caused by an extension of the Hohonu Range granitoids within the basement. In contrast to this, Hunt and Nathan (1976) described a similar magnetic anomaly in the Inangahua region, and proposed that it is caused by a lamprophyre source magma chamber, feeding the many dykes found in the area. Similar lamprophyre dykes are found in the Hohonu Range (the Hohonu Dyke Swarm), and it is also a possibility that the feeding magma chamber for these dykes is producing the magnetic anomaly.

4.4.2.3 Dextral Faults north of the Hohonu Range and around Granite Hill

East – west striking faults with apparent dextral separation are interpreted directly to the north and directly to the south of Granite Hill. This interpretation is based on the apparent dextral separation of north-south trending high magnetic intensity bands. The fault located south of Granite Hill may be an eastward continuation of the Rocky Creek Fault and the fault to the north, an eastward continuation of the fault inferred in fieldwork for the lower section of Sam Creek. Both east-west striking faults produce an apparent dextral separation of a NE-SW trending linear feature which is interpreted to be the Granite Hill Fault.

4.5 Construction of geological cross sections from available geological data

4.5.1 Selecting geological cross section traces

The location of the geological cross sections (see Figure 4-1) were decided for the principal purpose of observing the similarities and contrasts in Neogene deformation between the northern and southern parts of the study area. In the northern part of the study area, the Grey Valley Trough is broader, and deformation is more diffuse, while offshore, the basement is relatively undeformed and stable. In the southern part of the study area, the trough is much narrower and deeper with deformation localised on the Hohonu Fault. The southern offshore area contains the Takutai Half Graben (Bishop, 1992b), which has the potential to continue beneath the Paparoa Inversion Zone

and influence the structural development of the southern onshore region. Both geological cross sections constructed during this study have an orientation of 145°.

4.5.2 Depth Conversion of seismic profiles

Prior to interpretation, the seismic profiles that were to be projected onto the cross sections (see Figure 4-5) needed to be adequately depth converted in order for them to be tied with wells in the area. This study used the relatively simple method of using a best-fit quadratic or cubic function that approximated the average time-depth curve for the basin-fill sediments across the seismic profile. Many of the images of seismic profiles published in petroleum reports such as PR2275 (Kelman Seismic Processing, 1996) contained stacking velocities. As shown in Figure 4-12 the stacking velocities presented in these profile images were used to calculate the depths (Dsl) for each of the points in two way time. The depth calculation had to account for the thickness of sediment above the sea level datum (De) because average velocities (Va) were given from the surface. This meant that the total two way time over which Va was recorded is the two way time below the sea level datum (Tsl) plus the two way time above (Te). Using the simple relationship that distance equals velocity multiplied by time, the following equation for calculating the depth was produced:

$$Dsl = (((Tsl+Te)Va) / 2) - De$$

All of the calculated depth points were plotted against their corresponding two way time. A polynomial line of best fit was placed across the plotted points. The function for this curve represents the approximated average depth-time curve across the seismic profile and was used to depth convert the seismic line using the depth conversion tool in Move.

line	Va - Average TWT velocity (m/sec)	Tsl - two way Time (sec)	De - Elevation of surface (m)	Te - Surface time above datum (sec)	Dsl - depth below sea level (m)
gv10	2678	0.34	65	0.09	510.77
	2892	0.596	65	0.09	926.956
	2896	0.824	65	0.09	1258.472
	2906	1.172	65	0.09	1768.686
	3034	1.648	65	0.09	2571.546
	2573	0.448	54	0.08	625.272
	2601	0.756	54	0.08	1033.218
	2898	1.12	54	0.08	1684.8
	3239	1.672	54	0.08	2783.364
	2677	0.312	76	0.105	482.1545
	2746	0.62	76	0.105	919.425
	2906	0.936	76	0.105	1436.573
	3251	1.504	76	0.105	2539.4295
	2406	0.152	94	0.12	233.216
	2592	0.504	94	0.12	714.704
	2757	0.864	94	0.12	1262.444
	2881	1.192	94	0.12	1795.936
	2552	0.332	121	0.16	506.792
	3163	0.956	121	0.16	1643.954
	2627	0.096	165	0.2	223.796
	2981	0.512	165	0.2	896.236
	2820	0.244	115	0.165	461.69
	3051	0.66	115	0.165	1143.5375
	2946	1.292	115	0.165	2031.161

Figure 4-7: Method of producing a polynomial model equation for depth conversion

This method assumes that all of the basin fill across a seismic profile has effectively the same increase-of-velocity-with-depth properties and ideally has a horizontal layer-cake stratigraphy. For the post-Oligocene infill of the Grey Valley Trough the sediments are relatively consistently sand and siltstone. As seen in the Kokiri-1 well completion report (Carter, 1981), this results in a relatively regular increase of velocity with depth across the sedimentary package and suggests that the depth conversion technique used would give reasonable results. On the Paparoa Inversion Zone the basin infill is much more heterogeneous with a significant localised increase in wave velocity within the Cobden limestone. Because of the varying depth of the limestone across profiles in the Paparoa Inversion Zone, its localised increase in wave velocity cannot be accounted for by a cross-profile average function. This probably the most significant source of error in the depth conversion method used for this study and it may mean horizons can be misplaced several hundred metres in some locations. Another problem with this method of depth conversion was when there were significant lateral changes in stratigraphic character within single profiles such as in WV-4 (Figure 4-15) where parts of both the Grey Valley Trough and the Paparoa Inversion Zone are intersected. This problem could be mitigated to some degree by using different depth-time functions on either side of major boundaries in the stratigraphic character which in the case of WV-4 is the Grey Valley Fault.

4.5.3 Interpreting seismic profiles, and checking interpretations with projected boreholes

The depth conversion of the seismic profiles was validated by checking that the easily recognizable horizons such as the Late Miocene Unconformity and the Top Cobden Limestone matched with those in the wells that were on or nearby to the profile traces. In most cases, the depths of well horizons matched with the depth-converted seismic profiles to within a c. 5% error.

Once validated, more detailed interpretation of the relevant seismic profiles was undertaken by recognizing the typical seismic character of the units that comprise the basin fill (Figure 4-13) and applying this throughout the study area. GV-10 and WV-4 are given as examples of lines that have been depth converted and interpreted (Figure 4-14 and Figure 4-14) and were later used for constructing the northern and southern geological cross sections respectively.

Appearance in Seismic Profile	Description
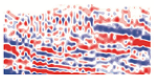	**Old Man Group:** Discontinuous reflectors, usually warped by being near the surface
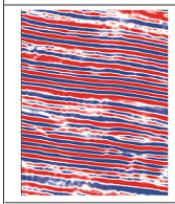	**Eight Mile Formation:** Usually contiuous, relatively bright reflectors
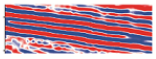	**Deep Creek Conglomerate/ Notown Coal Measures:** A small number of bright, continuous reflectors
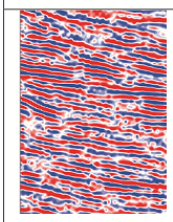	**Stillwater Mudstone and Inangahua Formation**: Relatively faint, discontinuous reflectors, sometimes exhibiting prograding clinoforms. Bright, more continuous reflectors appear within the Stillwater Mudstone in the southern Grey Valley Trough. These represent the Niagara Sandstone submarine turbidite deposits (c.f Diligenz, 2009)
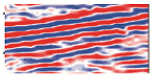	**Cobden Limestone:** A small number of bright, continuous reflectors
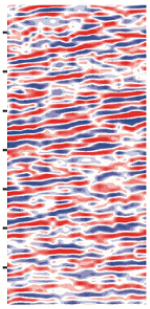	**Kiata Formation:** Relatively faint, discontinuous reflectors, sometimes exhibiting a band of brighter reflectors in the middle,which represents the Omotumotu Member.
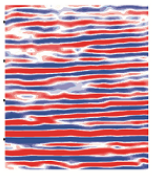	**Brunner and Paparoa Coal Measures:** Relatively bright, ranging from continuous to discontinuous reflectors.
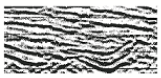	**Pororari Group:** Curved, tilted and truncated bright to faint reflectors.
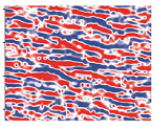	**Basement**: Random reflection brightness with minimal reflector continuity.

Figure 4-13: Chart of the generalized seismic stratigraphy of the study area

Figure 4-8: Original two-way-time profile and depth converted and interpreted profile of GV-10

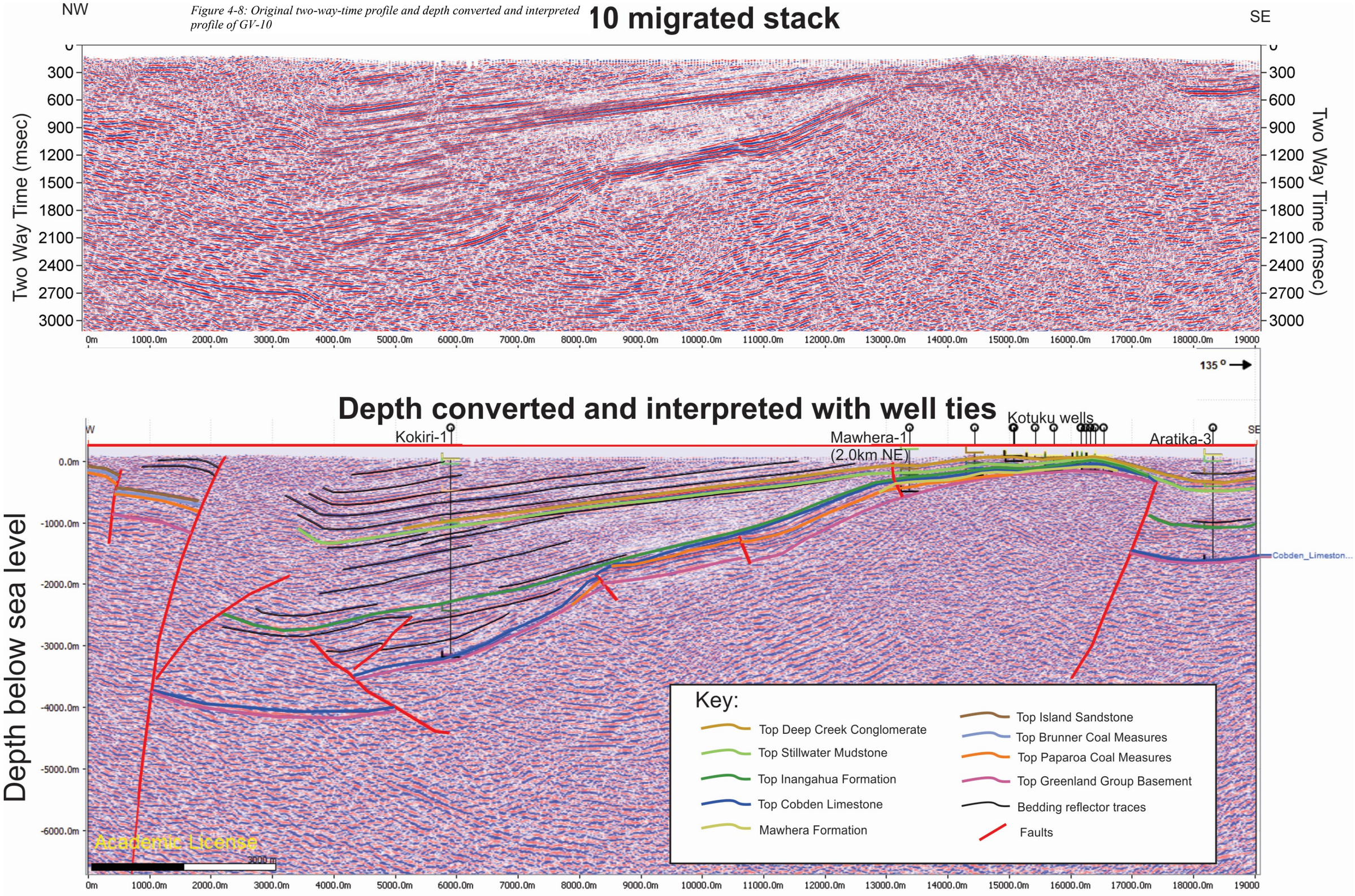

Figure 4-9: Original two-way-time profile and depth converted and interpreted profile of WV-04

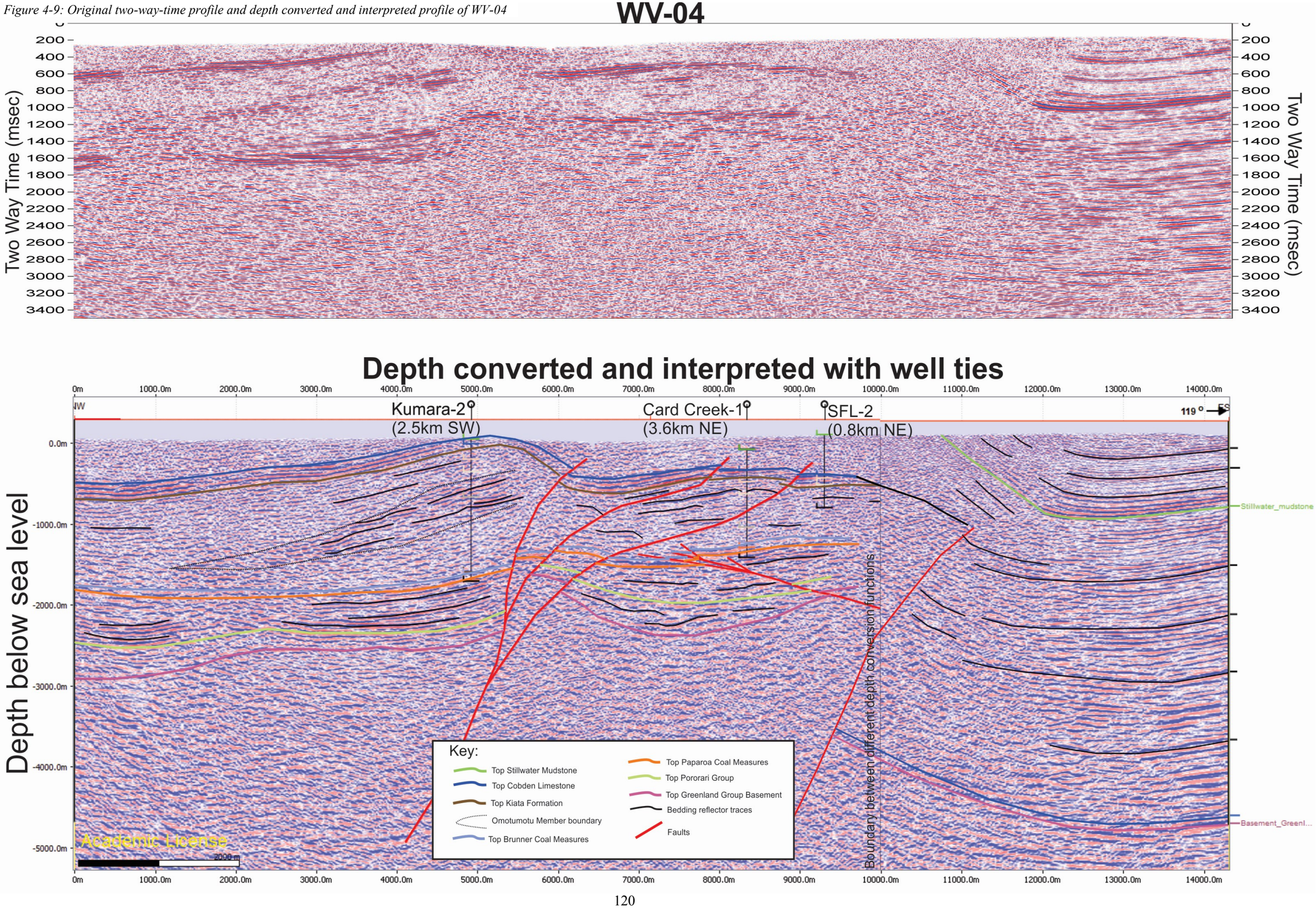

4.5.4 Projecting interpreted horizons to geological cross sections

Once depth converted and interpreted, the significant horizons in the adjacent seismic profiles, as well as borehole and surface dip data had to be projected onto the geological cross sections. As an example, a 3D image of the interpreted seismic data adjacent to the north cross section can be seen in Figure 4-16. Objects were projected along a 3D vector defined by a trend and a plunge. The vectors used for projecting the data were either horizontally along structure contours provided by horizon mapping in petroleum reports such as PR2298 (Buchan, 1997) or along fault strikes with an approximation of the plunge of the line where significant horizons are truncated by the fault plane. Once horizons from a number of nearby seismic profiles were projected onto the geological cross section, they were used as guides for drawing the final horizons.

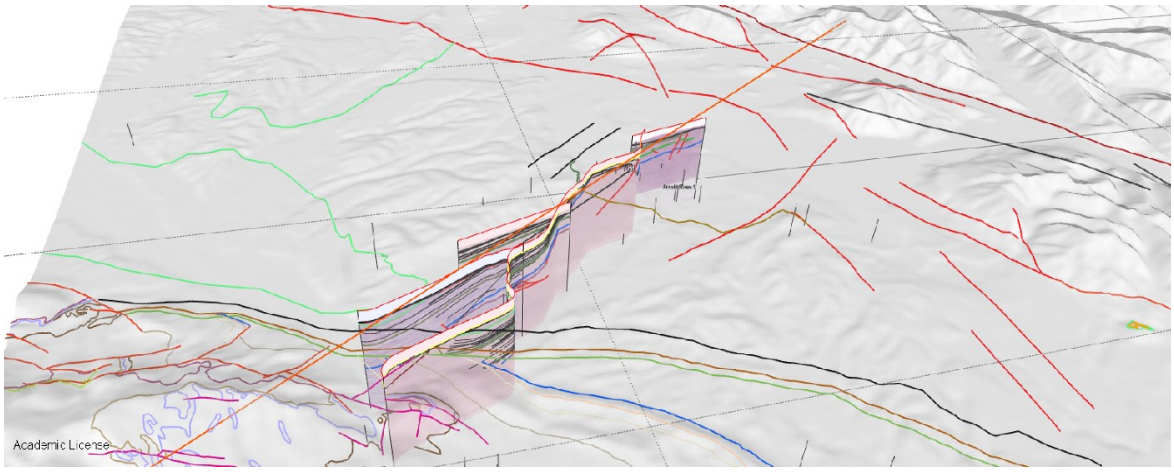

Figure 4-16: Example of seismic data adjacent to part of the northern section about to be projected. Boreholes and surface contacts also showing.

The projection of data onto the geological cross sections contains significant sources of error, particularly for objects projected from a larger distance (up to 5 km). An important source of error is that projection assumes that there is a parallel structural grain within the basin fill. To some extent this is true within the study area as it has a pervasive NNE-SSW structural grain developed through Paleogene extension and Neogene compression. However, the Cretaceous sediments have a predominantly WNW-ESE structural grain that has been deformed by later tectonic episodes, which makes their projection problematic. For this reason, as well as the fact that their boundaries and extent were difficult to determine in seismic profiles, the representation of the Paparoa Coal Measures and the Pororari Group is highly speculative across the parts of the geological cross sections constructed primarily from seismic interpretation.

4.5.5 Completing initial geological cross sections– using borehole, surface dip data and isopach maps

After projecting interpreted data from adjacent seismic profiles, there were still a number of gaps in the geological cross sections where no adjacent seismic surveys were available. Surface bedding dip and contact data gave a basic indication of the structural form of the area. Where no other data are available (such as along the coastal strip), the small amount of surface data, along with the assumption that the thickness of sedimentary units does not vary significantly, allows the cross section to be completed. For the northern transect, a large gap in data was present across the Greymouth Coalfield area. As a result of the extensive amount of exploration drilling that has occurred in the area, isopach maps created for each of the members within the Paparoa Coal Measures and are available in the coal report CR2395 (Bowman, 1984). These maps were georeferenced into the Move model and the thicknesses were used, along with the surface data mapped by Nathan (1978a) to complete the geological cross section.

4.6 Balancing and restoring geological cross sections

4.6.1 Introduction

Section restoration is a valuable tool for analyzing tectonic evolution as it can produce a geometrically admissible section as well as a representation of the section at the time of deposition of the horizon it has been restored to.

Groshong (2006) describes a balanced cross section as "generally understood to be one which is restorable to a geologically reasonable pre-deformation geometry, as well as maintaining constant area". Constructing a restorable cross section is typically easier with a large amount of data to constrain its geometry, and in the case of the sections constructed during this study, all available borehole, geophysical and surface data has been used.

The premises of balancing a cross section include:

(1) The assumption that the cross section area, or volume remains constant between the strained and unstrained states (Hossack, 1979).
(2) The depth to the detachment fault. This is the depth at which no vertical movement is assumed to have occurred across the base of a structure, therefore allowing a section with a finite base to be restored based on the constant area criterion (Groshong, 2006). In the study area, it is likely that large fault zones such as the Paparoa Tectonic Zone penetrate the crust deeply, and reactivation that has caused inversion may be controlled by a detachment structure at lower crustal depths.
(3) The section is constructed along the plane of transport with no lateral movement into or out of the section. If a section is constructed across a series of pure thrust faults, this means orientating the section perpendicular to them, and any movement on faults that intersect the

section that have a strike slip component cannot be balanced. This premise presents a significant source of error in the study area; to begin with, the Alpine Fault has a very large dextral component of movement (and therefore no attempt has been made to balance the section across it); fieldwork at Bell Hill shows a number of thrust faults (inferred to be part of the Hohonu Fault Zone) that also have large dextral components; and a series of east-west trending dextral strike slip faults have also been suggested to cross the Grey Valley Trough, specifically, the northern cross section (Section 1)

Retro deformation of a section is separated into two components:

(1) Removal of all deformation that has happened after the deposition of a given unit. In this study this is done using separate processes of removing slip that has occurred on faults, and removing the folding that has occurred. Paleodepth provides a template by which to restore to. For this, inferences on the paleobathymetry of the horizon to be restored to, based on fauna identification need to be made.

(2) Back stripping of a given unit and the decompaction of underlying units. This involves removing a given undeformed, overlying unit, and restoring the underlying units to their thickness before they were compacted by deposition and loading of the overlying unit (Allen and Allen, 2009).

Progressive retro-deformation is accomplished by removing the component of shortening/extension and progressive accumulation of fault separation that occurred during the time of deposition of a given unit. Progressive retro-deformation of a number of units in a geological cross section helps constrain fault propagation and growth across the history of the section. Erosion of underlying units during the deposition of a given unit may also have to be accounted for. In this case, eroded tops of units have to be reconstructed before they can undergo the retro-deformation process.

4.6.2 Basic elements of retrodeformation

Restoring to each of these horizons involved undertaking the following three processes:

1) Removing progressive fault separation. This is done using the Fault Parallel Flow algorithm (Egan et al., 1997; Kane et al., 1997) which is designed to kinematically model hangingwall blocks in fold and thrust belts where deformation is accommodated by fault-parallel shear.
2) Unfolding and reducing to paleodepth. Unfolding is done using the flexural slip algorithm which is outlined in Groshong (1999). This algorithm is used as it maintains orthogonal

bed thicknesses and bed length. This is important for the study area, especially in areas where bedding was re-oriented to become steeply dipping in the limbs of folds, and bed length conservation was necessary. Paleodepths for each restored horizon were derived from broad-scale estimates attained by referring to Suggate and Waight (1999)

3) Decompaction of overlying sediments using the Sclater and Christie (1980) method. Sclater & Christie assume that porosity decreases with increasing depth (Compaction) and increases with decreasing depth (Decompaction) and can be represented by the equation:

$$f = f_0\left(e^{-cy}\right)$$

- f is the present-day porosity at depth
- f_0 is the porosity at the surface
- c is the porosity-depth coefficient (km^{-1})
- y is depth (m)

For this method, surface porosity and porosity-depth coefficient values (Figure 4-17) are required for each of the basin – fill units (Figure 4-18). These were estimated based on their sandstone, siltstone and limestone contents with the average values taken from Allen and Allen (2009).

4.6.3 Methods of creating valid restorations of cross sections

The validation process involved undertaking the process described above for each of the horizons chosen as principal markers. These principal marker horizons were; the top Eight Mile horizon; the top Stillwater or late Miocene unconformity; and the top Cobden horizon which gave representations of the cross sections at c. 3.5Ma, c. 7.5 Ma and c. 25 Ma respectively. At the end of each restoration step, geometric inadmissibilities in the early draughts of the cross section became clear. These were addressed by editing the original section, and the restoration process was repeated to check that the corrections produced a geometrically admissible section. In order to construct valid representations of the more complex, inverted parts of the section (such as the eastern side of the Paparoa Inversion Zone), many iterations were needed, and often that part of the cross section was edited and restored separately in order to make it geometrically admissible. Horizons that were eroded in part before the overlying horizon was produced, had to be reconstructed after the removal of that overlying horizon in order for them to be restored. Once this iterative process was completed through to the top Cobden horizon, the final restored sequence was created.

	1:Rock Type	2:Sandstone(%)	3:Shale(%)	4:Limestone(%)	5:Porosity	6:DepthCoefficient	7:Compaction Curve	8:v0	9:k	10:Grain Size	11:Density	12:Young Modulus	13:Poisson Ratio
	Sandstone	100.0000	0.0000	0.0000	0.5600	0.3900	Default	2000.00	0.5000	0.38	2500.0000	15000.0	0.2950
	Shale	0.0000	100.0000	0.0000	0.6300	0.5200	Default	2500.00	0.5000	0.05	2720.0000	32500.0	0.3000
	Limestone	0.0000	0.0000	100.0000	0.4100	0.4000	Default	2600.00	0.5000	0.00	2710.0000	45000.0	0.2150
Unit		%	%	%	fraction	1/km		m/s		mm	g/cm^3	MPa	
1	Default				0.5600	0.3900	Sclater-Christie	2200.00	0.5000	0.21	2680.0000	23750.0	0.3000
2	ShalySand	60.0000	40.0000	0.0000	0.5880	0.4420	Sclater-Christie	2200.00	0.5000	0.24	2588.0000	22000.0	0.2970
3	Salt				0.0000	0.0000	None	4481.00	0.5000	0.00	2100.0000	11000.0	0.4000
4	Chalk				0.7000	0.7100	Sclater-Christie	2200.00	0.5000	0.00	2200.0000	14000.0	0.2000
5	NONE				0.0000	0.0000	None	0.00	0.0000	0.00	0.0000	0.0	0.0000
6	Matiri_Fmt_1_1				0.6800	0.3900	Sclater-Christie	3000.00	0.5000	0.21	2450.0000	30000.0	0.2500
7	Upper_Mangles_1_1				0.5600	0.3900	Sclater-Christie	1800.00	0.5000	0.21	2350.0000	14000.0	0.2500
8	Gravels				1.4000	0.3900	Sclater-Christie	1600.00	0.5000	0.21	1850.0000	10000.0	0.1500
9	Upper_BB_Horizon	50.0000	50.0000	0.0000	0.5950	0.4550	Sclater-Christie	2250.00	0.5000	0.21	2610.0000	23750.0	0.2975
10	Sea_Bottom_1_1				0.5600	0.3900	Sclater-Christie	1700.00	0.5000	0.21	1850.0000	14000.0	0.2000
11	Upper_Blue_Bottom=EightMile_1_1	35.0000	65.0000	0.0000	0.6055	0.4745	Sclater-Christie	2325.00	0.5000	0.16	2643.0000	26375.0	0.2983
12	Lower_Mangles_1_1				0.5600	0.3900	Sclater-Christie	2200.00	0.5000	0.21	2400.0000	15000.0	0.2400
13	Lower_Blue_Bottom_Undiff_1_1				0.5600	0.3900	Sclater-Christie	2200.00	0.5000	0.21	2400.0000	15000.0	0.2400
14	Sandstone_Mudstone	50.0000	50.0000	0.0000	0.5950	0.4550	Sclater-Christie	2250.00	0.5000	0.21	2610.0000	23750.0	0.2975
15	Fault_1_1				0.5600	0.3900	Sclater-Christie	2000.00	0.5000	0.21	2680.0000	23750.0	0.3000
16	Metamorphic_Low_Grade				0.2000	0.3900	Sclater-Christie	3000.00	0.5000	0.21	2680.0000	42400.0	0.2500
17	Coal_sandstone				0.5600	0.3900	Sclater-Christie	2200.00	0.5000	0.21	2200.0000	15000.0	0.2400
18	Limestone_003	10.0000	10.0000	80.0000	0.4470	0.4110	Sclater-Christie	2530.00	0.5000	0.05	2690.0000	40750.0	0.2315
19	Mudstone	5.0000	95.0000	0.0000	0.6265	0.5135	Sclater-Christie	2475.00	0.5000	0.06	2709.0000	31625.0	0.2998
20	Sandstone_002	90.0000	10.0000	0.0000	0.5670	0.4030	Sclater-Christie	2050.00	0.5000	0.34	2522.0000	16750.0	0.2955
21	Granite				0.2000	0.3900	Sclater-Christie	3200.00	0.5000	0.21	2680.0000	59300.0	0.3000
22	Basalt				0.5600	0.3900	Sclater-Christie	3500.00	0.5000	0.21	2680.0000	62000.0	0.2500
23	Horizon_Basement				0.2000	0.3900	Sclater-Christie	3500.00	0.0000	0.21	2680.0000	59300.0	0.2300
24	Water				0.0000	0.0000	None	1450.00	0.0000	0.21	1100.0000	22000.0	0.5000
25	Kiata_undiff	40.0000	50.0000	10.0000	0.5800	0.4560	Sclater-Christie	2310.00	0.5000	0.17	2631.0000	26750.0	0.2895
26	Breccia	100.0000			0.5600	0.3900	Sclater-Christie	2000.00	0.5000	0.38	2500.0000	15000.0	0.2950
27	Conglomerate	100.0000			0.5600	0.3900	Sclater-Christie	2000.00	0.5000	0.38	2500.0000	15000.0	0.2950

Figure 4-10: Rock properties assigned to the units of the study area

	1:Horizon	2:Colour	3:Rock Type
7	Quaternary		Gravels
8	Old_Man_Goup		Gravels
9	Upper_Blue_Bottom=EightMile		Upper_Blue_Bottom=EightMile_1_1
10	Lower_Blue_Bottom_Undiff		Lower_Blue_Bottom_Undiff_1_1
11	Rotohoku_coal		Sandstone
12	Deep_creek_conglomerate		Upper_Blue_Bottom=EightMile_1_1
13	Callaghans_greensand		Sandstone
14	Stillwater_mudstone		Lower_Blue_Bottom_Undiff_1_1
15	Niagara_sandstones		Lower_Blue_Bottom_Undiff_1_1
16	Hohonu_conglomerate		Lower_Mangles_1_1
17	Inangahua_Formation		Lower_Blue_Bottom_Undiff_1_1
18	Cobden_Limestones_nc		Limestone_002
19	Port_elizabeth_member_rkp		Kiata_undiff
20	Mawhera_fmt		Sandstone
21	Kaiata_Fmt_Undiff_rk		Kiata_undiff
22	Omotumotu_member_rko		Sandstone
23	Kiata_member_rkk		Shale
24	Island_sandstone_ri		Sandstone
25	Brunner_Coal_Meas_br		Coal_sandstone
26	Paparoa_coal_measures		Coal_sandstone
27	Basement_LK_Basalts		Basalt
28	Pororari_Group		Granite
29	Basement_Greenland		Horizon_Basement

Figure 4-11: Stratigraphic units of the Move model of the study area

4.6.4 **Results**

Figure 4-19 and Figure 4-20 show the balanced south (Section 2) and north (Section 1) geological cross sections respectively at each major stage in restoration. Figure 4-21 to Figure 4-24 show 3D views of the sections restored to each significant horizon.

The main tectonic stages during progressive Neogene deformation can be seen across both sections. In order of the time in which they occurred, these are:

1) The reconstruction of the top Cobden horizon at its inferred paleo-depth of c. 20-50 m below sea level can be achieved for the whole extent of the geological cross section, and is in agreement with the regional interpretations (cf. Nathan, 1986; King 2000) of a regional transgression of calcareous sediments associated with maximum marine flooding during post-rift subsidence and relative tectonic quiescence (Figure 4.21).
2) In the Early Miocene, an initial phase of inversion of the Paparoa Tectonic Zone took place, and the area now occupied by the Grey Valley Trough was converted from a basement high to a basement low. The north section shows that inversion of pre-

existing basin areas occurred in two areas; the Paparoa Inversion Zone; and the area on, and to the west of the Kotuku Anticline. This inversion was marked firstly by erosion on the western side of the Paparoa Inversion Zone, and a little on top of the Kotuku anticline, and deposition of the Inangahua Formation in the down-thrown areas.

3) In the Middle Miocene, the inversion process became more subdued or quiescent, leaving widespread subsidence and deposition of the Stillwater Mudstone to occur. It appears that during this time, there was still land to the east, from which the Niagara Sandstone turbidite fans were sourced
4) In the Late Miocene, compression, and an up-tilting of the whole area from the east occurred. This produced the Late Miocene unconformity, marked by the Top Stillwater horizon (figure 4.20).
5) Subsidence resumed across most of the study area in the latest Miocene and Early Pliocene. This occurred concurrently with the development of the Hohonu thrust fault in the west. Sediment input rates began to outpace subsidence rates in the Grey Valley Trough around the middle Pliocene, and the basin was infilled to become terrestrial. This point in time is represented by the top Eight Mile horizon, when the terrestrial Old Man Group begins to be deposited (figure 4. 19)
6) As compression continued into the Late Pliocene and Quaternary, re-activation of the Paparoa Inversion Zone occurred. During this time, the northern part of the inversion zone appeared to go under a greater degree of uplift than the south. This is characterized by faults that cut through the Miocene and Pliocene strata on the eastern side of the Paparoa Inversion Zone the north section. This is in contrast to the south section, where the smaller movement on the same fault was accommodated mostly by folding of the overlying Miocene and Pliocene strata.

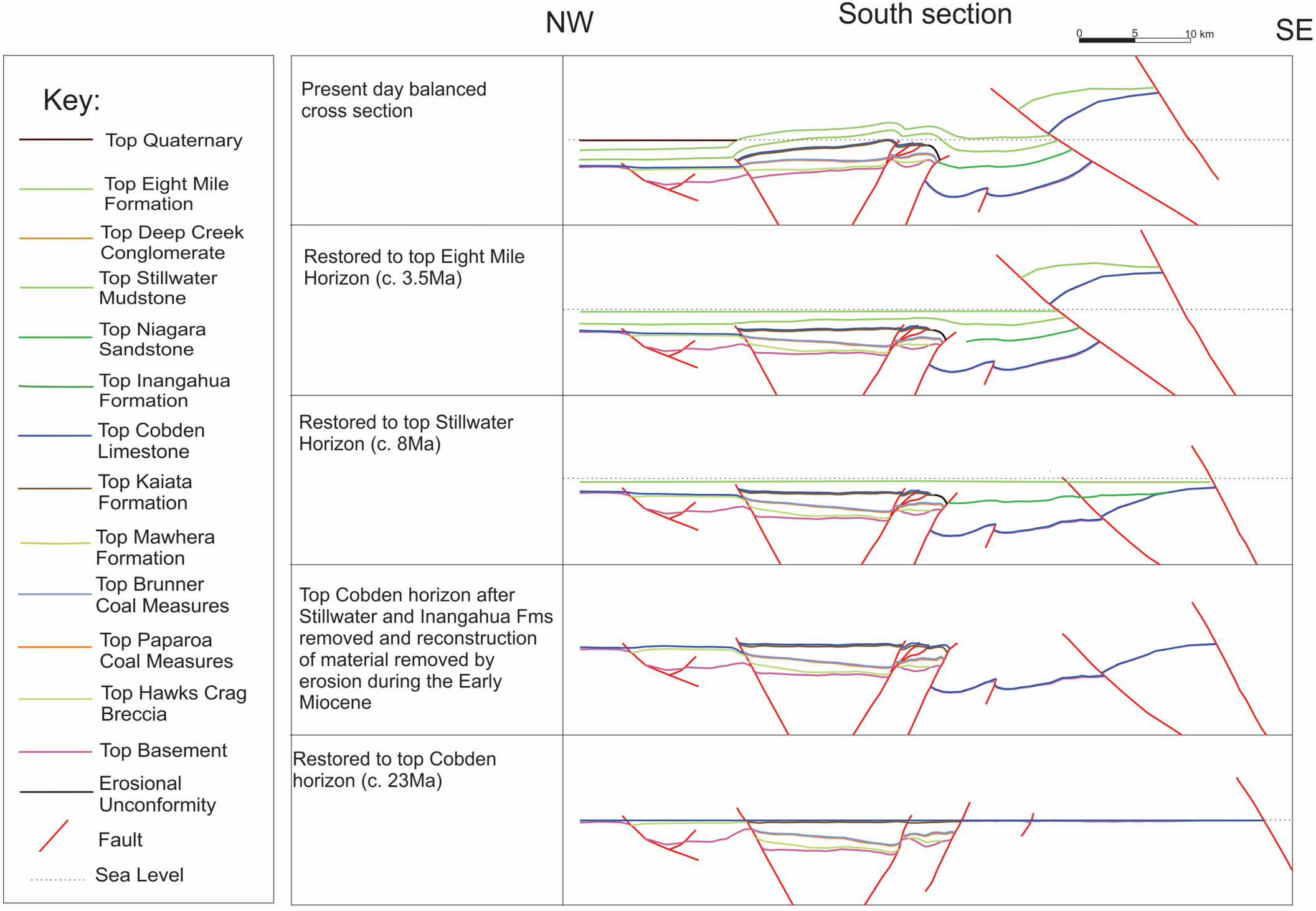

Figure 4-12: South section showing restoration to the major horizons

North section

NW

0 5 10 km

SE

Present day balanced cross section

Restored to top Eight Mile Horizon (c. 3.5Ma)

Restored to top Stillwater Horizon (c. 8Ma)

Top Cobden horizon after Stillwater and Inangahua Fms removed and reconstruction of material removed by erosion during the Early Miocene

Restored to top Cobden horizon (c. 23Ma)

Figure 4-13: North Section showing restoration to the major horizons, see figure 4.16 for key.

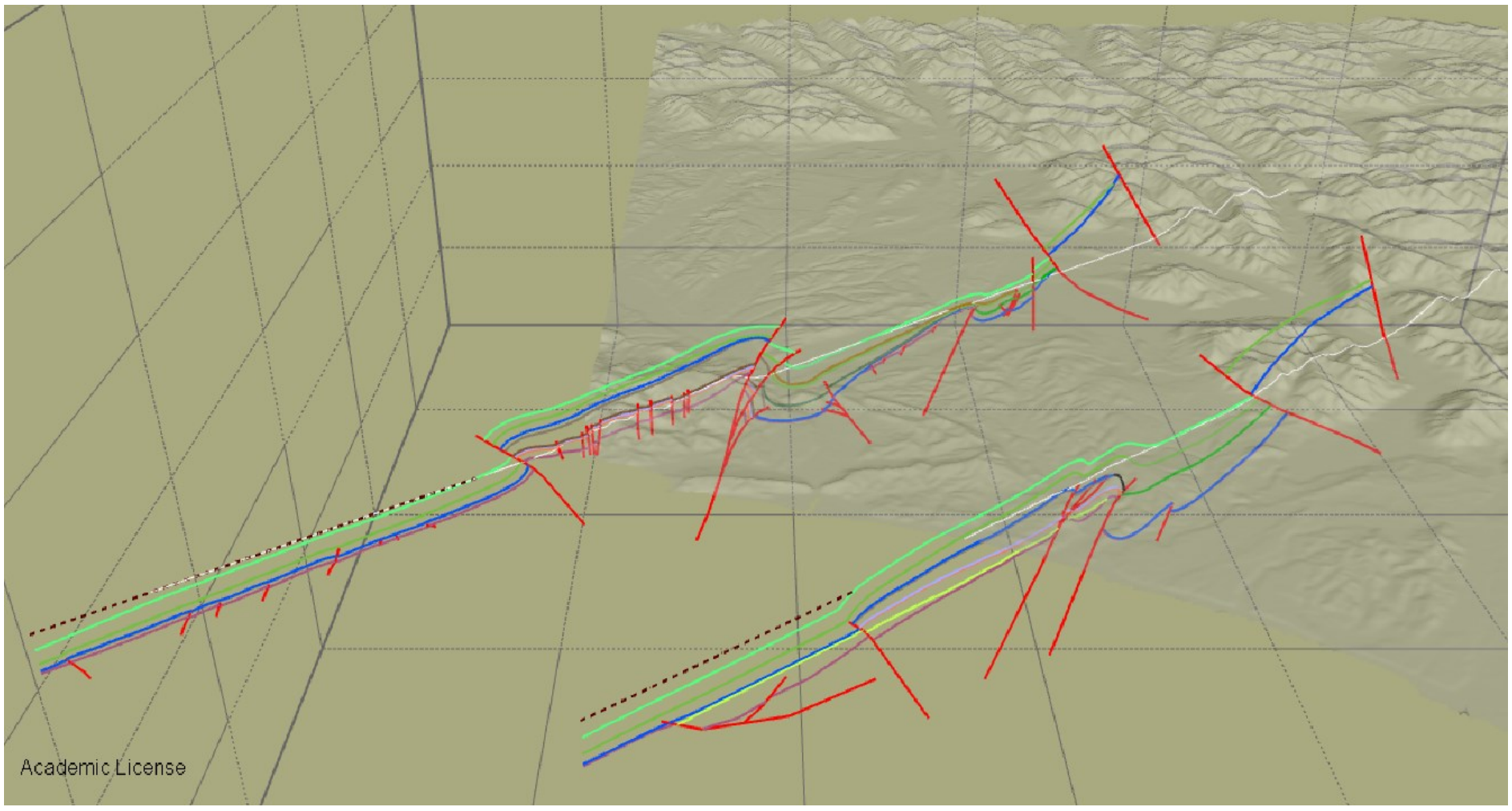

Figure 4-21: 3D view of balanced geological cross sections at the present day. DEM shown for reference.

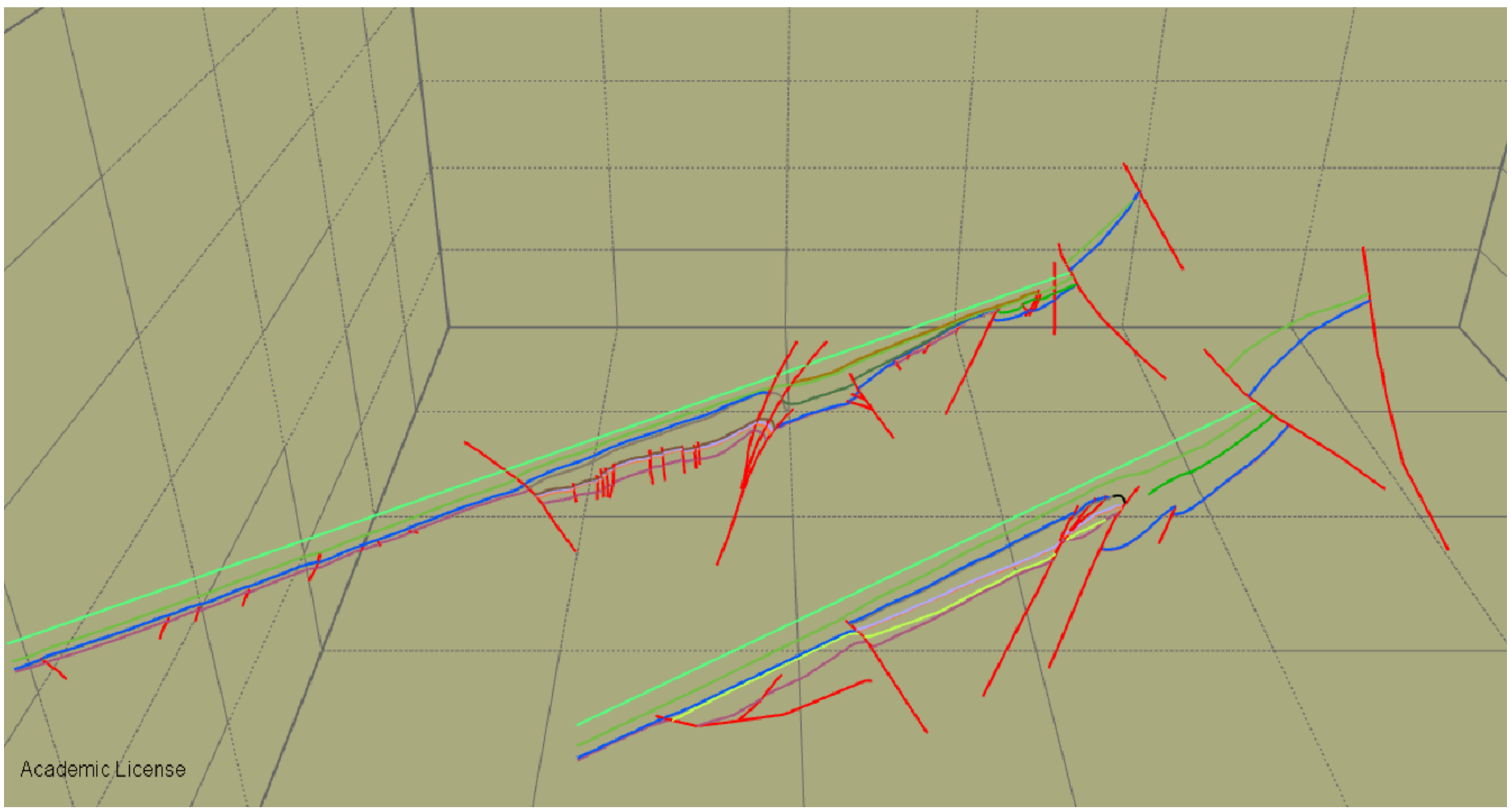

Figure 4-22: 3D view of sections restored to the to Eight Mile Fomation horizon (c. 3.5Ma)

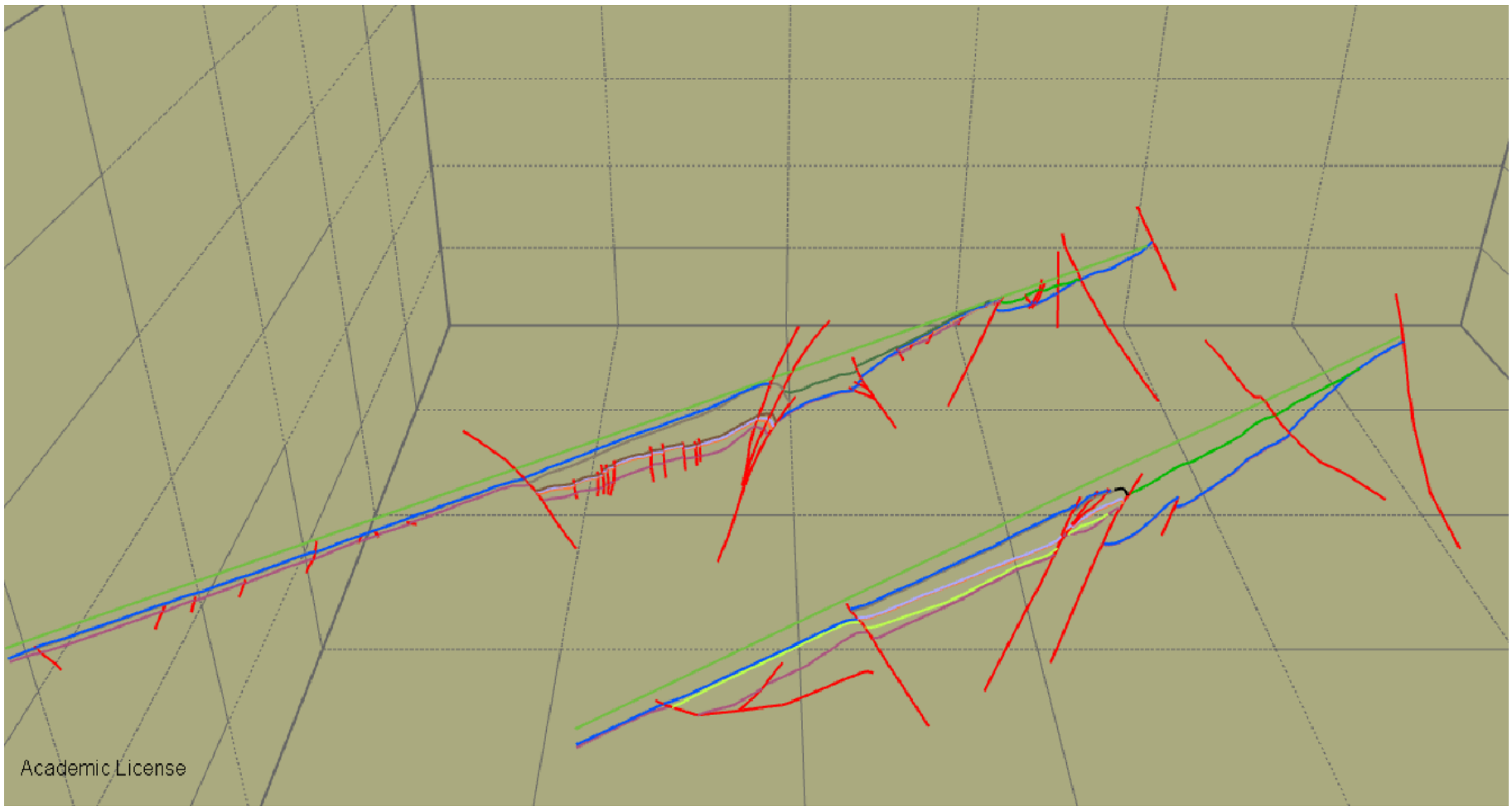

Figure 4-23: 3D view of sections restored to the top Stillwater Mudstone horizon (c. 8Ma)

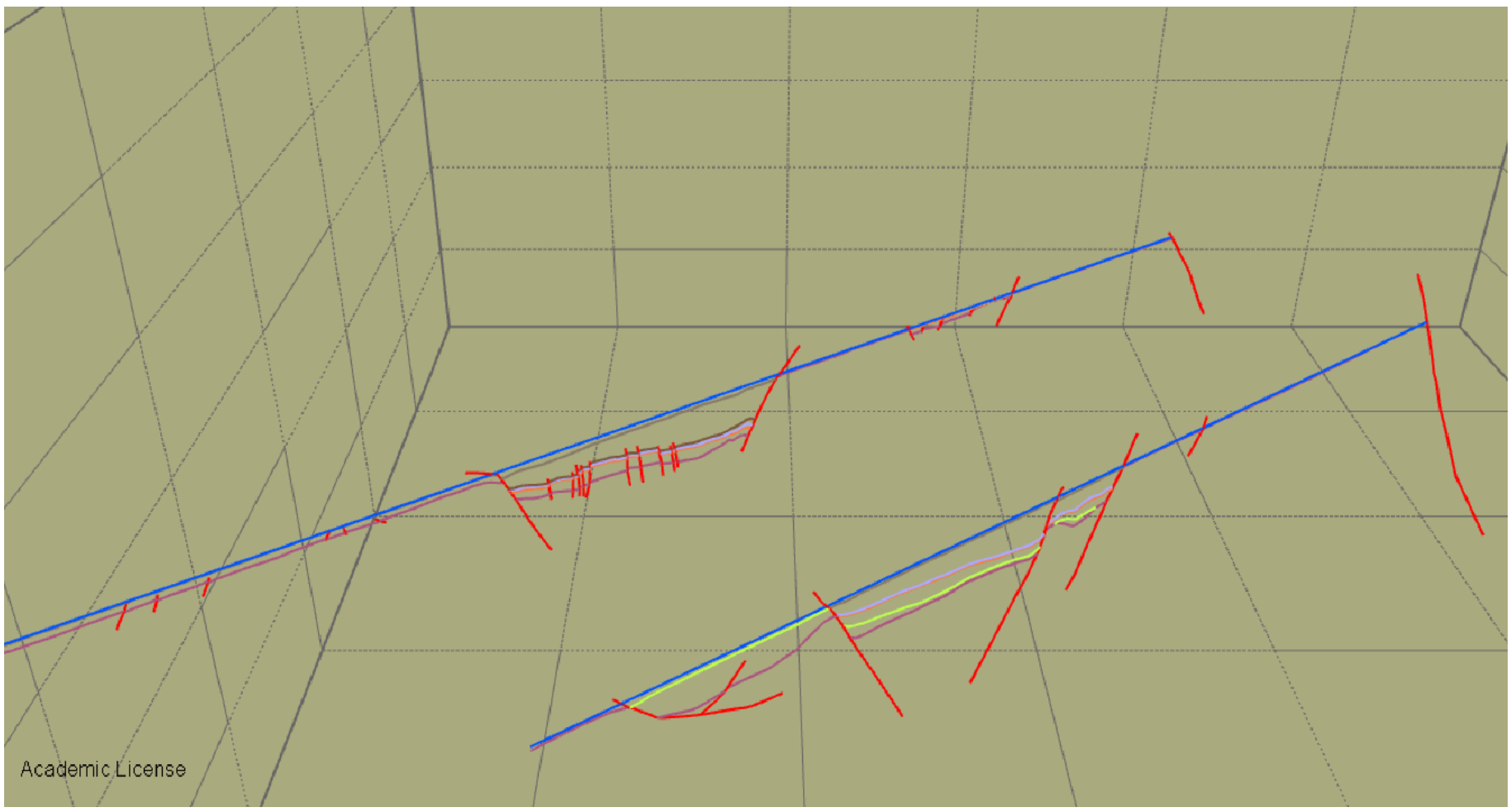

Figure 4-24: 3D view of sections restored to the top Cobden Limestone horizon (c. 23Ma)

CHAPTER 5. DISSCUSSION

5.1 General structure of this chapter

This chapter discusses firstly, the Neogene tectonic development of the study area, and provides explanations for the tectonic changes that occurred using previously published studies as a guide to the regional tectonic context (e.g. King, 2000; Sutherland et al. 2000; Furlong and Kamp, 2009). This is done by discussing three main phases in the development of the plate boundary: 1) the tectonic transition from the Challenger Rift System to the proto-Alpine Fault dextral transform from the Late Oligocene through to the Early Miocene; 2) the phase of relatively pure dextral-transform movement on the Alpine Fault during the Early and Middle Miocene; and 3) the phase of increased convergence across the plate boundary from the Late Miocene to the Present. This is followed by a discussion on the timing of activity on the Hohonu Fault based on findings in this study. Finally, the presence of WNW-ESE trending Cretaceous extensional structures across the study area, and what effect they may have had on Neogene tectonic development and present day seismic risk will be discussed.

5.2 The Challenger Rift System to Alpine Fault transition from the Late Eocene to Early Miocene

Understanding the reasons for the tectonic changes that occurred in the study area during the Late Eocene to Early Miocene requires knowledge of the regional tectonic context. The initial phase of inversion of the Paparoa Inversion Zone occurred during a transition from NW-SE-directed extension of the Late Eocene and Early Oligocene (the Challenger Rift System) to a NE-SW trending right lateral transform (the Alpine Fault) in the Late Oligocene and Early Miocene.

In plate motion reconstructions by Sutherland et al. (2000) and Furlong and Kamp (2009), during the Oligocene, the study area is shown to be situated on the western rift shoulder of the Challenger Rift System. To the south of the field area, a greater degree of Eocene and Oligocene extension resulted in seafloor spreading and the opening of the Emerald Basin. As shown in Figure 5-1, the study area was situated close to the transition zone between incipient rifting in continental crust to the north, and where extension had progressed to seafloor spreading in the south. The movement of the pole of rotation of the Pacific Plate during the Eocene and Oligocene (Figure 5-1 and Figure 5-2) show the Challenger Rift System to have originally opened in the Eocene as a result of WNW-ESE directed extension (Sutherland et al., 2000, Furlong and Kamp, 2009). As the rift system developed further during the Oligocene, it became trans-tensional with an increasing dextral component. Inception of a through-going transform fault (the proto-Alpine Fault) is associated with the dextral component of movement becoming dominant across the Challenger Rift System in the Late Oligocene and Early Miocene (Kamp, 1986; Sutherland et al., 2000). Furlong and Kamp (2009) and Sutherland et al., (2000) show that in the early Miocene, in

conjunction with the development of a right-lateral transform, the western side of the northern Emerald Basin began to subduct beneath the southern margin of the Fiordland block (see Figure 5-2).

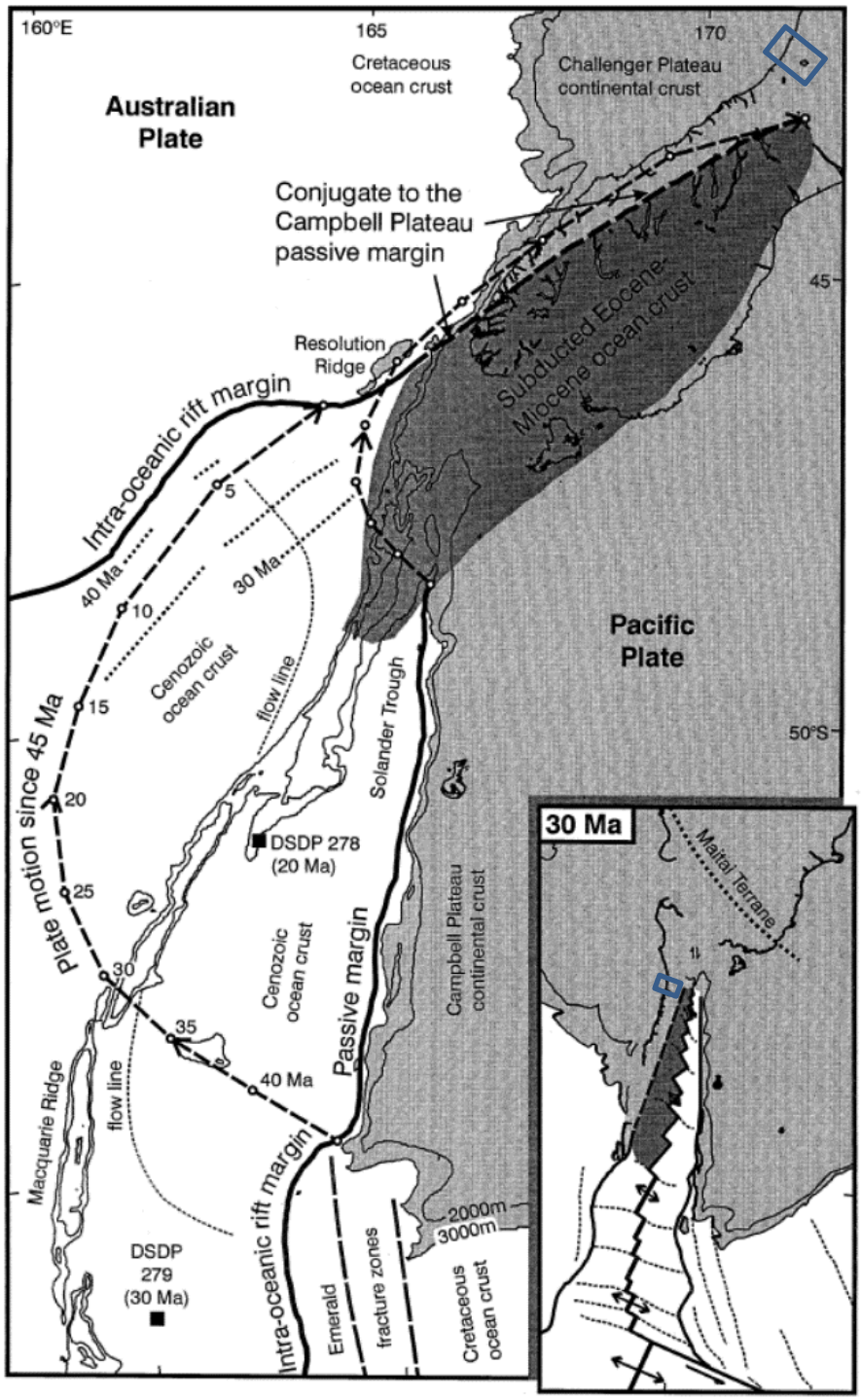

Figure 5-1: Plate motion reconstructions from 45 Ma to present showing the subduction of the western side of the Emerald Basin beneath the Fiordland Block (modified from Sutherland et al, 2000). The location of the study area on the Australian plane is shown with a blue rectangle.

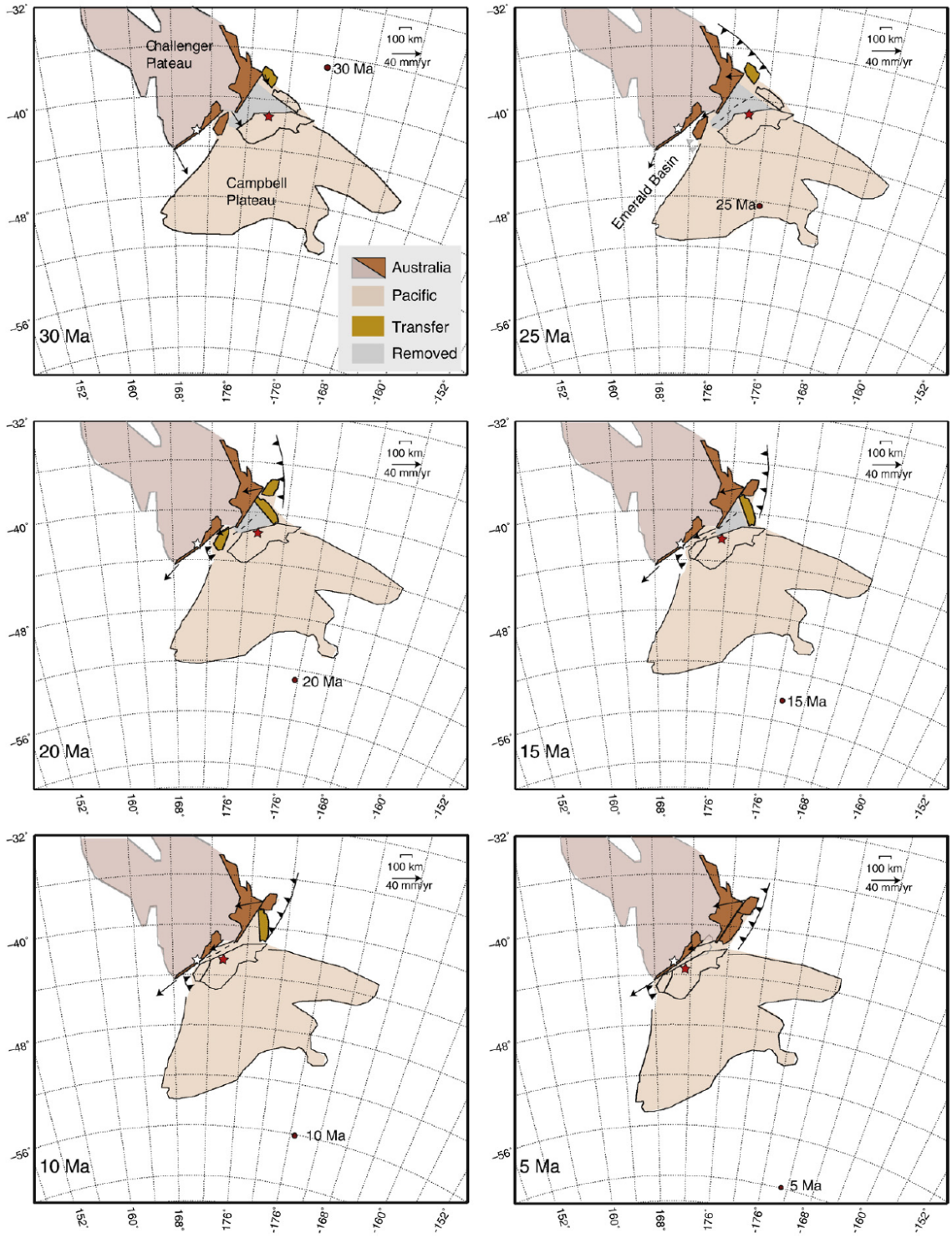

Figure 5-2: Simplified plate motions of New Zealand over the last 30 Ma with Pacific Plate pole of rotation shown (taken from Furlong and Kamp, 2009).

In the study area, the Paparoa Trough formed during the initial development of the Challenger Rift System in the Late Eocene, with activity on the eastern bounding normal fault (the Paparoa Tectonic Zone) probably continuing into the late Oligocene. It has been inferred by Sircombe

(1993) and Sutherland et al. (2000) that the present position of the Alpine Fault, at least for the section of the fault that is to the south of the study area, approximates the position of the rifted margin of Challenger Plateau with the Emerald Basin that formed c. 45 Ma. It is therefore likely that to the east of the study area, during Oligocene times, there was a well-developed continental rift system in which seafloor spreading may have initiated. Although not well constrained, it is likely that southward movement of the Fiordland block, and the subduction of the northern Emerald Basin crust beneath it began relatively nearby, to the east of the study area in the Early Miocene. An initial, rapid phase of inversion during the Early Miocene in which the subsidence rates in the Grey Valley Trough greatly outstripped sediment supply rates is shown in the restored cross sections (Figure 4-19 and Figure 4-20). This inversion phase is here inferred to be related to a phase of compression associated with the Fiordland block starting to move southward as part of the Pacific Plate. This was associated with the development of the proto Alpine Fault transform along the western margin, and the northern Emerald Basin oceanic crust beginning to subduct beneath the southern margin of the Fiordland block.

Previous analysis of the structure of the study area by Suggate and Waight (1999) suggested that Early Miocene subsidence in the Grey Valley Trough, complemented with uplift in the Paparoa Inversion Zone was not associated with 'true' inversion of the Paparoa Tectonic Zone (they believe this didn't occur until the Quaternary), i.e. subsidence in the Grey Valley Trough was caused by broad scale warping of the basement rock, and not by reverse movement on pre-existing normal faults. The view that the warping of the basement in the Early Neogene is not associated with the reactivation of basement structures is contested in this study. Suggate and Waight's (1999) interpretation relies on the assumption that basement deformation is diffuse. Fieldwork conducted during this study shows that diffuse deformation through tectonic activation of cleavage is entirely plausible for Greenland Group rocks. Therefore, diffuse deformation is accepted here as likely to be a significant component of basement deformation. However, the positioning of the transition between subsidence and uplift co-linear with the Paparoa Tectonic Zone during the Early Miocene is not thought to be a coincidence, and is inferred here to be indicative of normal fault re-activating with a reverse sense of slip.

Models of inverted structures (Bonini et al., 2012; Freidman et al., 1976; 1980) show that as an Andersonian normal fault (dipping c. 60º) (Anderson, 1905) began to re-activate with a reverse sense of slip, shallower reverse faults at a more optimal orientation (c. 30º) began to cut through the footwall towards the front of a developing monocline at the surface. As the structure continued to invert, a series of reverse faults with shallower dips than the original normal fault developed close to the surface. This process shows that inversion of a crust-penetrating normal fault (like the one thought to control the section of the Paparoa Tectonic Zone within the study area) may be

expressed by reverse-slip activation along the original normal fault at depth, but closer to the surface, the strain is distributed along a number of shallower reverse faults, which results in the formation of a monocline-like structure across the top basement unconformity. The primary reason Suggate and Waight (1999) argue that inversion did not occur in the Early Miocene is because there is no evidence of localized reverse faulting on the eastern margin of the Paparoa Inversion Zone for that time. The 'warping' of the top basement unconformity described by Suggate and Waight (1999) is here suggested to be caused by reverse-slip reactivation of the Paleogene normal fault at depth with diffusion of deformation into a series of shallower reverse faults closer to the surface. The diffusion of deformation would have meant that the overlying sediments were not locally cut by faults but folded.

5.3 Pure transform movement on the Alpine Fault between c. 20Ma and c. 10Ma

Plate reconstructions by Sutherland et al., (2000), and King, (2000) show the Alpine Fault to have become a pure dextral transform structure during the Early and Middle Miocene (see Figure 5-1). During this phase, the lack of convergence meant that minimal compressional deformation took place across the study area, and it went through a phase of relative tectonic quiescence. Parts of the Grey Valley Trough had water depths up to 2km that were inherited from the earliest Miocene phase of inversion (Spanninga, 1993), and these were progressively in-filled with the Stillwater Mudstone. The Alpine Fault was active as a dextral transform to the east of the study area (some distance further east of its present location). Little previous work has been done to asess if any land was uplifted sub aerially and eroding on the eastern side of the Alpine Fault adjacent to the study area at this time. During the Early and Middle Miocene, active convergence and uplift was occurring hundreds of kilometres further north across the Taranaki Fault (Holt and Stern, 1994). Given the uniform, fine grained nature of the Stillwater Mudstone, it is possible that it is the distally transported sediment that was sourced from an uplifting area to the east of the Taranaki Fault (Holt and Stern, 1994). The coarser Niagara Sandstone units within the Stillwater Mudstone have been interpreted to be sourced from a more proximal sediment source to the east (Matthews, 1990; Diligenz, 2009). Based on this, it is suggested here that relatively small amounts of uplift and erosion associated with activity on the adjacent Alpine Fault may have been occurring during this time.

5.4 Increased convergence across the Alpine Fault since the Late Miocene

The exact timing that convergence began to increase across the Alpine Fault, and the Southern Alps began to uplift has remained controversial. Taking into account evidence from a number of

different workers, increased convergence and uplift across the Alpine Fault may have begun to occur any time between 11 Ma and 6 Ma (Walcott, 1998; Cande and Stock, 2004), with it likely to have started earlier in the north (Kamp et al., 1992). The start of increased convergence across the plate boundary during Late Miocene would have significantly affected the tectonic setting of the study area, as it was situated in on the margin of the rising Southern Alps Orogen. Although the timing is poorly constrained, the formation of the Late Miocene unconformity across the study area correlates with this change in tectonic setting. This also approximately correlates with the timing that the Westland Basin changed tectonic setting into what has been identified as a foreland basin system (Kamp et al., 1992; Sircombe, 1993; Sircombe and Kamp, 1998; Harrison, 1999).

A number of pieces of evidence suggest that the study area developed as a westward migrating foreland basin system during the Late Miocene. The process of outward migration of a foreland basin system during the growth of an orogen has been well documented (eg. Horton and Decelles, 1997). In the study area, initial broad scale uplift is thought to have produced the widespread late Miocene unconformity. This is consistent with the most of the study area being situated on the forebulge depozone of the foreland system at this time. This situation is thought to have occurred in the early phases of mountain building when the western side of the fold and thrust belt was much further east, and the orogen was relatively narrow. The Hohonu Fault is not thought to have been active at this time, instead, the Hohonu Block would likely have been in the position of the foredeep and has since been inverted (cf. Kamp et al. 1992). Resumption of sedimentation above the unconformity across the Paparoa Inversion Zone and Grey Valley Trough show a migration into the foredeep depozone. This was possibly associated with the advancing of the western boundary of the fold and thrust belt close to the present position of the Hohonu Fault. The Deep Creek Conglomerate, which directly overlies the Late Miocene unconformity in the northern Grey Valley Trough shows a relatively rapid initiation of subsidence. This is interpreted to have occurred as a result of a rapid advancement of the fold and thrust belt through the activation of a new range front thrust. The Callaghans Greensand which directly overlies the Late Miocene unconformity on the Paparoa Inversion Zone is thought to have been deposited in a shallow water setting, far away from land, with minimal sediment input. This is consistent with it being situated on the margin of the forebulge, with subsequent sedimentation showing it migrating into the foredeep.

As shortening continued, the orogen-bounding Hohonu Fault began to activate. Greenland Group derived debris flow deposits within the mostly granite-derived Eight Mile Formation in the direct footwall of the Hohonu Fault on the northwest side of the Hohonu Range provide evidence of active unroofing of granites in frontal-thrust blocks during the Pliocene. The main trace of the Hohonu Fault at this time is interpreted as being an eroding active fault scarp on the seafloor with

large amounts of granite-derived sediment transported from uplifted areas further east being deposited on the subsiding footwall side. Uplift of the Hohonu Range since the Late Miocene is consistent with fission track data from further south along the same faulted block (White and Green 1986; Kamp et al., 1992; Batt et al., 2004; Ring and Bernet, 2010).

As the Southern Alps Orogen developed further during the Pliocene, continuing foreland flexure provided more accommodation space in which the Eight Mile Formation was deposited. The deposition of the Old Man Group in the Late Pliocene may represent a time when the foreland basin became overfilled, and therefore became terrestrial.

It appears that the foreland basin system became perturbed from around 2-3 Ma with the reactivation of the inverted faults bounding the Paparoa Inversion Zone (Suggate and Waight, 1999; Kamp et al., 1999). In terms of development as a foreland system (c.f Decelles and Giles, 1996), the whole onshore region of the northwest South Island may be considered to be part of the fold and thrust belt of the orogen, or the wedge-top depozone (cf. Ghisetti et al., 2014). The deformation front of the fold and thrust belt in the present setting would be the Cape Foulwind Fault; the offshore platform, the foredeep; and the forebulge, around 50km offshore (Ghisetti et al., 2014, Harrison, 1999). This view necessitates the presence of an active detachment at depth transferring deformation to the present thrust margin and this has been speculated to be the case (Ghisetti et al., 2014).

5.5 Hohonu Fault Development

As described above, the development of the Hohonu Fault is inferred here to be directly related to the development of the study area as a foreland-type system from the Late Miocene. Some previous workers have described the Hohonu block as being an uplifting and eroding zone since the Early Miocene (Suggate and Waight, 1999; Matthews, 1990). This view is primarily based on the presence of the Hohonu Conglomerate, which has only been found adjacent to the Hohonu Range, and is therefore inferred to be sourced from material that has eroded from its mass. Based on observations of the in-faulted wedge of Oligocene and Early Miocene sediments on the western margin of the Hohonu Range (Figure 3-7), a previous Early Miocene phase of thrust faulting is inferred to be related to the production of conglomerates and probably not the Hohonu Fault. The fault that was observed in this study bounding the western side of this in faulted wedge (site 6.12 – see Figure 3-7) is best explained as an Early Miocene reverse fault, likely to have originally been west-dipping that has been cross-cut by the east-dipping Hohonu Fault since the late Miocene, and rotated. The implication is that there were probably thrust faults that were associated with the uplifting of nearby eroding areas from which the Hohonu conglomerates were sourced, but this

was probably not due to movement on the Hohonu Fault itself, which in inferred here to have developed as a large NE-SW trending thrust fault since convergence increased across the Alpine Fault in the Late Miocene.

5.6 WNW-ESE trending Cretaceous extensional structures

This section discusses the evidence for both the presence and the influence on Neogene tectonic activity of WNW-ESE trending Cretaceous extensional structures in each of the main tectonic domains across the study area. In the offshore platform tectonic domain, the presence of WNW-ESE oriented Cretaceous structures is well documented. Further east, the continuation of these structures is less well documented, but evidence suggesting their presence gathered during this study will be discussed.

5.6.1 Offshore platform

Offshore of Greymouth, a half graben structure (the Takutai Half Graben) up to 1500 m deep and c. 10 km wide has been mapped. This structure extends for over 40 km approximately perpendicular to the coast from where it appears to be truncated by the Cape Foulwind Fault c. 5 km offshore (Geophysical Service Inc., 1981; Bishop, 1992b; Reynolds, 2009). The Takutai Half Graben has not been drilled, so estimates of its exact age are largely speculative. Both the Pororari Group and early part of the Paparoa Coal Measures onshore have similar WNW-ESE depositional trends, and this has been used by Bishop (1992b) to infer that it formed in the Late Cretaceous, although it is uncertain if it was active mainly before and/or after the start of seafloor spreading in the Tasman Sea c. 83 Ma. The main bounding fault of this half graben is on its northern side. Warping of Oligocene - Recent sediments is particularly noticeable above this northern bounding fault (see Figure 5-3). This warping could be explained by a greater degree of compaction of the half graben infill relative to the shouldering basement rock, with no reactivation of the fault (in a normal sense of slip) necessarily occurring. However, observation of the earthquakes that have been recorded in the area (from www.geonet.org.nz) show a clear WNW- ESE trending linear swarm of earthquakes occurring c. 10 km north of the Takutai Half Graben during the years 2002 and 2003 (see Figure 5-4). Another, similar sized WNW-ESE half graben structure has been mapped c. 30 km further north by Geophysical Service Inc. (1981) with a bounding fault on the southern side, although very little work has been done to constrain the size and origin of this structure.

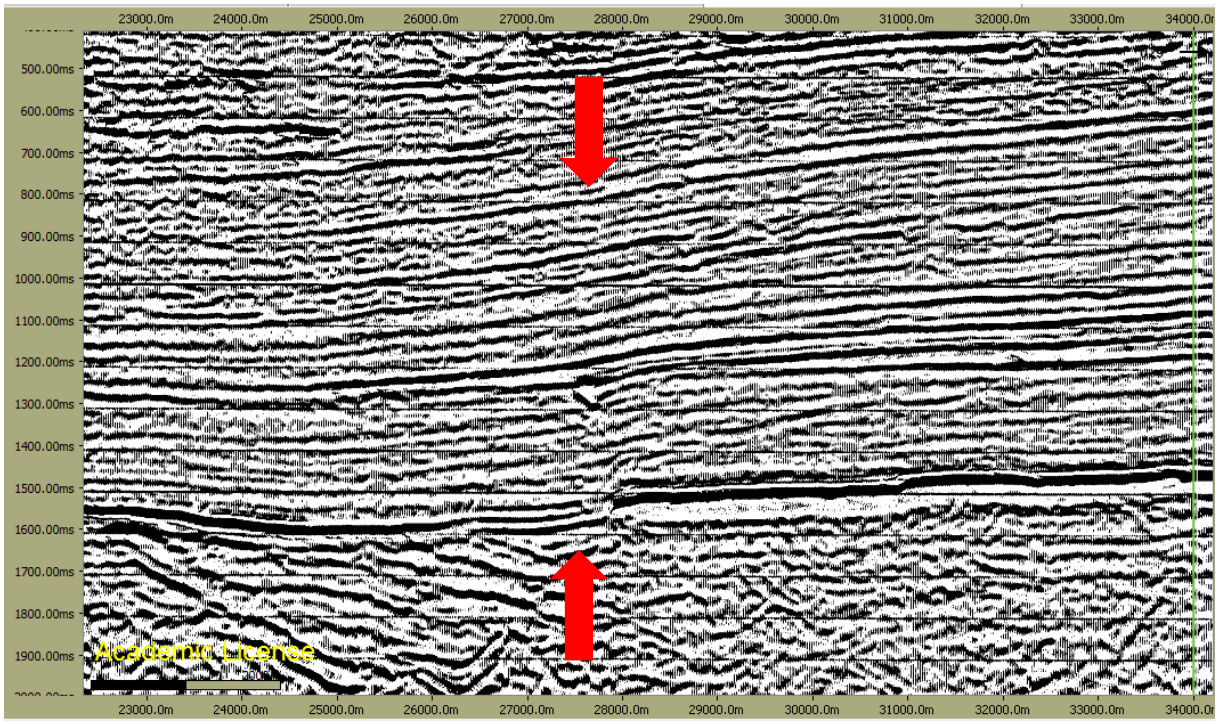

Figure 5-3: Warping of Oligocene to recent sediments (indicated with red arrows) above the northern bounding fault of the Takutai Half Graben on seismic profile DS3-82-07.

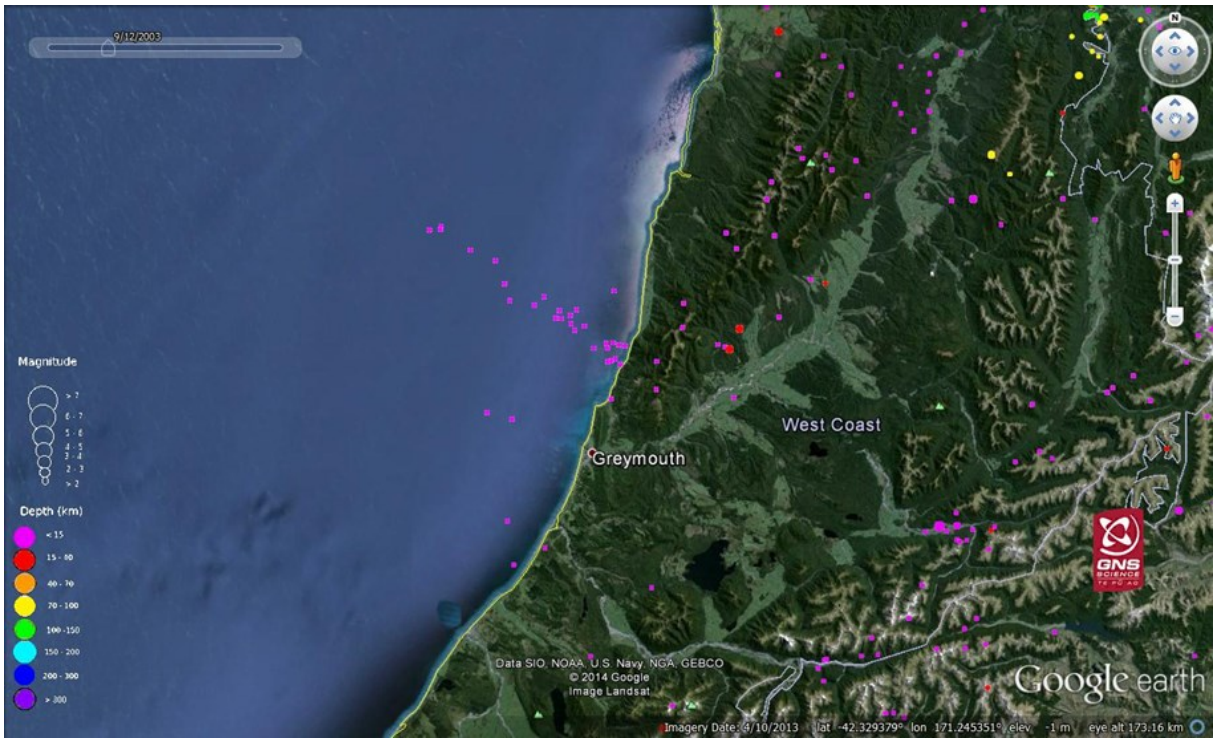

Figure 5-4: Earthquakes recorded in the study area during the years 2002 and 2003. It shows cluster of M2-M3 earthquakes forming a clear WNW-ESE trend offshore Greymouth that are parallel with the the Takutai Half Graben. Source: GNS earthquake database, displayed on Google Earth.

5.6.2 Paparoa Inversion Zone

No definite WNW-ESE trending structures have been identified in the seismic as crossing the Paparoa Inversion Zone during this study (Figure 4-7). This may be largely due to the poor quality of seismic and the stratigraphic level at which these structures occur. As stated above, WNW-ESE trending normal faults are thought to have controlled the deposition of the Pororari Group and lower part of the Paparoa Coal Measures. Across the Paparoa Inversion Zone, the overlying strata are typically over 2 km thick, and have been deformed by faulting and folding. Due to the difference in conditions, the relatively subtle seismic response of the Cretaceous rift structure that is seen along straight seismic profiles through flat overlying sediments offshore, is not able to be distinguished onshore due to the much poorer quality.

The aeromagnetic data (from www.nzpam.govt.nz) provide some evidence for the continuation of the Takutai Half Graben onshore. The diffuse northeast boundary of the Kumara Magnetic Anomaly (see Figure 4-11) across the Paparoa Inversion Zone defines a linear belt that is almost exactly co-linear with the northern bounding fault of the Takutai Half Graben. This firstly suggests that the Takutai Half Graben may continue onshore, however, no seismic profiles are present across this part of the Paparoa Inversion Zone to confirm the northern bounding faults presence. Secondly, it suggests that either the northern bounding fault of the half graben is also the northern boundary of the intrusive body that creates the magnetic anomaly, or that the half graben is infilled with volcani-clastics that also have a high magnetic intensity and are associated with the intrusion. Unfortunately, the aeromagnetic data do not extend offshore, meaning that the northern boundary of the Kumara Magnetic Anomaly cannot be directly correlated with the position of the Takutai Half Graben.

Potential influences on Neogene tectonic development of the inferred onshore continuation of the Takutai Half Graben across the Paparoa Inversion Zone include:

1) The fact that the Cobden Limestone escarpment of the Brunner –Mt Davy Anticline plunges southward, beneath the Miocene sediments at the point where it crosses the northern boundary of the Kumara Magnetic Anomaly. The Cobden Limestone makes a good marker for Neogene tectonic deformation as it was originally deposited across a relatively flat surface between 50 and 200 m below sea level. This means that the locations where it is presently observed to be uplifted and eroded approximate the places where there has been a net uplift of the basement during the Neogene. The presence of the Cobden Limestone escarpment across the Paparoa Inversion Zone therefore approximately marks the transition between where there has been net uplift to the north and net subsidence to the south. It is suggested here that the inferred onshore continuation of the

Takutai Half Graben could be associated with this transition from net uplift to net subsidence during the Neogene.

2) A WNW-ESE trending fault cutting the Early Miocene Inangahua Formation and Oligocene Cobden Limestone mapped by Nathan (1978) across the western flank of the anticline to the south of Greymouth is directly above the inferred onshore continuation of the northern bounding fault of the Takutai Half Graben. This fault (and the Inangahua Formation outcrop) is not mapped by Suggate and Waight (1999), so its presence may be questionable, but if it is present, it may be associated with localized, fault controlled subsidence of the Takutai Half Graben in the Early Miocene.

5.6.3 Grey Valley Trough

The south-eastward continuation of the diffuse northern boundary of the Kumara Magnetic Anomaly into the Grey Valley Trough suggests that the northern bounding fault of the Takutai Half Graben continues further east, across the Paparoa Tectonic Zone. Again, lack of seismic coverage means that this is not able to be comprehensively confirmed, although there is what appears to be a half graben in the right location on profile GV08 (see Figure 5-5).

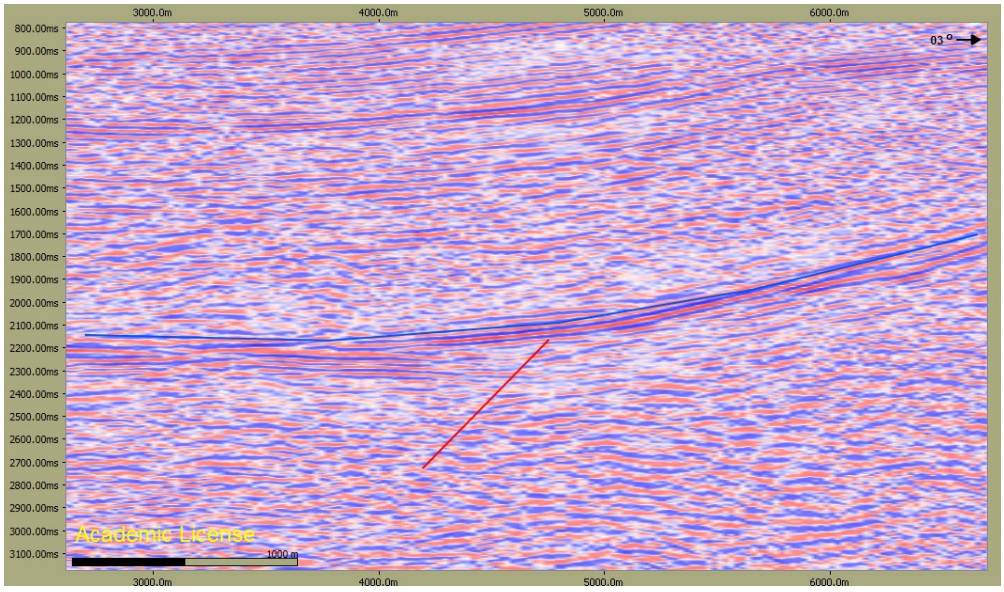

Figure 5-5: A section of line GV-08 showing a potential half-graben structure beneath the top Cobden reflector, at the location where it crosses the northern boundary of the Kumara Magnetic Anomaly.

WNW-ESE trending faults inferred in seismic lines from the bending of reflectors across vertical planes in the southern Grey Valley Trough are also likely to be associated with the Cretaceous structures in the underlying basement. As mentioned in chapter 4, the basement structures that control the development of these features were not identified due to the poor quality of the seismic profiles. However, the wide zone over which the reflectors have bent, and that the reflectors are

bent around a vertical axial plane is consistent with differential compaction like that seen relatively easily in the seismic profiles across the Takutai Half Graben offshore. Faults in a WNW-ESE orientation have been mapped in this location by Toomath and Palmer (1987) and Haskell (1991) (see Figure 5-6). Booth's (2008) map of the top basement unconformity across the southern part of the study area (Figure 5-7) shows a NW-SE trending section where the basement dips steeply to the north across the southern part of the Grey Valley Trough. These interpretations support the interpretations made in this study of WNW-ESE trending structures in the southern Grey Valley Trough. A significant observation made in this study is the link between a clear monoclonal bend in the reflectors of profile WD-7 (a straight profile that trends NNE-SSW down the centre of the southern Grey Valley Trough – see Figure 3-3) with the southern boundary of the Kumara Magnetic Anomaly (see Figure 5-8). This again suggests that the presence of the magnetic anomaly is associated with basement structures.

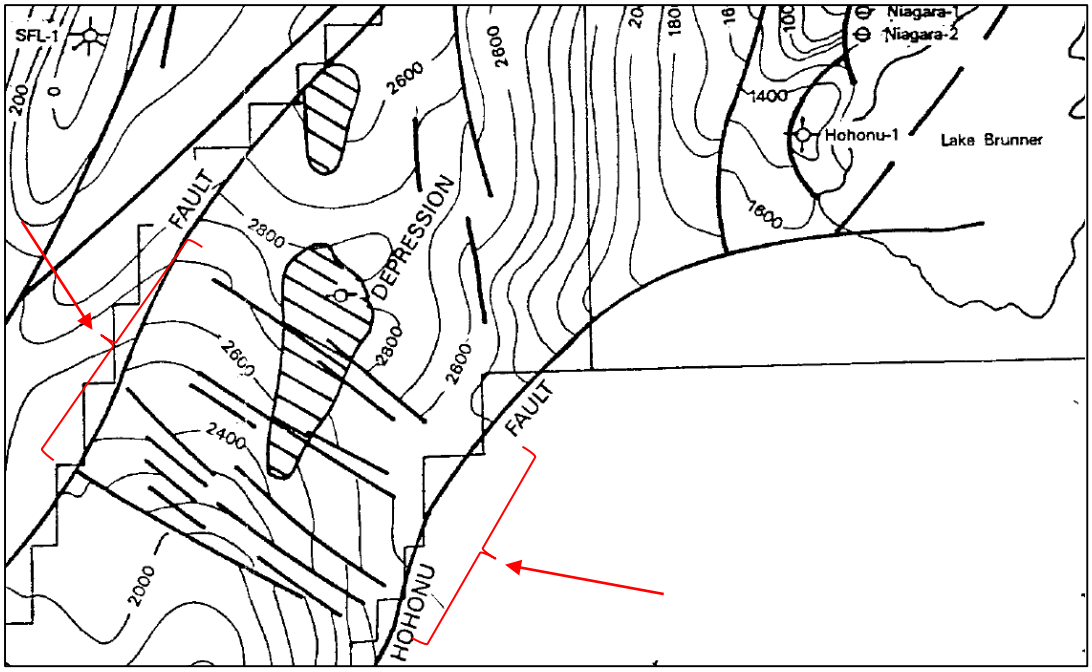

Figure 5-6: Part of the top-basement two-way-time (in milliseconds) structure contour map produced by Haskell (1991). WNW-ESE trending faults indicated with red arrows.

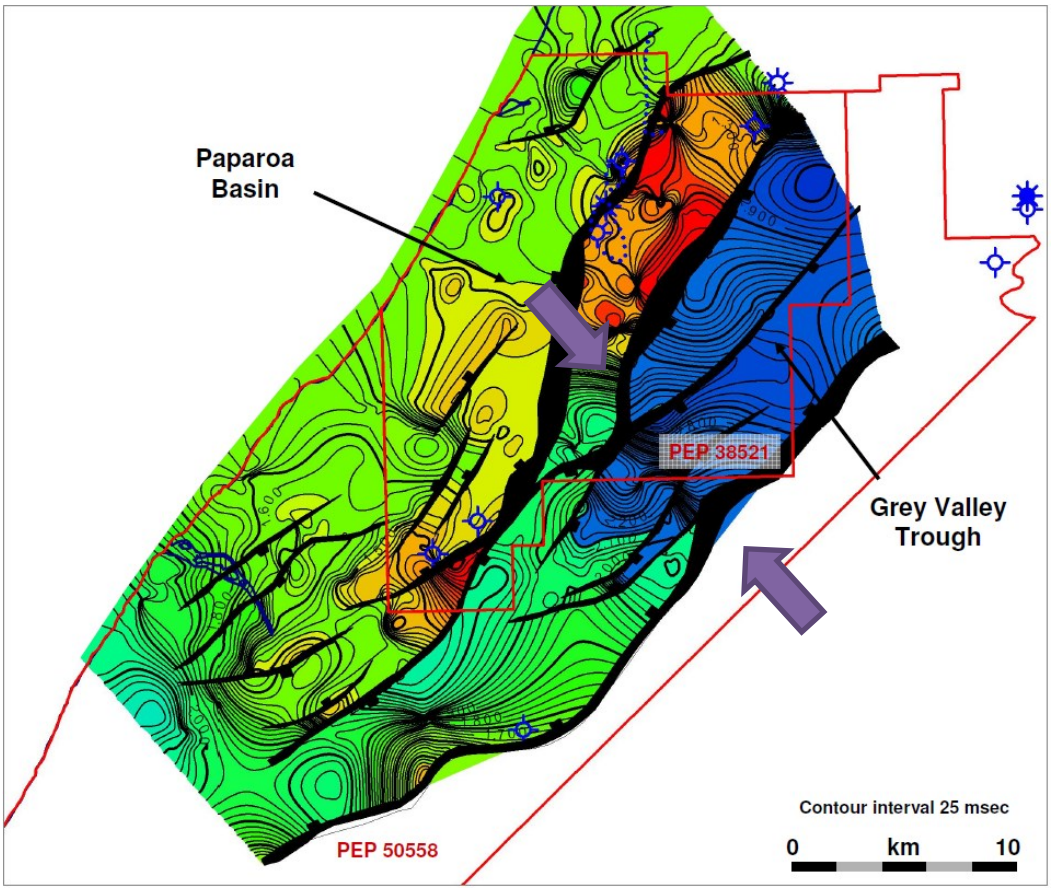

Figure 5-7: Two-way-time top basement structure contour map produced by Booth (2008). A NW-SE orientated, steeply dipping section of the top basement unconformity is indicated with purple arrows.

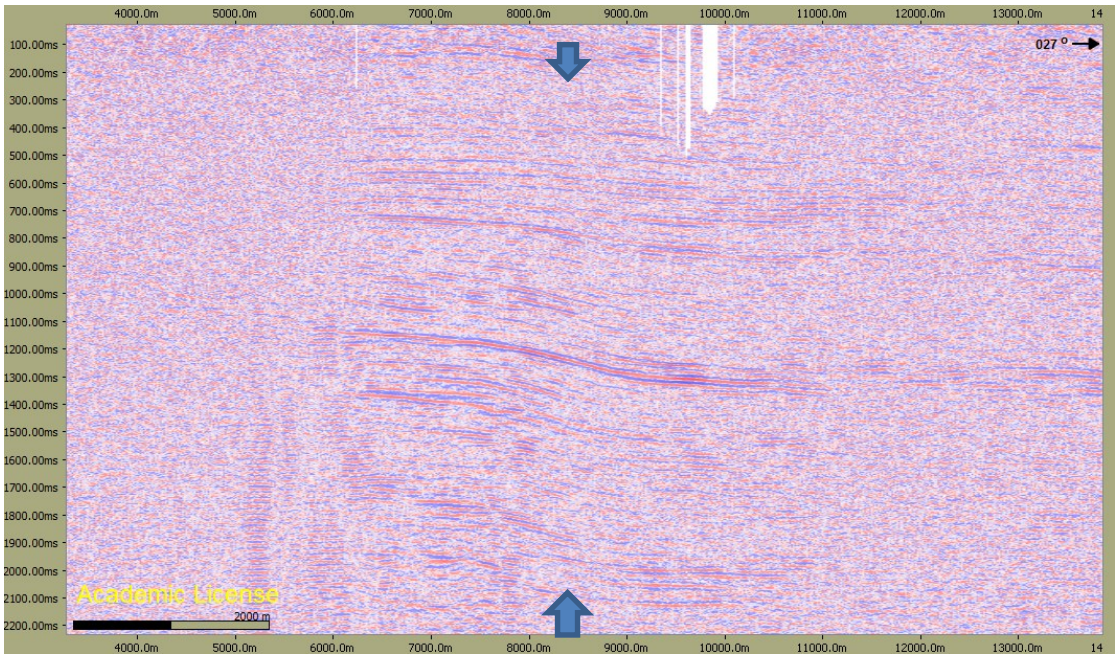

Figure 5-8: A section of the southern part seismic profile WD-7, showing a down-stepping of reflectors from south to north (indicated with arrows), which occurs where the line crosses the southern boundary of the Kumara Magnetic Anomaly.

Yet another suggestion that the Kumara Magnetic Anomaly is associated with structural features is that where it is present across the Grey Valley Trough almost exactly coincides with an anomalous depth to basement of 5 km or more (value calculated during this study, and also in Suggate and Waight, 1999).This is c. 2 km deeper than the deepest parts of the trough to the north and south. This might well be the result of a greater degree of Neogene subsidence, but discussing the reason why this greater degree of subsidence appears to be directly related to the presence of the Kumara Magnetic Anomaly is beyond the scope of this study.

5.6.4 **Hohonu Block**

Because all the cover sediment, and large amounts of basement rock has been eroded from the Hohonu Block, WNW-ESE to NW-SE trending Cretaceous structures are much more difficult to recognize, and very little was able to be done in this regard. However, the possibility remains that if the presence of the Cretaceous structures appears to be linked to the presence of the Kumara Magnetic Anomaly, which in turn is likely to be caused by intrusive rocks, then it is likely that in the Hohonu Range where the magnetic anomaly is projected further to the southeast, evidence of the intrusive rocks that produce the magnetic anomaly will be present. As mentioned in the geological setting chapter, the French Creek Granite (the outcrop of which is confined to the width of the adjacent magnetic anomaly) and Hohonu Dyke swarm were likely to have been emplaced in a zone of continental rifting, at a time almost exactly contemporaneous with the start of seafloor spreading in the Tasman Sea. Given that extension was occurring in a NNE-SSW direction at the time of emplacement, it is likely that the intrusives were sourced from a WNW-ESE trending magma body beneath, and the strong WNW-ESE preferential orientation of the dykes (see Figure 5-9) supports this. The Kumara Magnetic Anomaly could be explained by the presence of such a magma body. A similar scenario is described by Hunt and Nathan (1976) for Inangahua region, where lamprophyre dykes of similar age to those in the Hohonu Range overly another magnetic anomaly, which is also thought to represent the dykes' source.

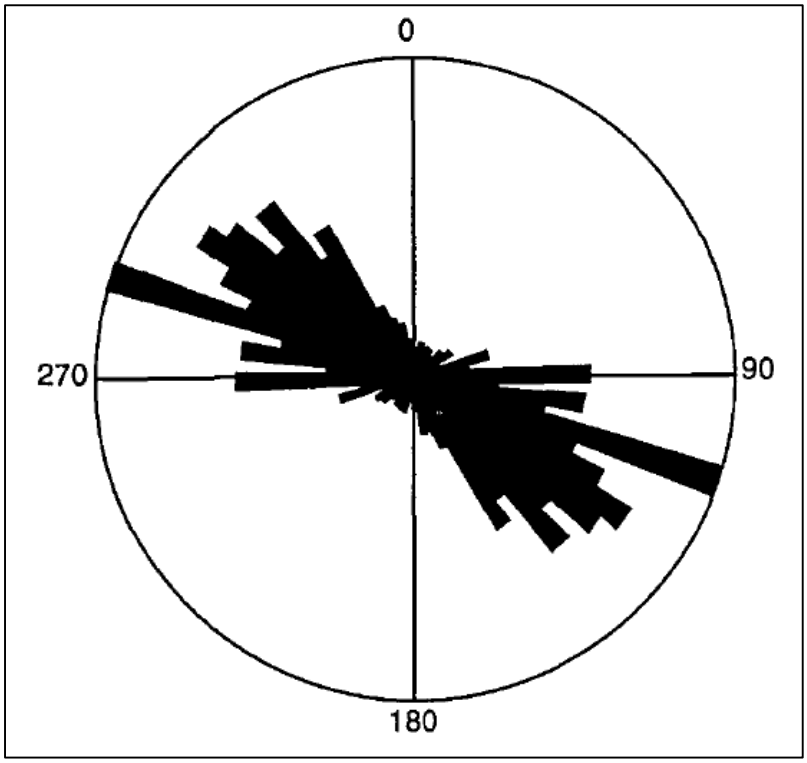

Figure 5-9:Rose plot of strike directions for the Hohonu Dyke Swarm (taken from Waight et al., 1998b).

5.7 Conjugate strike slip faulting across the Hohonu Block and Grey Valley Trough

Important changes to this overall strike of the Hohonu Fault can be seen in the vicinity of the Hohonu Range, and investigating the reasons for these changes is of principal interest for this study. A key thing to note when observing the geology of the Hohonu Range is the orientations of its margins. Taking into account that the maximum horizontal stress is c. 115º (Townend et al, 2012), the east-west striking northern margin and the NW-SE striking southwest margin are seen as potential conjugate strike-slip faults that cut across the main NE-SW striking Hohonu Fault and offset it dextrally and sinistrally respectively.

Both the field observations (Figure 3-2 and Figure 3-3) and aeromagnetic data (Figure 4-11) suggest the existence of a number of significant east-west striking dextral faults across the area between Mt Te Kinga and Lake Ahaura. The most southerly of these is the east-west striking Rocky Creek Fault, a likely eastward continuation of the dextral fault inferred to exist across the northern margin of the Hohonu Range (see Figure 3-2). Kinematic data from the Rocky Creek Fault suggests that at least some component of dextral slip has occurred. This is not conclusive evidence that this fault operated primarily as a strike slip fault, and other kinematic evidence suggests it may be an oblique fault with dip-slip components of undetermined sense. The Rocky

Creek Fault is co-linear with the northern margin of the Hohonu Range which suggests that they may be part of a significant east-west trending structure. The aeromagnetic data (Figure 4-11) show that if this fault continues eastward up to the southern side of Granite Hill, it coincides with apparent dextral separation of magnetically prominent bands of rock. Apparent dextral separation of magnetically prominent bands of rock can also be seen at the northern end of Granite Hill. The fault offsetting these units probably trends east-west, linking with the fault in the lower reaches of Sam Creek (site 2.14 – see Figure 3.3). From here it appears to continue further west to create the northern boundary of the highly magnetic granites at Pah Point. Other dextral east-west striking faults are inferred to intersect the upper reaches of Sam Creek, and the northern flank of Bell Hill. Fieldwork and observations of topography further suggest the existence of a sinistral strike slip in the Bell Hill area. This fault strikes along the upper, NW trending straight section of Deep Creek, forming the gouge zone at site 2.9 (Figure 3.3). It then crosses the ridge into Jones Creek where it is likely to be associated with the fault observed at site 2.6 (Figure 3.3). The inferred fault is then thought to intersect Jones Creek, extend along the hillside on the true left above the gorge section, before intersecting the creek again where it flattens out. The left-lateral separation of the hill front where the creek comes out at the bottom may be associated with activity on the fault.

There is also evidence that east-west dextral strike-slip structures continue across the Grey Valley trough. As mentioned in chapter 4, two possible strike slip faults appear to intersect seismic profile GV-08. These faults appear to be dextral east-west striking faults based on the following evidence: 1) reflector terminations in the surrounding, poorer quality seismic data appear to link up along an east-west strike; and 2) east-west trending linear features in the aeromagnetic data cross those points in GV08 and appear to show apparent dextral separation in shallowly dipping sedimentary horizons.

Based on panoramic field views (Figure 5-10) and Google Earth satellite photos (Figure 5-11), east-west striking dextral faults are also thought to occur in the Hohonu Range, near the summit of Mt French and French Creek. Dextral strike slip kinematics were measured on a fault in upper French Creek and the analysis of a possible fault trace on Google Earth suggests that the fault found in French Creek may be an eastward continuation of that seen intersecting the ridge near Mt French.

Figure 5-10: Southeast dipping faults seen cutting the ridge top adjacent to Mt French.

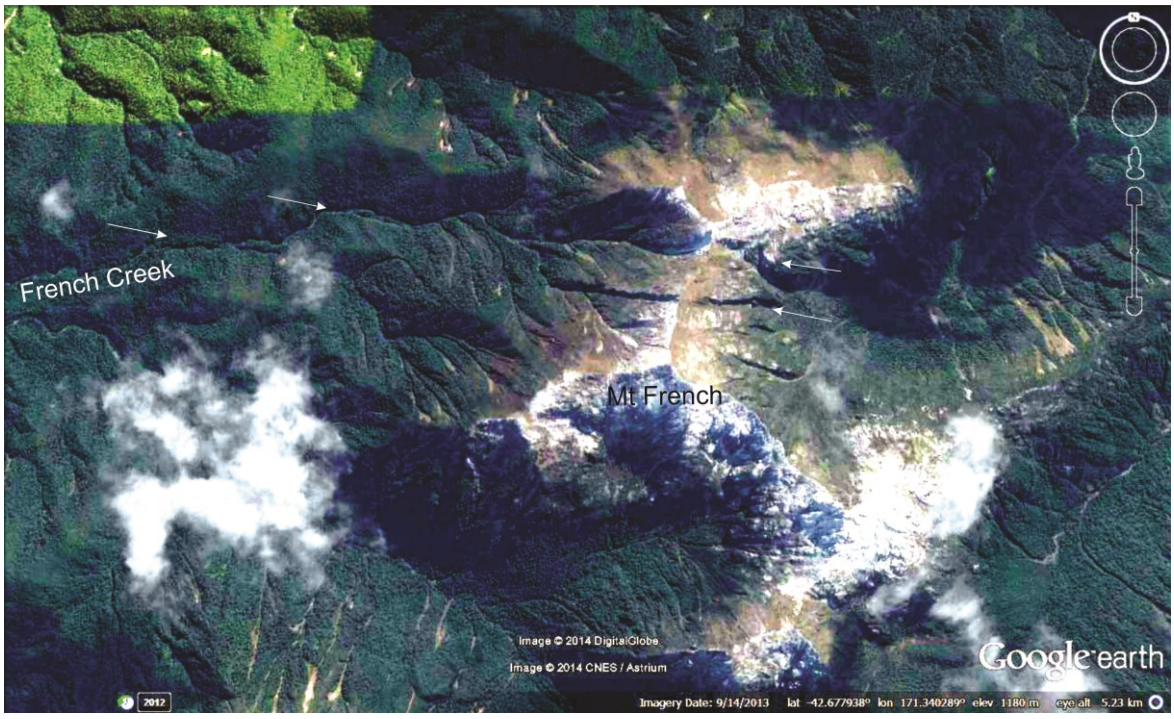

Figure 5-11: Possible fault traces on Google Earth, marked with white arrows. Dextral strike slip kinematic data was gathered from the western end of the southern fault trace.

As mentioned above, it is also suggested in this study that there is a NW-SE trending sinistral fault present beneath the straight section of the Taramakau River on the southwest margin of the Hohonu Range. This hypothesis is largely based on the left lateral separation of the range-front at this location, as well as the strikingly straight edge of steep topography on that side of the range. The poor quality of seismic data leaves it open as a possibility that this fault extends across the Grey Valley Trough. Co-linear features in the aeromagnetic data across the Grey Valley Trough also suggest its existence. The occurrence of an earthquake swarm that began on 1st December 2008, and lasted for around 20 days with 30 M2-3 and 7 M3-3.6 earthquakes provides further support for the existence and present activity of the fault. The locations of earthquake epicentres in this swarm formed a NW-SE trend co-linear with the inferred fault and extended from beneath the Alpine Fault through to the western side of the Grey Valley Trough (Figure 5-12). Unfortunately, the earthquakes were too small to obtain focal solutions from.

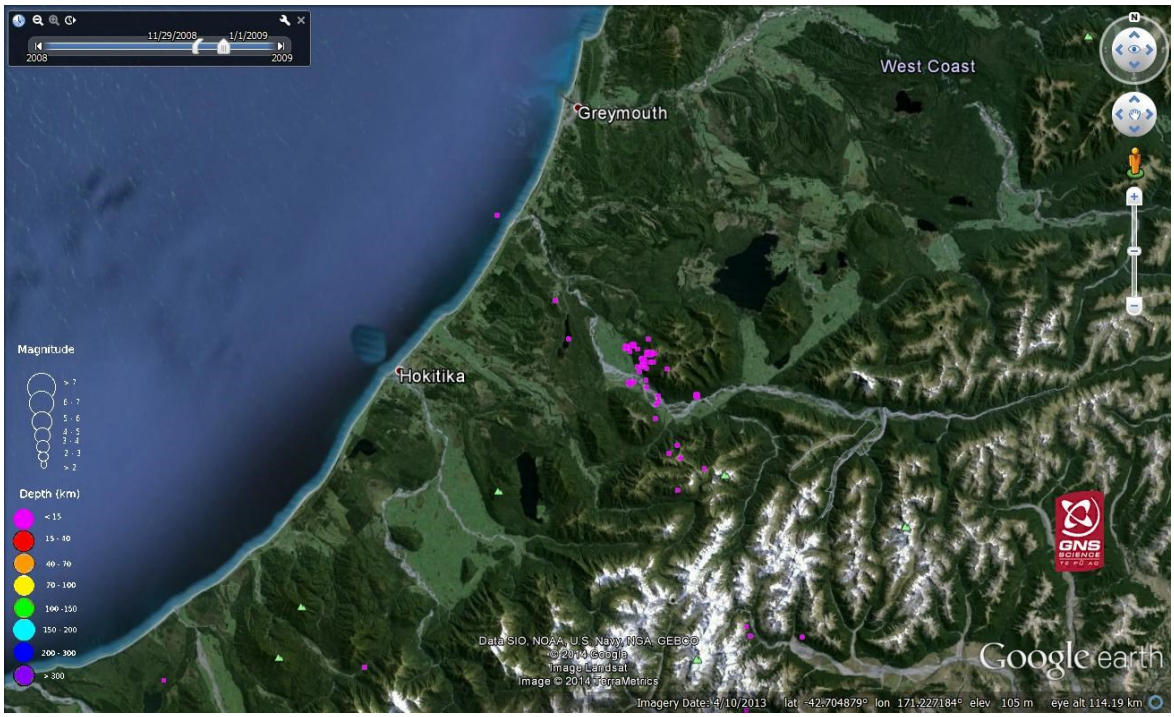

Figure 5-12: Earthquakes that occurred in the study area during the month of December, 2008. The swarm forms a linear feature parallel with the southwest margin of the Hohonu Range. Source: GNS earthquake database, displayed on Google Earth.

Steeply dipping, east-west striking faults with dextral slip components have been described on the western side of the Alpine Fault. Lund Snee et al (2013) describe a fault of this nature at Smithy Creek near Franz Joseph and suggest it is likely to be recently active. There is also evidence for NW-SE striking sinistral faults elsewhere on the West Coast: 1) the focal mechanism for M 4.2

earthquake that occurred on the 30th November 2013 at the northern end of the Paparoa Range appears to show sinistral slip on a vertical NW-SE trending fault (Figure 5-14); and 2), further interpretation of the aeromagnetic data inland of Ross (Figure 5-13) shows NW-SE trending faults sinistrally offsetting a series of linear bands of high magnetic intensity (probably dykes within the Greenland Group).

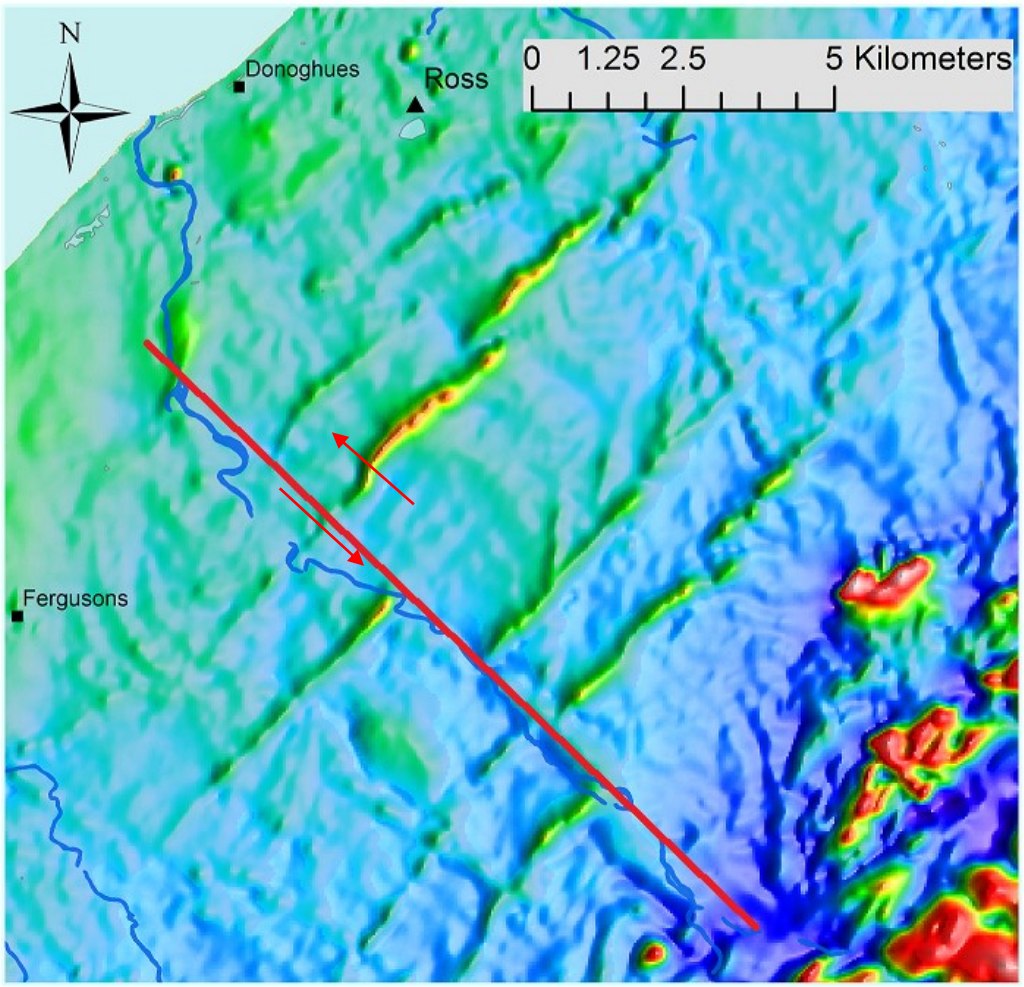

Figure 5-13: Aeromagnetic data near Ross, c. 30km to the south west of the study area (courtesy of New Zealand Petroleum and Minerals. NE trending bands of high magnetic intensity (probably dykes) cross what has been mapped as Greenland Group (Nathan et al 2002). The magnetic bands show a series of apparent regular c. 1.5km left-lateral offsets along the line of the Mikonui River likely to be attributed to the presence of co-linear sinistral strike-slip fault.

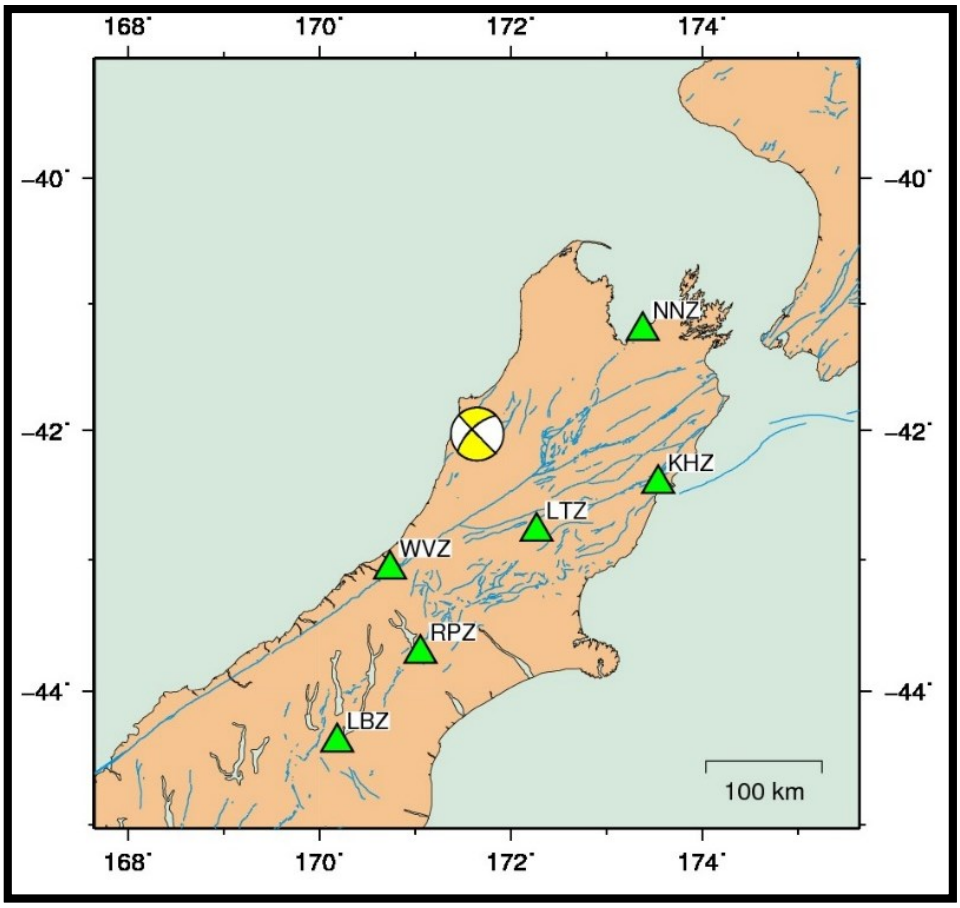

Figure 5-14: Strike-slip focal mechanism (interpreted as NW striking sinistral) for a M.4.2 earthquake that occurred at the northern end of the Paparoa Range on 30th November 2013 (courtesy of John Ristau, GNS)

The evidence presented above suggests that conjugate strike-slip faults, active under the current stress field where SHmax = c. 115º (Townend et al. 2012) are likely to be playing an important role in the Pliocene and Quaternary deformation of the study area. It is suggested here that the presence of these strike – slip faults are associated with the presence of WNW-ESE trending Cretaceous structures. Particularly for the NW-SE trending sinistral fault inferred on the southwest margin of the Hohonu Range, it appears that Cretaceous extensional faults has been reactivated in the current stress field as strike slip fault. A similar phenomenon has been documented for the recent 2010 Darfield earthquake in Canterbury (Campbell et al. 2012; Ghisetti and Sibson, 2012). The E-W trending dextral faults inferred to the north of the Hohonu Range are also thought to be exploiting weaknesses created by the presence of WNW-ESE trending Cretaceous faults. The inferred dextral fault bounding the northern side of the Hohonu Range is considered to be the most significant of these because its position appears to be controlled by the inland extension fault of the northern boundary of the Takutai Half Graben.

5.8 Potential seismic hazard in present day

Earthquakes swarms shown in Figure 5-12 and Figure 5-4 suggest that there is presently seismic activity occurring associated with the presence of the Cretaceous extensional structures. The seismic hazard potential of the structurally important Cretaceous extensional structure identified here, which orthogonally intersects the highly active Alpine Fault plate boundary has not been previously researched, and an in-depth look into this is beyond the scope of this study.

CHAPTER 6. CONCLUSIONS AND RECOMMENDATIONS

6.1 Conclusions

The major findings that have come from this research can be summarized into the following main points:

1) The Neogene tectonic development of the study area involves an initial phase of compressional inversion during the Early Miocene (c. 20 Ma). This was followed by a period of relative tectonic quiescence until compressional deformation, associated with increased rates of convergence across the plate boundary began to occur between 12 and 7 Ma. The widespread Late Miocene unconformity suggests that in the initial phases of orogenesis, most of the study area was situated in on the forebulge depozone in which minor uplift occurred. This was followed by the westward advancing of the fold and thrust belt towards the present position of the Hohonu Fault and the migration of most of the study area into the foredeep depozone. As the plate boundary developed further and compressional deformation continued to occur across the study area during the Late Pliocene, a second phase of compressional inversion began with the re-activation of the faults bounding the Paparoa Inversion Zone. In a sense, this can be considered as the time that the onshore part of the study area became part of the fold and thrust belt of the foreland system.
2) The Hohonu Thrust began to develop as a major structural feature from the latest Miocene. Over the course of its development, it has been perturbed from developing as a typical thrust into the foreland through being intersected by a series of conjugate strike slip faults. The amount of down-throw of the footwall of the fault also varies greatly.
3) A WNW-ESE trending, c. 25 km wide zone of Late Cretaceous extensional faulting, likely to be associated with magmatism extends from the Takutai Half Graben offshore, through to the Hohonu Range. This has had a significant influence on Neogene deformation in the Grey Valley Trough and Hohonu Block. In the Grey Valley Trough, the zone of Cretaceous extensional faulting coincides with an area where the basement has subsided c. 2 km deeper (up to 6 km) than any part of the trough to the north or south. The conjugate strike slip faults inferred to the southwest and north of the Hohonu Range are thought to be either reactivated or controlled by the presence of pre-existing Cretaceous extensional faults.

6.2 Recommendations

The conclusions that have been proposed in this study are new and require further research in order to be either accepted or disregarded by the wider scientific community. Following are suggestions for further research required to either prove, or count against the hypothesis stated in this thesis:

1) Both targeted and widespread kinematic mapping across the Hohonu Block. This would be done by examining both aeromagnetic data and satellite photos for likely fault zones and assessing the kinematics of them. Principal targets include:
    a. The inferred dextral strike-slip faults both to the north and south of Granite Hill and the Granite Hill Fault on the western side of Granite Hill
    b. The east-west striking faults across the summit of Mt French.
    c. The fault at the head of Eel Creek on the north side of the Hohonu Range
    d. Assess whether the French Creek Granite is fault bounded
    e. Assess the kinematics of the a fault mapped by Waight (1995) in the Grahams Creek on the north side of Mt Turiwhate
    f. Assess the kinematics of potential shears in the creeks that drain the southwest margin of the Hohonu Range to see if they comply with the existence of the significant sinistral-reverse fault proposed to run along the base of the hill.
    g. Mapping of fault zones, cleavage and bedding in creeks on the northern side of Bell Hill.
2) For suspected active faults, use small scale, shallow geophysics to assess their recent history of activation. Specific targets for this method include:
    a. Where a proposed sinistral fault exits the north-western side of Bell Hill at Jones Creek.
    b. Gravels against base of the southwestern margin of the Hohonu Range to test for the presence of the proposed sinistral fault in that location.
    c. The east-west trending strike - slip faults that have been interpreted in both seismic and aeromagnetic data across the Kotuku Anticline to the north of the Hohonu Range. There may also be surface outcrop evidence for the presence of these faults.

REFERENCES

Adams, C. J. (2004). Rb-Sr age and strontium isotope characteristics of the Greenland Group, Buller Terrane, New Zealand, and correlations at the East Gondwanaland margin. New Zealand Journal of Geology and Geophysics, 47(2), 189-200

Anderson, E.M. (1905). The dynamics of faulting. Transactions of the Edinburgh Geological Society. 8, 387-402.

Allen, Philip A.; Allen, John R. (2009). Basin Analysis: Principles and Applications

Allmendinger, R. W., Cardozo, N. C., and Fisher, D., 2012, Structural Geology Algorithms: Vectors & Tensors: Cambridge, England, Cambridge University Press, 289 pp.

Batt, G. E., Baldwin, S. L., Cottam, M. A., Fitzgerald, P. G., Brandon, M. T., & Spell, T. L. (2004). Cenozoic plate boundary evolution in the South Island of New Zealand: New thermochronological constraints. Tectonics, 23(4).

Baur, J., Sutherland, R., & Stern, T. (2013). Anomalous passive subsidence of deep-water sedimentary basins: a prearc basin example, southern New Caledonia Trough and Taranaki Basin, New Zealand. Basin Research.

Beaumont, C., Kamp, P. J., Hamilton, J., & Fullsack, P. (1996). The continental collision zone, South Island, New Zealand: Comparison of geodynamical models and observations. Journal of Geophysical Research: Solid Earth (1978–2012), 101(B1), 3333-3359.

Bishop, D. J. (1992a). Middle Cretaceous - Tertiary Tectonics and Seismic Interpretation of North Westland and Northwest Nelson, New Zealand. PhD Thesis, Victoria University of Wellington.

Bishop, D. J. (1992b). Extensional tectonism and magmatism during the middle Cretaceous to Paleocene, North Westland, New Zealand. New Zealand journal of geology and geophysics, 35(1), 81-91.

Bishop, D. J., & Buchanan, P. G. (1995). Development of structurally inverted basins: a case study from the West Coast, South Island, New Zealand. Geological Society, London, Special Publications, 88(1), 549-585.

Bonini, M., Sani, F., & Antonielli, B. (2012). Basin inversion and contractional reactivation of inherited normal faults: A review based on previous and new experimental models. Tectonophysics, 522, 55-88.

Bowman, R.G. (1984). Greymouth Coalfield report, New Zealand Coal resources survey. Unpublished report to Mines Division, Ministry of Energy. Institute of Geological and Nuclear Sciences open file coal report 136.

Bradshaw, J. D. (1989). Cretaceous geotectonic patterns in the New Zealand region. Tectonics, 8(4), 803-820.

Buchan, R.J., (1997).Westland Basin seismic interpretation report. PEP38505 and PEP38506, South Island, New Zealand. Unpublished open-file petroleum report PR2298. Ministry of Economic Development, Wellington.

Campbell, J. K., Pettinga, J. R., & Jongens, R. (2012). The tectonic and structural setting of the 4 September 2010 Darfield (Canterbury) earthquake sequence, New Zealand. New Zealand Journal of Geology and Geophysics, 55(3), 155-168.

Cande, S. C., & Stock, J. M. (2004). Pacific–Antarctic–Australia motion and the formation of the Macquarie Plate. Geophysical Journal International, 157(1), 399-414.

Carter, M.J., (1981). Kokiri-1 Well Completion Report, PPL 38038. Unpublished open-file petroleum report PR799. Ministry of Economic Development, Wellington.

Catuneanu, O. (2004). Retroarc foreland systems—evolution through time. Journal of African Earth Sciences, 38(3), 225-242

Christie, L. J. (2007). Cretaceous and Cenozoic Basin Evolution Based on Decompacted Sediment Thickness from Petroleum Wells around New Zealand. Masters Thesis, Victoria University of Wellington.

Davey, F.J., Henyey, T., Kleffmann, S., Melhuish, A., Okaya, D., Stern,T.A., Woodward, D.J., 1995. Crustal refections from the Alpine Fault zone, South Island, New Zealand. New Zealand Journal of Geology and Geophysics 38, 601-604.

DeCelles, P. G., & Giles, K. A. (1996). Foreland basin systems. Basin Research, 8(2), 105-123.

DILIGENZ, (2009). The Potential For Submarine Fan Plays In The Grey Valley Trough, West Coast Basin, South Island, NZ. Unpublished open-file petroleum report PR4081. Ministry of Economic Development, Wellington.

Egan, S.S., Buddin, T.S., Kane, S.J., Williams, G.D., (1997). Three-dimensional modelling and visualization in structural geology: new techniques for the restoration and balancing of volumes. In: Proceedings of the 1996 Geoscience Information Group Conference on Geological Visualization, Electronic Geology, 1, Paper 7, pp. 67-82.

Friedman, M., Hugman, R. H. H., & Handin, J. (1980). Experimental folding of rocks under confining pressure, Part VIII—Forced folding of unconsolidated sand and of lubricated layers of limestone and sandstone. Geological Society of America Bulletin, 91(5), 307-312.

Friedman, M., Handin, J., Logan, J. M., Min, K. D., & Stearns, D. W. (1976). Experimental folding of rocks under confining pressure: Part III. Faulted drape folds in multilithologic layered specimens. Geological Society of America Bulletin, 87(7), 1049-1066.

Furlong, K. P., & Kamp, P. J. (2009). The lithospheric geodynamics of plate boundary transpression in New Zealand: Initiating and emplacing subduction along the Hikurangi margin, and the tectonic evolution of the Alpine Fault system. Tectonophysics, 474(3), 449-462.

Furlong, K. P., & Kamp, P. J. (2013). Changes in plate boundary kinematics: Punctuated or smoothly varying—Evidence from the mid-Cenozoic transition from lithospheric extension to shortening in New Zealand. Tectonophysics, 608, 1328-1342.

Gage, M. (1952). The Greymouth Coalfield (No. 45). RE Owen, Govt. Printer.

Geophysical Service Inc., (1981). Marine Seismic Survey PPL38129. Unpublished open-file petroleum report PR855. Ministry of Economic Development, Wellington.

Ghisetti, F. C., & Sibson, R. H. (2006). Accommodation of compressional inversion in north-western South Island (New Zealand): Old faults versus new? Journal of Structural Geology, 28(11), 1994-2010.

Ghisetti, F. C., & Sibson, R. H. (2012). Compressional reactivation of E–W inherited normal faults in the area of the 2010–2011 Canterbury earthquake sequence. New Zealand Journal of Geology and Geophysics, 55(3), 177-184.

Ghisetti, F. C., Barnes, P. M., & Sibson, R. H. (2014). Deformation of the Top Basement Unconformity west of the Alpine Fault (South Island, New Zealand): seismotectonic implications. New Zealand Journal of Geology and Geophysics, (ahead-of-print), 1-24.

Groshong, R. H. (2006). 3 D structural geology: a practical guide to quantitative surface and subsurface map interpretation. 2nd. ed. corr.

Hamill, L. J. (1972). Geology of the western Hohonu Range, north Westland. Unpublished BSc (Hons.) thesis, University of Otago.

Harrison, A. J. (1999). Multi-channel Seismic and Flexural Analysis of the Westland Sedimentary Basin, South Island, New Zealand. Masters Thesis, Victoria University of Wellington.

Haskell, T.R., (1991). An assessment of the Pounamu Structure, Grey Valley, Westland, New Zealand, as an oil prospect. PPL38070. Unpublished open-file petroleum report PR1752. Ministry of Economic Development, Wellington.

Haskell, T.R., (2009). Pertroleum systems in the Grey Valley Trough, PEP50558, West Coast, New Zealand. Unpublished open-file petroleum report PR4045. Ministry of Economic Development, Wellington.

Hiess, J., Ireland, T., & Rattenbury, M. (2010). U-Th-Pb zircon and monazite geochronology of Western Province gneissic rocks, central-south Westland, New Zealand. New Zealand Journal of Geology and Geophysics, 53(4), 241-269.

Holt, W. E., & Stern, T. A. (1994). Subduction, platform subsidence, and foreland thrust loading: The late Tertiary development of Taranaki Basin, New Zealand. Tectonics, 13(5), 1068-1092.

Horton, B. K., & DeCelles, P. G. (1997). The modern foreland basin system adjacent to the Central Andes. Geology, 25(10), 895-898.

Hossack, J. R. (1979). The use of balanced cross-sections in the calculation of orogenic contraction: a review. Journal of the Geological Society, 136(6), 705-711.

Hunt, T., & Nathan, S. (1976). Inangahua magnetic anomaly, New Zealand. New Zealand journal of geology and geophysics, 19(4), 395-406.

Ivanovskaya, T. A., Gor'kova, N. V., Karpova, G. V., Pokrovskaya, E. V., & Drits, V. A. (2003). Chloritization of Globular and Platy Phyllosilicates of the Glauconite Series in Terrigenous Rocks of the Upper Riphean Päräjarvi Formation (Srednii Peninsula). Lithology and Mineral Resources, 38(6), 495-508.

Kamp, P. J. (1986). The mid-Cenozoic Challenger Rift System of western New Zealand and its implications for the age of Alpine fault inception. Geological Society of America Bulletin, 97(3), 255-281.

Kamp, P. J., Green, P. F., & Tippett, J. M. (1992). Tectonic architecture of the mountain front-foreland basin transition, South Island, New Zealand, assessed by fission track analysis. Tectonics, 11(1), 98-113.

Kamp, P. J., Whitehouse, I. W., & Newman, J. (1999). Constraints on the thermal and tectonic evolution of Greymouth coalfield. New Zealand Journal of Geology and Geophysics, 42(3), 447-467.

Kane, S.J., Williams, G.D., Buddin, T.S., Egan, S.S., Hodgetts, D., (1997). Flexural-slip Based Restoration in 3D, a New Approach. AAPG Annual Convention Official Program, p. A58.

Kelman Seismic Processing, (1996). Reprocessing Programme, PEP38505 and PEP38506, Westland Basin. Unpublished open-file petroleum report PR2275. Ministry of Economic Development, Wellington.

Kimbrough, D. L., Tulloch, A. J., & Rattenbury, M. S. (1994). Late Jurassic-Early Cretaceous metamorphic age of Fraser Complex migmatite, Westland, New Zealand. New Zealand journal of geology and geophysics, 37(2), 137-142.

King, P.R. (2000). Tectonic reconstructions of New Zealand: 40 Ma to the Present, New Zealand Journal of Geology and Geophysics, 43:4, 611-638.

Koons, P. O. (1990). Two-sided orogen: Collision and erosion from the sandbox to the Southern Alps, New Zealand. Geology, 18(8), 679-682.

Koons, P. O., & Henderson, C. M. (1995). Geodetic analysis of model oblique collision and comparison to the Southern Alps of New Zealand. New Zealand journal of geology and geophysics, 38(4), 545-552.

Koons, P. O., Norris, R. J., Craw, D., & Cooper, A. F. (2003). Influence of exhumation on the structural evolution of transpressional plate boundaries: An example from the Southern Alps, New Zealand. Geology, 31(1), 3-6.

Laird, M. G. (1968). The Paparoa tectonic zone. New Zealand journal of geology and geophysics, 11(2), 435-454.

Laird, M. G. (1988). Sheet S37, Punakaiki, Geological Map of New Zealand, 1: 63,360. NZ Department of Science and Industrial Research, Wellington.

Laird M.G. (1993). Cretaceous continental rifts, New Zealand region. In: Balance P.F. ed. Sedimentary basins of the world; south Pacific sedimentary basins. Amsterdam, Elsevier. Pp. 37–49.

Laird, M. G., Shelley, D. (1974). Sedimentation and early tectonic history of the Greenland Group, Reefton, New Zealand. New Zealand Journal of Geology and Geophysics 17: 839-854.

Laird, M. G., & Bradshaw, J. D. (2004). The break-up of a long-term relationship: the Cretaceous separation of New Zealand from Gondwana. Gondwana Research, 7(1), 273-286.

Lund Snee, J. E., Toy, V. G., & Gessner, K. (2013). Significance of brittle deformation in the footwall of the Alpine Fault, New Zealand: Smithy Creek Fault zone. Journal of Structural Geology.

Marrett, R. A., and Allmendinger, R. W., (1990). Kinematic analysis of fault-slip data: Journal of Structural Geology, v. 12, p. 973-986.

Matthews, E.R. (1990). Exploration in the onshore Westland Basin. Pp. 62-69 *in* 1989 New Zealand oil exploration conference proceedings 1. Energy and resources division, Ministry of Commerce, Wellington.

Miller, J. F., & Mitra, S. (2011). Deformation and secondary faulting associated with basement-involved compressional and extensional structures. AAPG bulletin, 95(4), 675-689.

Mortimer, N. (2004). New Zealand's geological foundations. Gondwana Research, 7(1), 261-272.

Mutter, J. C., A Hegarty, K., Cande, S. C., & Weissel, J. K. (1985). Breakup between Australia and Antarctica: a brief review in the light of new data. Tectonophysics, 114(1), 255-279.

Nathan, S. (1978a). Sheet S44 - Greymouth (1st ed.). Geological map of New Zealand 1:63360. Wellington, New Zealand. Department of Scientific and Industrial Research.

Nathan, S. (1978b). Cretaceous and Cenozoic history of north Westland. New Zealand unpublished open-file petroleum report PR731. Ministry of Economic Development, New Zealand.

Nathan, S., Anderson, H. J., Cook, R. A., Herzer, R. H., Hoskins, R. H., Raine, J. I., & Smale, D. (1986). Cretaceous and Cenozoic sedimentary basins of the West Coast region, South Island, New Zealand (p. 90). Wellington,, New Zealand: Department of Scientific and Industrial Research.

Nathan, S., Rattenbury, M. S., & Suggate, R. P. (2002). Geology of the Greymouth area. Institute of Geological & Nuclear Sciences 1: 250,000 geological map 12. Institute of Geological and Nuclear Sciences: Lower Hutt, New Zealand.

Naylor, M., & Sinclair, H. D. (2008). Pro-vs. retro-foreland basins. Basin Research, 20(3), 285-303.

Newman, J. (1985). Paleoenvironments, coal properties, and their interrelationship in the Paparoa and selected Brunner Coal Measures on the West Coast of the South Island. PhD Thesis, University of Canterbury.

Norris, R. J., Koons, P. O., & Cooper, A. F. (1990). The obliquely-convergent plate boundary in the South Island of New Zealand: implications for ancient collision zones. Journal of structural geology, 12(5), 715-725.

Norris, R. J. and Cooper, A. F. (1995) Origin of small-scale segmentation and transpressional thrusting along the Alpine fault, New Zealand. Bulletin of the Geological Society of America 107, 231-240.

Norris, R. J., & Cooper, A. F. (2001). Late Quaternary slip rates and slip partitioning on the Alpine Fault, New Zealand. Journal of Structural Geology, 23(2), 507-520.

Ocean Harvest International Ltd, (2008). Seismic Acquisition 2008-1, Reprocessing and Interpretation Report. Unpublished open-file petroleum report PR3799. Ministry of Economic Development, Wellington.

Petit, J. P. (1987). Criteria for the sense of movement on fault surfaces in brittle rocks. Journal of Structural Geology, 9(5), 597-608.

Reynolds, G., (2009). Widespread Energy, Prospectivity Report for Offshore West Coast South Island. Unpublished open-file petroleum report PR3998. Ministry of Economic Development, Wellington.

Sclater, J.G. & Christie, P.A.F. 1980. Continental stretching: an explanation of the post-Mid-Cretaceous subsidence of the Central North Sea Basin. Journal of Geophysical Research, v.85, No. B7. Pp. 3711-3739

Sibson, R. H. (1977). Fault rocks and fault mechanisms. Journal of the Geological Society, 133(3), 191-213.

Sibson, R. H. (2009). Rupturing in overpressured crust during compressional inversion—The case from NE Honshu, Japan. Tectonophysics, 473(3), 404-416.

Sircombe, K. N., & Kamp, P. J. (1998). The South Westland Basin: seismic stratigraphy, basin geometry and evolution of a foreland basin within the Southern Alps collision zone, New Zealand. Tectonophysics, 300(1), 359-387.

Spanninga, G. A. (1993). Evolution of the Grey Valley Trough, Masters Thesis, University of Waikato.

Stern, T. A., & Holt, W. E. (1994). Platform subsidence behind an active subduction zone. Nature, 368(6468), 233-236.

Suggate, R. P. (1987). Active folding in North Westland, New Zealand. New Zealand journal of geology and geophysics, 30(2), 169-174.

Suggate, R. P., & Waight, T. E. (1999). Geology of the Kumara-Moana area, scale 1:50 000 Institute of Geological and Nuclear Sciences geological map, 24. 1 sheet +124 p. Lower Hutt, New Zealand: institute of Geological and Nuclear Sciences Limited.

Sutherland, R., Davey, F., & Beavan, J. (2000). Plate boundary deformation in South Island, New Zealand, is related to inherited lithospheric structure. Earth and Planetary Science Letters, 177(3), 141-151.

Thrasher, G. P. (1990). Tectonics of the Taranaki rift. In New Zealand Petroleum Conference (1989: Queenstown, NZ) (pp. 124-133).

Tippett, J. M., & Kamp, P. J. (1993). Fission track analysis of the late Cenozoic vertical kinematics of continental Pacific crust, South Island, New Zealand. Journal of Geophysical Research: Solid Earth (1978–2012), 98(B9), 16119-16148.

Toomath, A., Palmer, J., (1987). Seismic interpretation report, Grey Valley Trough, Westland. PPL38070. Unpublished open-file petroleum report PR1327. Ministry of Economic Development, Wellington.

Townend, J., Sherburn, S., Arnold, R., Boese, C., & Woods, L. (2012). Three-dimensional variations in present-day tectonic stress along the Australia–Pacific plate boundary in New Zealand. Earth and Planetary Science Letters, 353, 47-59.

Tulloch, A. J. (1987). Magnetic susceptibilities of Westland-Nelson plutonic rocks: discrimination of Paleozoic and Mesozoic granitoid suites. New Zealand journal of geology and geophysics, 32(2), 197-203.

Tulloch, A. J., & Kimbrough, D. L. (1989). The Paparoa metamorphic core complex, New Zealand: cretaceous extension associated with fragmeotation of the pacific margin of Gondwana. Tectonics, 8(6), 1217-1234.

Vidanovich, P., (2013). Summary Report on the West Coast Airborne Geophysical Survey 2011-2013. Report prepared for New Zealand Petroleum and Minerals

Waight, T. E. (1995). The geology and geochemistry of the Hohonu Batholith and adjacent rocks, North Westland, New Zealand. PhD Thesis, University of Canterbury.

Waight, T. E., Weaver, S. D., & Muir, R. J. (1998a). Mid-Cretaceous granitic magmatism during the transition from subduction to extension in southern New Zealand: a chemical and tectonic synthesis. Lithos, 45(1), 469-482.

Waight, T. E., Weaver, S. D., Maas, R., & Eby, G. N. (1998b). French Creek Granite and Hohonu Dyke Swarm, South Island, New Zealand: Late Cretaceous alkaline magmatism and the opening of the Tasman Sea. Australian Journal of Earth Sciences, 45(6), 823-835.

Walcott, R. I. (1998). Modes of oblique compression: Late Cenozoic tectonics of the South Island of New Zealand. Reviews of Geophysics, 36(1), 1-26.

Weissel, J. K., Hayes, D. E., & Herron, E. M. (1977). Plate tectonics synthesis: The displacements between Australia, New Zealand, and Antarctica since the late Cretaceous. Marine geology, 25(1), 231-277.

Wellman, H.W., (1949). Geology of the Pike River coalfield, North Westland. New Zealand Journal of Science and Technology 30, 84-95.

Wellman, H.W. (1950). Tertiary Geology of Sheet S51 Kumara, with notes on the Cretaceous and Tertiary outliers to the south (S57, S58, S64). Unpublished manuscript in the library of the Institute of Geological and Nuclear Sciences.